

Synthetic Oversampling: Theory and A Practical Approach Using LLMs to Address Data Imbalance

Ryumei Nakada^{1*} Yichen Xu^{2*} Lexin Li^{3†} Linjun Zhang^{4†}

June 7, 2024

Abstract

Imbalanced data and spurious correlations are common challenges in machine learning and data science. Oversampling, which artificially increases the number of instances in the underrepresented classes, has been widely adopted to tackle these challenges. In this article, we introduce OPAL (**O**versam**P**ling with **A**rtificial **L**LM-generated data), a systematic oversampling approach that leverages the capabilities of large language models (LLMs) to generate high-quality synthetic data for minority groups. Recent studies on synthetic data generation using deep generative models mostly target prediction tasks. Our proposal differs in that we focus on handling imbalanced data and spurious correlations. More importantly, we develop a novel theory that rigorously characterizes the benefits of using the synthetic data, and shows the capacity of transformers in generating high-quality synthetic data for both labels and covariates. We further conduct intensive numerical experiments to demonstrate the efficacy of our proposed approach compared to some representative alternative solutions.

1 Introduction

Imbalanced data and spurious correlations are common challenges in machine learning and data science Haixiang et al. (2017); Ye et al. (2024). Imbalanced data occurs when classes in a dataset are not equally represented, such as in fraud detection or rare disease diagnosis, where positive samples are much less frequent than negative ones. Spurious correlations arise from misleading statistical relationships between variables due to irrelevant features. Imbalanced data can lead to spurious correlations, e.g., when some features predominantly present in the majority class, giving the illusion that these features are more predictive than they actually are. In both situations, statistical analyses may suffer from biased models that favor the majority group, or overfitting to irrelevant spurious features, which eventually lead to poor model performance, misleading insights, and compromised model generalizability and fairness.

Oversampling, which artificially balances the data by increasing the number of instances in the underrepresented classes, is a widely adopted technique to address the challenges of imbalanced data and spurious correlations Gosain and Sardana (2017). This approach

*Equal contribution.

†Corresponding author.

¹Rutgers University. Email: rn375@rutgers.edu.

²University of California, Berkeley. Email: yichen_xu@berkeley.edu.

³University of California, Berkeley. Email: lexinli@berkeley.edu.

⁴Rutgers University. Email: lz412@stat.rutgers.edu.

provides a more comprehensive view of the data landscape, helps achieve fairness in predictions, and improves the model’s generalization capability.

In the era of AI-driven innovations, large language models (LLMs) have risen to prominence as indispensable tools across a wide spectrum of applications. By leveraging the knowledge learned from training on vast amounts of data, LLMs generate coherent and contextually relevant text, often resembling human-generated content.

In this article, we introduce a systematic oversampling framework, which we term as OPAL (**O**versam**P**ling with **A**rtificial **L**LM-generated data), to generate high-quality synthetic data for underrepresented classes. Leveraging the capacity of large language models (LLMs), specifically the transformer-based GPT models, we apply in-context learning to tabular data. We develop a novel theoretical framework that elucidates the conditions under which adding synthetic data is beneficial for reducing the variance and improving the minority group performance in the presence of imbalanced data and spurious correlations. Our theory rigorously characterizes the benefits of using synthetic data, and provides an exact dependence of the convergence rate on the synthetic data bias. In addition, we theoretically demonstrate the capacity of transformers to generate high-quality synthetic data for both labels and covariates given in-context examples, which contrasts with existing theories that mostly focus on prediction or inference from in-context examples Xie et al. (2021); Garg et al. (2022); Zhang et al. (2023a); Bai et al. (2023). Our proposal thus differs from recent studies on synthetic data generation, which have primarily targeted prediction tasks Huang et al. (2022); Jain et al. (2024). In contrast, we focus specifically on the challenges of imbalanced data and spurious correlations, and we establish the corresponding theoretical guarantees. Finally, we validate our approach against conventional oversampling techniques such as random replication Loyola-González et al. (2016) and SMOTE Chawla et al. (2002), demonstrating the empirical competitiveness of our method. In summary, by harnessing the sophisticated generative capabilities of LLMs, our proposed method addresses the limitations of traditional oversampling methods, and provides a scalable and effective solution to improve the performance on imbalanced data and mitigate spurious correlations.

Outline of the paper. Section 2 introduces the problem set-up and a general framework for oversampling with synthetic samples generated by GPT. Section 3 first presents how the synthetic data quality affects the performance of the proposed method theoretically, and then analyzes the data quality of the synthetic data generated by transformers. Section 4 provides numerical evidence that our proposed method is better than conventional oversampling methods and other baseline methods.

1.1 Related works

LLM-based synthetic data generation. Current works primarily focus on pre-training and fine-tuning GPT on specific datasets. Borisov et al. (2023) proposed GReaT, a pipeline to fine-tune GPT-2 on tabular datasets to generate synthetic samples. Solatorio and Dupriez (2023) extended this and proposed REalTabFormer that synthesizes relational tabular data. Zhang et al. (2023b) developed TAPTAP that is pre-fine-tuned from GPT-2 using 450 public tables to incorporate more prior knowledge. Zhao et al. (2023) proposed Tabula that involves iterative fine-tuning to address the long training times of LLMs for tabular data. Gulati and Roysdon (2023) proposed TabMT that employs masking to enable different data types and imputation. Seedat et al. (2024) developed Curated LLM to monitor the confidence and uncertainty to screen out lower-quality synthetic data. More recently, Huang et al. (2022) presented catalytic priors, which use synthetic data to improve Bayesian

analysis when data is scarce. This approach combines the observed and synthetic data from simpler models for stable and interpretable inferences. Jain et al. (2024) explored how to improve machine learning by using “surrogate” data to supplement limited original data, proposed a weighted empirical risk minimization method, and introduced a scaling law to optimize the use of surrogate data. They showed that integrating surrogate data can significantly reduce test error, both theoretically and empirically.

Oversampling techniques. Oversampling has been widely adapted for handling imbalanced data and spurious correlation Vilorio et al. (2020); An et al. (2020); Ye et al. (2024). Synthetic Minority Oversampling Technique (SMOTE) Chawla et al. (2002) and its variants Han et al. (2005); Bunkhumpornpat et al. (2009); Douzas et al. (2018) are popular oversampling methods that demonstrate significant improvements in handling class imbalance by oversampling. He et al. (2008) further proposed ADASYN by adaptively generating more synthetic data for the minority class that is harder to learn. More recently, Douzas and Bacao (2018); Oh et al. (2019); Jo and Kim (2022) have started to employ Generative Adversarial Networks (GANs) Goodfellow et al. (2014) for oversampling Douzas and Bacao (2018) leveraged GANs to create more realistic synthetic samples, enhancing the diversity and quality of the oversampled data. See also Krawczyk (2016) for a review on oversampling techniques. On the other hand, Chawla et al. (2004); Fernández et al. (2018); Johnson and Khoshgoftaar (2019) have shown that the oversampling minority group could lead to overfitting. Chatterji et al. (2022) theoretically proved that undersampling the majority group to balance out the groups is minimax optimal in handling the imbalanced data for non-parametric classification. These results highlight the room for improvement in oversampling methodology.

2 Oversampling with artificial LLM-generated data

2.1 Problem setup

In many real-world datasets, individual samples are naturally organized into groups. Machine learning models trained on such datasets often perform poorly on the under-represented minority groups. To enhance the performance, we introduce the synthetic data that mimic the raw data in these groups.

We first introduce the problem setup. Let \mathcal{G} denote the set of groups. For each group $g \in \mathcal{G}$, let n_g be the number of observed raw samples, while we further generate m_g synthetic samples for this group. Let $n_{\text{total}} := \sum_{g \in \mathcal{G}} n_g$, and $m_{\text{total}} := \sum_{g \in \mathcal{G}} m_g$ be the total number of raw and synthetic data, respectively. We aim to investigate the effect of the synthetically balanced data on the risk of both majority and minority groups. Denote the observed raw data for group g as $\{(\mathbf{x}_i^{(g)}, y_i^{(g)})\}_{i \in [n_g]}$, and the generated synthetic data for group g as $\{(\tilde{\mathbf{x}}_i^{(g)}, \tilde{y}_i^{(g)})\}_{i \in [m_g]}$. Given a loss function $\ell(\boldsymbol{\theta}; \mathbf{x}, y)$ parameterized by $\boldsymbol{\theta} \in \Theta$, we define the empirical risk with the raw and synthetic data as follows:

$$\widehat{\mathcal{R}}_{\text{syn}}(\boldsymbol{\theta}) := \frac{1}{n_{\text{total}} + m_{\text{total}}} \left(\sum_{g \in \mathcal{G}} \sum_{i \in [n_g]} \ell(\boldsymbol{\theta}; \mathbf{x}_i^{(g)}, y_i^{(g)}) + \sum_{g \in \mathcal{G}} \sum_{i \in [m_g]} \ell(\boldsymbol{\theta}; \tilde{\mathbf{x}}_i^{(g)}, \tilde{y}_i^{(g)}) \right). \quad (1)$$

We minimize the above empirical risk to obtain the parameter estimate $\widehat{\boldsymbol{\theta}}_{\text{syn}}$. Our goal is to analyze the group specific risk $\mathcal{R}_g(\widehat{\boldsymbol{\theta}}_{\text{syn}})$, where $\mathcal{R}_g(\boldsymbol{\theta}) := \mathbb{E}[\ell(\boldsymbol{\theta}; \mathbf{x}_1^{(g)}, y_1^{(g)})]$, for $g \in \mathcal{G}$. We next consider two specific situations: imbalanced classification and spurious correlations.

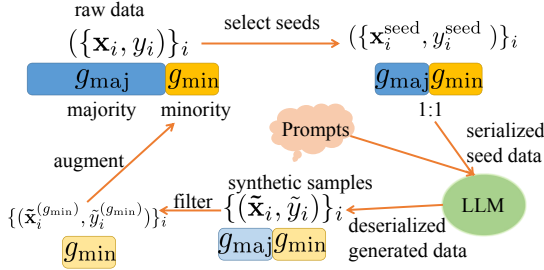


Figure 1: Overview of Synthetic Oversampling by OPAL.

Algorithm 1 OPAL

Input:

Raw data $\{(\mathbf{x}_i, y_i)\}_i$; an LLM; the minority group g_{\min} ; m_{\min} , the number of samples to augment g_{\min} .

Output:

Augmented data $\{(\mathbf{x}_i, y_i)\}_i \cup \{(\tilde{\mathbf{x}}_i, \tilde{y}_i)\}_i$

Procedure:

- 1: $\{(\mathbf{x}_i^{\text{seed}}, y_i^{\text{seed}})\}_i \leftarrow$ select balanced seed data from $\{(\mathbf{x}_i, y_i)\}_i$.
 - 2: $\{(\tilde{\mathbf{x}}_i, \tilde{y}_i)\}_i \leftarrow$ serialize the seed data, prompt LLM with $\{(\mathbf{x}_i^{\text{seed}}, y_i^{\text{seed}})\}_i$, deserialize the generated contents.
 - 3: $\{(\tilde{\mathbf{x}}_i^{(g_{\min})}, \tilde{y}_i^{(g_{\min})})\}_i \leftarrow$ choose m_{\min} samples from $\{(\tilde{\mathbf{x}}_i, \tilde{y}_i)\}_i$ for g_{\min} .
 - 4: **Return** $\{(\mathbf{x}_i, y_i)\}_i \cup \{(\tilde{\mathbf{x}}_i^{(g_{\min})}, \tilde{y}_i^{(g_{\min})})\}_i$
-

Imbalanced classification. We observe the pairs of label and covariate $(\mathbf{x}_i, y_i)_{i \in [n_{\text{total}}]} \subset \mathcal{X} \times \mathcal{Y}$, where \mathcal{X} is the set of covariates, \mathcal{Y} is the label set, and there is an unequal distribution among the group labels. For this task, the group structure is determined by the label, i.e., $\mathcal{G} = \mathcal{Y}$. Our goal is to improve the minority group risk for predicting y_i given \mathbf{x}_i .

Spurious correlations. We observe the triples of the core feature, the spurious feature, and the label $(\mathbf{z}_i, \mathbf{a}_i, y_i)_{i \in [n_{\text{total}}]} \subset \mathcal{X} \times \mathcal{A} \times \mathcal{Y}$. Such a setting is commonly used in the spurious correlations literature Sagawa et al. (2019, 2020); Chaudhuri et al. (2023); Ye et al. (2024). For this task, the group structure is determined by the combination of the label and spurious feature, i.e., $\mathcal{G} = \mathcal{Y} \times \mathcal{A}$. Our goal is to disentangle \mathbf{a}_i and y_i , and improve the prediction performance of y_i for the minority groups.

2.2 A general algorithm

We propose OPAL, short for **O**versamPling with **A**rtificial **L**LM-generated data, a new oversampling approach that leverages the capability of large language models (LLMs) to generate high-quality synthetic data for minority groups. We illustrate our approach in Figure 1 and Algorithm 1 with the setting of two groups, the minority group g_{\min} and the majority group g_{maj} . More specifically, to prepare the tabular data to feed into the LLM, we follow Borisov et al. (2023) to convert the numeric values into the sentence serialized format $[f_j \text{ "is" } v_{ij}]$, where f_j is the j -th feature name and v_{ij} is the value of the j -th feature of i -th data sample. To ensure that the LLM captures the characteristics of the minority group, we balance the input seed data by subsampling a balanced dataset from the original data (Algorithm 1, line 1). We then craft prompts that instruct the LLM to identify the underlying patterns, understand the data distributions, and generate synthetic samples that are distinct from the input data (line 2). The details of the prompts and the format of the serialized data are elaborated in Appendix E.1. Finally, we choose the synthetic samples that correspond to the minority group, and augment them to the raw data (line 3), completing the oversampling process.

3 Theoretical Analysis

We establish the theoretical guarantees for effective oversampling with synthetic data when employing a high-quality synthetic data generator. Furthermore, we theoretically

demonstrate that the transformers are indeed capable of producing such high-quality synthetic data.

3.1 Oversampling with synthetic data

We first investigate the performance of the general empirical risk minimizer of the risk $\widehat{\mathcal{R}}_{\text{syn}}$ in equation 1. We then study the imbalanced classification and spurious correlations settings, respectively. We present the main results here, while giving a more rigorous characterization in Appendix B.

We define the population-level balanced risk that puts equal weights on all groups as

$$\mathcal{R}_{\text{bal}}(\boldsymbol{\theta}) := \frac{1}{|\mathcal{G}|} \sum_{g \in \mathcal{G}} \mathcal{R}_g(\boldsymbol{\theta}), \quad \text{where} \quad \mathcal{R}_g(\boldsymbol{\theta}) := \mathbb{E}[\ell(\boldsymbol{\theta}; \mathbf{x}_1^{(g)}, y_1^{(g)})]. \quad (2)$$

Let the minimizer of $\widehat{\mathcal{R}}_{\text{syn}}$ and \mathcal{R}_{bal} be $\widehat{\boldsymbol{\theta}}_{\text{syn}}$ and $\boldsymbol{\theta}_{\text{bal}}$, respectively. Note that $\boldsymbol{\theta}_{\text{bal}}$ is the oracle solution, balancing out the parameters over all groups present in the dataset. We assume that \mathcal{B}_g and \mathcal{R}_g are twice differentiable around $\boldsymbol{\theta}_{\text{bal}}$ with bounded Lipschitz Hessians, and $\sum_g \nabla^2 \mathcal{R}_g(\boldsymbol{\theta})$ is strictly positive definite around $\boldsymbol{\theta}_{\text{bal}}$.

Our goal is to investigate the effect of bias present in the synthetic data to the estimator $\widehat{\boldsymbol{\theta}}_{\text{syn}}$, by measuring the risk of group g : $\mathcal{R}_g(\widehat{\boldsymbol{\theta}}_{\text{syn}}) - \mathcal{R}_g(\boldsymbol{\theta}_{\text{bal}})$. To demonstrate the scaling behavior of this risk, we consider the regime where $\min_{g \in \mathcal{G}} n_g$ grows. Define the bias of the risk for group g as $\mathcal{B}_g(\boldsymbol{\theta}) := \mathbb{E}[\ell(\boldsymbol{\theta}; \tilde{\mathbf{x}}_1^{(g)}, \tilde{y}_1^{(g)})] - \mathbb{E}[\ell(\boldsymbol{\theta}; \mathbf{x}_1^{(g)}, y_1^{(g)})]$. We introduce some regularity assumptions.

Assumption 3.1. Assume that $\sup_{\boldsymbol{\theta} \in \Theta} |\mathcal{B}_g(\boldsymbol{\theta})| \vee \|\nabla \mathcal{B}_g(\boldsymbol{\theta})\| = o(1)$ for all $g \in \mathcal{G}$.

Assumption 3.2. Assume that $\sup_{\boldsymbol{\theta} \in \Theta} |\widehat{\mathcal{R}}_{\text{syn}}(\boldsymbol{\theta}) - \mathcal{R}_{\text{syn}}(\boldsymbol{\theta})| = o_p(1)$, and that

$$\inf_{\boldsymbol{\theta} \in \Theta: \|\boldsymbol{\theta} - \boldsymbol{\theta}_{\text{syn}}\| \geq \epsilon} \mathbb{E}[\widehat{\mathcal{R}}_{\text{syn}}(\boldsymbol{\theta})] > \mathbb{E}[\widehat{\mathcal{R}}_{\text{syn}}(\boldsymbol{\theta}_{\text{syn}})], \quad \text{and} \quad \inf_{\boldsymbol{\theta} \in \Theta: \|\boldsymbol{\theta} - \boldsymbol{\theta}_{\text{bal}}\| \geq \epsilon} \mathcal{R}_{\text{bal}}(\boldsymbol{\theta}) > \mathcal{R}_{\text{bal}}(\boldsymbol{\theta}_{\text{bal}}).$$

Assumption 3.3. Assume that $\ell(\boldsymbol{\theta}; x, y)$ and $\ell(\boldsymbol{\theta}; \tilde{x}, \tilde{y})$ are differentiable around $\boldsymbol{\theta}_{\text{bal}}$ almost surely under the distributions for the raw data (\mathbf{x}, y) and the synthetic data $(\tilde{\mathbf{x}}, \tilde{y})$, with the second order moments of gradient Lipschitz around $\boldsymbol{\theta}_{\text{bal}}$.

Assumption 3.1 describes the regime where the bias for each group $g \in \mathcal{G}$ decreases as the amount of seed data increases. It is satisfied when the synthetic data generator improves its output quality with more seed data. Assumptions 3.2 and 3.3 are standard assumptions in proving the consistency and asymptotic normality of the estimators in statistical learning Van der Vaart (2000); Jain et al. (2024).

Theorem 3.1. Under Assumptions 3.1-3.3, for any $g \in \mathcal{G}$,

$$\mathcal{R}_g(\widehat{\boldsymbol{\theta}}_{\text{syn}}) = \mathcal{R}_g(\boldsymbol{\theta}_{\text{bal}}) - \{\nabla \mathcal{R}_g(\boldsymbol{\theta}_{\text{bal}})\}^\top \{\nabla^2 \mathcal{R}_{\text{bal}}(\boldsymbol{\theta}_{\text{bal}})\}^{-1} \mathbf{b} + O_p\left(\frac{v_g}{\sqrt{n_{\text{total}} + m_{\text{total}}}} + \frac{1}{m_{\text{total}} \wedge n_{\text{total}}} + \|\mathbf{b}\|^2\right),$$

where $\mathbf{b} := \sum_{g' \in \mathcal{G}} \frac{m_{g'}}{n_{\text{total}} + m_{\text{total}}} \nabla \mathcal{B}_{g'}(\boldsymbol{\theta}_{\text{bal}})$, and $v_g > 0$ is given in equation 7.

Within the O_p term, $v_g / \sqrt{n_{\text{total}} + m_{\text{total}}}$ accounts for the variance of the gradients, arising from the finite sample variation of $\widehat{\mathcal{R}}_{\text{syn}}$. We observe that the group-specific risk is influenced by the bias term $\{\nabla \mathcal{R}_g(\boldsymbol{\theta}_{\text{bal}})\}^\top \{\nabla^2 \mathcal{R}_{\text{bal}}(\boldsymbol{\theta}_{\text{bal}})\}^{-1} \mathbf{b}$. The term \mathbf{b} originates from two sources: the group-specific bias $\|\mathcal{B}_{g'}(\boldsymbol{\theta}_{\text{bal}})\|$ introduced by the synthetic data, and the ratio $m_{g'} / (n_{\text{total}} + m_{\text{total}})$ of the group-specific synthetic data size to the total number of

raw and synthetic samples, which reflects the data imbalance. A direct consequence of Theorem 3.1 is that choosing $m_{g'} \asymp \frac{v_g^2}{|\mathcal{G}|\|\nabla\mathcal{B}_{g'}(\boldsymbol{\theta}_{\text{bal}})\|^2}$ for all $g' \in \mathcal{G}$ gives

$$|\mathcal{R}_g(\widehat{\boldsymbol{\theta}}_{\text{syn}}) - \mathcal{R}_g(\boldsymbol{\theta}_{\text{bal}})| = O_p(\max_{g' \in \mathcal{G}} \|\nabla\mathcal{B}_{g'}(\boldsymbol{\theta}_{\text{bal}})\| \vee n_{\text{total}}^{-1}).$$

Therefore, having a high-quality synthetic data generator is beneficial for the convergence of the risk. We also briefly note that the notation O_p hides the constants in the assumptions and the constants depending on \mathcal{R}_g .

3.1.1 Imbalanced classification

We first apply the general result in Section 3.1 to the binary imbalanced classification task with the label set $\mathcal{G} = \mathcal{Y} = \{0, 1\}$, where group 0 is treated as the minority group and group 1 as the majority group. For imbalanced data classification, we add the synthetic data only to the minority group $g = 0$, such that the total number of samples for each group becomes equal, i.e., $n_0 + m_0 = n_1$. Let \mathcal{R}_{bal} be the balanced risk defined in equation 2 with $\mathcal{G} = \mathcal{Y}$. We are interested in the performance of $\widehat{\boldsymbol{\theta}}_{\text{syn}}$ against $\boldsymbol{\theta}_{\text{bal}}$ for the minority group. Recall that $\mathcal{R}_0(\boldsymbol{\theta}) := \mathbb{E}[\ell(\boldsymbol{\theta}; \mathbf{x}_1, y_1) | y_1 = 0]$ in our setting.

Corollary 3.1. *Under Assumptions 3.1-3.3, if $n_0 \leq cn_1$ holds for some constant $c \in (0, 1)$, then,*

$$\mathcal{R}_1(\widehat{\boldsymbol{\theta}}_{\text{syn}}) = \mathcal{R}_0(\boldsymbol{\theta}_{\text{bal}}) - \frac{n_1 - n_0}{2n_1} b_{0,0} + O_p\left(\frac{1}{\sqrt{n_1}} v_0 + \|\nabla\mathcal{B}_0(\boldsymbol{\theta}_{\text{bal}})\|^2\right),$$

where $b_{0,0} = \{\nabla\mathcal{R}_0(\boldsymbol{\theta}_{\text{bal}})\}^\top \{\nabla^2\mathcal{R}_{\text{bal}}(\boldsymbol{\theta}_{\text{bal}})\}^{-1} \nabla\mathcal{B}_0(\boldsymbol{\theta}_{\text{bal}})$ and $v_0 > 0$ is given in equation 13.

The term $\frac{n_1 - n_0}{2n_1} b_{0,0}$ represents the bias introduced by the addition of the synthetic data for group $g = 1$. The variance term is proportional to $n_1^{-1/2}$. This corollary indicates that $\widehat{\boldsymbol{\theta}}_{\text{syn}}$ achieves similar minority-group performance as $\boldsymbol{\theta}_{\text{bal}}$ when the introduced bias is small.

3.1.2 Spurious correlations

We next apply the general result in Section 3.1 to the spurious correlations setting with a binary label and a discrete-value spurious feature, i.e., $\mathcal{Y} = \{-1, 1\}$ and $\mathcal{A} = \{-\gamma, \gamma\}$ with some $\gamma \in \mathbb{R}^q$. A similar setting has been used in the learning theory under spurious correlations Arjovsky et al. (2019); Ye et al. (2023). We observe $\mathbf{x}_i = (\mathbf{z}_i, \mathbf{a}_i)$ and y_i , where $\mathbf{z}_i \in \mathbb{R}^p$ is the core feature and $\mathbf{a}_i \in \mathcal{A}$ is the spurious feature. We assume the conditional independence of \mathbf{a}_i and \mathbf{z}_i given y_i . For simplicity, assume $n_{(-1, \gamma)} = n_{(1, -\gamma)} = n_{\text{min}} < n_{\text{maj}} = n_{(1, \gamma)} = n_{(-1, -\gamma)}$, so that groups $(-1, -\gamma)$ and $(1, \gamma)$ are the majority groups. We choose the synthetic data size for group $g = (y, a) \in \mathcal{G}$ by $m_{(y, a)} = (n_{\text{maj}} - n_{\text{min}}) \mathbb{1}\{y = a\}$ to equal the raw and synthetic data size for each group. Define the reweighted risk and its minimizer by

$$\mathcal{R}_{\text{rw}}(\boldsymbol{\theta}) := \frac{1}{2} \sum_y \mathbb{E}[\ell(\boldsymbol{\theta}; \mathbf{x}'_1, y_1) | y_1 = y], \quad \text{and} \quad \boldsymbol{\theta}_{\text{rw}} := \arg \min_{\boldsymbol{\theta} \in \Theta} \mathcal{R}_{\text{rw}}(\boldsymbol{\theta}).$$

where $\mathbf{x}'_1 = (\mathbf{z}_1, \mathbf{a}'_1)$ with $\mathbf{a}'_1 \sim \text{Unif}(\{-\gamma, \gamma\})$ independent of y_1 . Note that \mathcal{R}_{rw} is the so-called reweighted loss Shimodaira (2000); Byrd and Lipton (2019); Sagawa et al. (2020) beneficial in handling spurious correlations. It successfully decouples the correlation between y_i and a_i , mitigating the effect of spurious correlations. We are interested in the performance of $\widehat{\boldsymbol{\theta}}_{\text{syn}}$ against $\boldsymbol{\theta}_{\text{rw}}$, measured in the worst group risk $\max_{g \in \mathcal{G}} \mathcal{R}_g(\boldsymbol{\theta}) := \max_{y \in \mathcal{Y}, \mathbf{a} \in \mathcal{A}} \mathbb{E}[\ell(\boldsymbol{\theta}; (\mathbf{z}_1, \mathbf{a}_1), \mathbf{y}_1) | y_1 = y, \mathbf{a}_1 = \mathbf{a}]$.

Corollary 3.2. *Under Assumptions 3.1-3.3, if $n_{\min} \leq cn_{\text{maj}}$ holds for some constant $c \in (0, 1)$, then,*

$$\max_{g \in \mathcal{G}} \mathcal{R}_g(\hat{\boldsymbol{\theta}}_{\text{syn}}) = \max_{g \in \mathcal{G}} \mathcal{R}_g(\boldsymbol{\theta}_{\text{rw}}) + O_p \left(\|\nabla \mathcal{B}_{(-1, \gamma)}(\boldsymbol{\theta}_{\text{rw}})\| + \|\nabla \mathcal{B}_{(1, -\gamma)}(\boldsymbol{\theta}_{\text{rw}})\| + \frac{\max_{g \in \mathcal{G}} v_g}{\sqrt{n_{\text{maj}}}} \right),$$

where $v_g > 0$ is given in equation 15.

Within the O_p term, there are bias terms for the minority groups, and a variance term of order $n_{\text{maj}}^{-1/2}$. The worst group risk of $\hat{\boldsymbol{\theta}}_{\text{syn}}$ becomes close to the worst group risk of $\boldsymbol{\theta}_{\text{rw}}$ when the bias of the minority group, coming from the synthetic data generation, decreases.

3.2 Transformers are high-quality synthetic data generators

We next provide theories to quantify the data quality generated by the transformers. Recall that Algorithm 1 utilizes the balanced seed data selected from the raw dataset. For our theoretical analysis, we consider a dataset that is already balanced and omit the “seed” superscript for the raw data. Let \mathcal{X} be any space containing the covariates and labels. Suppose that we have n i.i.d. seed data $\mathcal{D}_n := (X_i, Y_i)_{i \in [n]}$, where $X_i, Y_i \in \mathcal{X}$. Given \mathcal{D}_n in-context, we aim to show that the transformers can generate the high-quality synthetic data $(\tilde{X}_1, \tilde{Y}_1), (\tilde{X}_2, \tilde{Y}_2), \dots$ that mimic the distribution of (X_1, Y_1) . We also provide more technical details in Appendix A and Appendix C.

3.2.1 Data generating process

We first introduce the data generating process for $(X_i, Y_i)_{i \in [n]}$. As assumed in the literature on word representations Arora et al. (2015); Khalife et al. (2021); Li et al. (2022), we consider a Bayesian setting for the token embeddings, where $\mathbf{u}_1, \dots, \mathbf{u}_d \in \mathbb{R}^r$ are modeled as i.i.d. realizations of $N(0, I_r/r)$. Let $U = [\mathbf{u}_1, \dots, \mathbf{u}_d]^\top$. We assume that X_i and Y_i take values in a finite set $\mathcal{X} = [d]$, reflecting the treatment of tabular data as a collection of finite tokens for language models. We define a “subject” as any background information providing context for each tabular data. For instance, the data on heart failure rates could be specified by the subject “heart failure”.

We then introduce the data generating process for tabular data: generative models for covariates and discriminative models for labels given the covariates. Specifically, $(X_i, Y_i) \in \mathcal{X}^2$ given subject $T = t$ and discriminative function index $M = m$ follows a multinomial distribution defined by,

$$\begin{aligned} \mathbb{P}(X_i = x; T = t, U, \eta) &\propto \exp(\eta^{-1} \langle \mathbf{z}^{(t)}, \mathbf{u}_x \rangle), \\ \mathbb{P}(Y_i = y | X_i = x; M = m, U, \eta) &\propto \exp(\eta^{-1} \langle f^{(m)}(\mathbf{u}_x), \mathbf{u}_y \rangle), \end{aligned} \quad (3)$$

where $t \in \mathcal{T}$, $m \in \mathcal{M}$ are possible indices of subjects and discriminative function indices, $\eta > 0$ is a parameter, $\mathbf{u}_x \in \mathbb{R}^r$ is the embedding of the token $x \in \mathcal{X}$, $\mathbf{z}^{(t)} \in \mathbb{R}^r$ is the representation of subject t , and $f^{(m)} : \mathbb{R}^r \rightarrow \mathbb{R}^r$ is a discriminative function with index m . We consider the case where $|\mathcal{M}| \geq |\mathcal{T}|$ for simplicity. We allow η to vary on the interval $[(1/\sqrt{r}) \log d, \infty)$, while assume $\|\mathbf{z}^{(t)}\| = 1$ for any $t \in \mathcal{T}$ and $\sup_{\mathbf{u} \in \mathbb{B}_r(\log d)} \|f^{(m)}(\mathbf{u})\| \leq 1$ for identifiability. A similar model has been proposed and used in the language modeling literature Mnih and Hinton (2007); Arora et al. (2015, 2017); Shi et al. (2017); Khalife et al. (2021). Denote the joint distribution of X_1 and Y_1 by $P_{X_1, Y_1; T=t, M=m, U, \eta}$ and (conditional) distributions of X_1 and $Y_1 | X_1$ under model 3 by $P_{X_1; T=t, U, \eta}$ and $P_{Y_1 | X_1; M=m, U, \eta}$, respectively. Based on the intuition that the transformers are pre-trained on vast amount of data, we further assume that the candidate of subject embeddings $\{\mathbf{z}^{(t)}\}_{t \in \mathcal{T}}$ and candidate of functions $\{f^{(m)}\}_{m \in \mathcal{M}}$ are known to the transformers.

Finite known candidates of subject embeddings and functions Based on the intuition that transformers are pre-trained on vast amount of data, we further assume that the transformer knows the candidate of subject embeddings $\{\mathbf{z}^{(t)}\}_{t \in \mathcal{T}}$ and candidate of functions $\{f^{(m)}\}_{m \in \mathcal{M}} \subset \mathcal{F}(L_0, r_0) \subset \{\text{FFN}_{\nu_{\text{pre}, L_0}} \circ \text{FFN}_{\nu_{\text{pre}, L_0-1}} \circ \dots \circ \text{FFN}_{\nu_{\text{pre}, 1}} : \nu_{\text{pre}, \ell} \in \mathbb{R}^{r_0 \times r} \times \mathbb{R}^{r \times r_0} \text{ for } \ell \in [L_0]\}$ with $L_0, r_0 \in \mathbb{N}^+$.

We remark that our modeling differs from those in in-context learning theory papers. For instance, Xie et al. (2021); Garg et al. (2022); Zhang et al. (2023a); Bai et al. (2023) consider settings where seed data is directly treated as tokens. In contrast, our approach is motivated by the use of proprietary text-based LLMs with serialised tabular data, rather than training tabular transformers from scratch. Therefore, it is more natural to consider tokens *indirectly* embed the seed data in our setting.

3.2.2 Preliminaries of transformers

We follow the notations in Akyürek et al. (2022); Von Oswald et al. (2023); Bai et al. (2023) to introduce the transformers, which consist of two main types of layers: the self-attention, and the feed-forward transformation. Denote the input by $H = [\mathbf{h}_1, \mathbf{h}_2, \dots, \mathbf{h}_N] \in \mathbb{R}^{D \times N}$, where $\mathbf{h}_s \in \mathbb{R}^D$ is a column vector denoting the embedding of the s -th token. A transformer layer is defined as the composition of a self-attention layer and a feedforward layer. Specifically, given an attention layer Attn_μ and FFN_ν defined below, we define TF_ψ with $\psi = (\mu, \nu)$ as $\text{TF}_\psi := \text{FFN}_\nu \circ \text{Attn}_\mu$. With a slight abuse of notation, we write multiple transformer layers as $\text{TF}_{(\psi_1, \dots, \psi_L)} := \text{TF}_{\psi_L} \circ \dots \circ \text{TF}_{\psi_1}$.

Self-attention layer. Given a matrix $H \in \mathbb{R}^{D \times N}$, the self-attention layer with J heads and parameters $\mu = \{(Q_j, K_j, V_j)\}_{j=1}^J$ takes H as input and outputs

$$\text{Attn}_\mu(H)_s := \mathbf{h}_s + \sum_{j \in [J]} \sum_{s' \in [N]} \sigma(\langle Q_j \mathbf{h}_s, K_j \mathbf{h}_{s'} \rangle) V_j \mathbf{h}_{s'}, \quad s \in [N],$$

where σ is the ReLU activation function, and $Q, K, V \in \mathbb{R}^{D \times D}$.

Feed-forward transformation layer. Given a matrix $H \in \mathbb{R}^{D \times N}$, the feed-forward transformation layer with parameters $\nu = (W_1, W_2) \in \mathbb{R}^{D' \times D} \times \mathbb{R}^{D \times D'}$ takes H as input and outputs

$$\text{FFN}_\nu(H) := H + W_2 \sigma(W_1 H).$$

Input tokens for tabular data. We assume that tokens $(\mathbf{h}_i^Y)_{i \in [n]}$ correspond to $(Y_i)_{i \in [n]}$, and $(\mathbf{h}_i^X)_{i \in [n]}$ correspond to $(X_i)_{i \in [n]}$. The input of the transformer is given by

$$H_n = [\mathbf{h}_1^X; \mathbf{h}_1^Y; \mathbf{h}_2^X; \mathbf{h}_2^Y; \dots; \mathbf{h}_n^X; \mathbf{h}_n^Y].$$

We consider the composite type positional encoding, i.e., the forms of \mathbf{h}_i^X and \mathbf{h}_i^Y are given by $\mathbf{h}_i^X = (\mathbf{u}_{X_i}^\top, \mathbf{0}^\top, \mathbf{p}_{2i-1, n}^\top)^\top$ and $\mathbf{h}_i^Y = (\mathbf{u}_{X_i}^\top, \mathbf{0}^\top, \mathbf{p}_{2i, n}^\top)^\top$, respectively. Note that this differs from the practical additive positional encoding. Specifically for $i \in [n]$, the positional encoding $\mathbf{p}_{s, n} \in \mathbb{R}^4$ is defined as

$$\mathbf{p}_{s, n} = \left(\left[\frac{s}{2} \right], (s \bmod 2), 2n, 1 \right)^\top,$$

where $s \bmod 2$ is 0 for even s and 1 for odd s . The first coordinate specifies the index of the current token, and the second coordinate indicates whether the current token corresponds to X_i or Y_i . The third coordinate takes the length of the given tokens. The last coordinate is a constant added for technical convenience.

Output distribution. Given the initial input tokens $H_n \in \mathbb{R}^{D \times 2n}$, a transformer parameterized by Ψ sequentially outputs $\mathbf{h}_{2n+1}, \mathbf{h}_{2n+2}, \dots$ corresponding to the synthetic data from a categorical distribution given the last output from the transformer layers. At each step $\ell \in \mathbb{N}^+$, given all previous tokens H_n and $\mathbf{h}_{2n+1}, \mathbf{h}_{2n+2}, \dots, \mathbf{h}_{2n+\ell-1}$, the next token $\mathbf{h}_{2n+\ell}$ is given by $\mathbf{h}_{2n+\ell} = (\mathbf{v}_{2n+\ell}^\top, \mathbf{0}^\top, \mathbf{p}_{2n+\ell, n}^\top)^\top$, where $\mathbf{v}_{2n+\ell} \in \mathbb{R}^r$ is drawn from a categorical distribution with softmax probability over all possible tokens $\mathbf{u}_1, \dots, \mathbf{u}_d \in \mathbb{R}^r$:

$$\mathbb{P}(\mathbf{v}_{2n+\ell} = \mathbf{u}_x) \propto \exp(\tau^{-1} \langle \mathbf{u}_x, (\tilde{\mathbf{h}}_{2n+\ell-1})_{1:r} \rangle),$$

where

$$\tilde{\mathbf{h}}_{2n+\ell-1} := (\text{TF}_\Psi([H_n, \mathbf{h}_{2n+1}, \mathbf{h}_{2n+2}, \dots, \mathbf{h}_{2n+\ell-1}]))_{2n+\ell-1},$$

and $\tau > 0$ is the temperature parameter. Since we expect the outputs $\mathbf{h}_{2n+1}, \mathbf{h}_{2n+2}, \mathbf{h}_{2n+3}, \mathbf{h}_{2n+4}, \dots$ from a transformer TF_Ψ correspond to $\tilde{X}_1, \tilde{Y}_1, \tilde{X}_2, \tilde{Y}_2, \dots$, we write the joint distribution of $\mathbf{v}_{2n+2s-1}$ and \mathbf{v}_{2n+2s} as

$$Q_{\tilde{X}_s, \tilde{Y}_s; \Psi, \tau, \mathcal{D}_n}(x, y) := \mathbb{P}(\mathbf{v}_{2n+2s-1} = \mathbf{u}_x, \mathbf{v}_{2n+2s} = \mathbf{u}_y).$$

We similarly denote the marginal and conditional distributions of \tilde{X}_s and $\tilde{Y}_s | \tilde{X}_s$ by $Q_{\tilde{X}_s; \Psi, \tau, \mathcal{D}_n}(x)$ and $Q_{\tilde{Y}_s | \tilde{X}_s; \Psi, \tau, \mathcal{D}_n}(y)$. For an overview of the input and output tokens, see Table 2 in Appendix.

We introduce an assumption for the identifiability of functions as follows.

Assumption 3.4. There exists a constant $C > 0$ and $\epsilon > 0$ such that for any $\epsilon' \leq \epsilon$ and $m, m' \in \mathcal{M}$, if $|\mathbb{E}[f^{(m')}(\mathbf{u}_{X_1})^\top f^{(m)}(\mathbf{u}_{X_1})] - \mathbb{E}[\|f^{(m)}(\mathbf{u}_{X_1})\|^2]| \leq \epsilon'$, then $|\mathbb{E}[\|f^{(m')}(\mathbf{u}_{X_1}) - f^{(m)}(\mathbf{u}_{X_1})\|^2]| \leq C\epsilon'$ holds with high probability in U , where the expectation is taken with respect to $P_{X_1; T=t, U, \eta}$.

Assumption 3.4 requires that for any $f^{(m')}$ whose projection to $f^{(m)}$ is approximately $f^{(m)}$, it must be close to $f^{(m)}$ on average. At the high level, this assumption requires that $\{f^{(m)}\}_{m \in \mathcal{M}}$ locally takes values on a sphere on average. Note that this assumption is trivially satisfied by considering functions that take values on a sphere in \mathbb{R}^r on average, and introducing layer-normalization in the transformers.

We consider the regime where d and r both grows with $r = o(\log d)$, and investigate the capacity of language models to recover the original distribution measured by the Kullback-Leibler divergence.

Theorem 3.2. Suppose that Assumption 3.4 holds. Fix any $d, r, r_0, L_0 \in \mathbb{N}^+$, $(\mathbf{z}^{(t)})_{t \in \mathcal{T}}$ and $(f^{(m)})_{m \in \mathcal{M}} \subset \mathcal{F}(L_0, r_0)$. Then, there exists transformer layers TF_{Ψ^*} with $O(|\mathcal{M}|)$ attention heads such that for any $t \in \mathcal{T}$, $m \in \mathcal{M}$, and $\eta \geq r^{-1/2} \log d$,

$$D_{\text{KL}}(P_{X_1; T=t, U, \eta} \| Q_{\tilde{X}_s; \Psi^*, \tau, \mathcal{D}_n}) \lesssim \frac{1}{\sqrt{d}} + \frac{\log d}{\sqrt{n}},$$

$$\mathbb{E} \left[D_{\text{KL}}(P_{Y_1 | X_1; M=m, U, \eta} \| Q_{\tilde{Y}_s | X_1; \Psi^*, \tau, \mathcal{D}_n}) \mid M = m, T = t, U, \eta \right] \lesssim \frac{1}{\sqrt{d}} + \frac{\log d}{\sqrt{n}},$$

and

$$\min_{\tau > 0} D_{\text{KL}}(P_{X_1, Y_1; T=t, M=m, U, \eta} \| Q_{\tilde{X}_s, \tilde{Y}_s; \Psi^*, \tau, \mathcal{D}_n}) \lesssim \frac{1}{\sqrt{d}} + \frac{\log d}{\sqrt{n}}$$

hold for all $s \in \mathbb{N}^+$ with probability $1 - \exp(-\Omega(\log^2 d))$ in U .

In Theorem 3.2, the upper bound consists of the bias and variance terms. In a typical in-context learning setting, the number of possible tokens is huge while the number of in-context examples are small. Thus the dominating term in the upper bound is $\tilde{O}(n^{-1/2})$. From the results in Section 3.1, the minority group risk for imbalanced data and the worst group risk for spurious correlations settings depend on the quality of synthetic data via $\|\nabla\mathcal{B}_g(\theta_{\text{bal}})\|$, which in turn can be controlled by the KL divergence stated in Theorem 3.2. Therefore, language models indeed produce high-quality data, supporting the use of LLMs for synthetic oversampling. We defer the details of the constructed transformer to Proposition C.1 and Theorem C.1 in Appendix C.

4 Numerical Experiments

4.1 Experiment setup

We conduct intensive numerical experiments to demonstrate the efficacy of OPAL.¹ We use the GPT-4 turbo gpt-4-1106-preview (<https://platform.openai.com/docs/models/gpt-4-turbo-and-gpt-4>) for synthetic data generation. We give more details on the prompt we use in Appendix E.1. We consider three datasets, Diabetes, HeartFailure, and Gender, all with binary classification tasks Sigillito (2014); hea (2020); Issadeen (2020). We apply three classifiers, logistic regression, CatBoost Prokhorenkova et al. (2018), and random forest Breiman (2001), where the tuning parameters are selected by three-fold cross-validation. Due to the token size limit, to ensure that all the data can be fed into GPT-4, we randomly sample a small size, i.e., 100, 50, and 50, of data points from each of the three datasets as the raw data. We then sample 20 data points from the raw data to serve as the seed data to feed into GPT-4. We further randomly sample another 200, 100, and 1000 data points as the test data. The dataset information is summarized in Table 1. Following Buda et al. (2018), we create imbalanced data and introduce spurious correlation by deliberately constructing disparities in the raw data. These imbalances manifest as uneven distributions in labels for classification tasks, and in label-attribute pairs for spurious correlations. The imbalanced ratio, i.e., the ratio of the number of majority samples to that of the minority samples, is set as 9 : 1, 4 : 1, and 4 : 1 for the three datasets. To assess the impact of synthetic data, we first train the model using all the raw data. Then, we gradually augment the training set with synthetic samples in subsequent steps. We follow a sequence of synthetic-to-raw data ratios: {0%, 20%, 40%, 60%, 80%, 100%}. For instance, if the raw data size is 50 and the syn/raw = 80%, we add 40 synthetic samples to the raw data.

We compare OPAL with two benchmark alternative solutions: the duplication method Loyola-González et al. (2016), and the synthetic-minority oversampling technique (Chawla et al., 2002, SMOTE). The former randomly picks samples from the minority group to add to the raw data. The latter generates the synthetic samples through linear interpolation between a minority class sample and its nearest neighbors within the same class, and we

¹The code is available at github.

Table 1: Summary of datasets used in numerical experiments.

Dataset	Total Size	# Features	Target	Task	Source	Raw	Test	Remain
Diabetes	768	8	indicator of diabetes	classification	OpenML	100	200	468
HeartFailure	299	12	death event	classification	UCI ML	50	100	149
Gender	5001	7	gender	classification	Kaggle	50	1000	3551

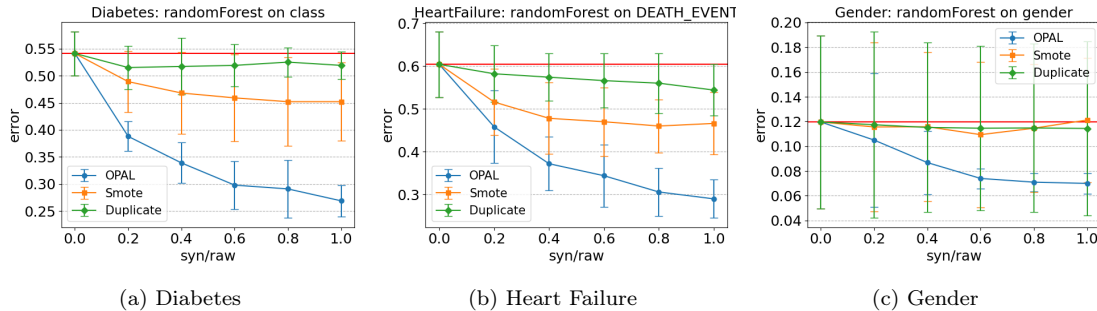


Figure 2: Imbalanced classification: comparison of OPAL, SMOTE, and duplication, with three datasets, Diabetes, Heart Failure, Gender, and the random forest classifier. The red line represents the mean error of the classifier trained with the raw data.

use the default value of 5 neighbors as in the *imblearn* package Lemaître et al. (2017) in our implementation.

We next conduct the experiments for the imbalanced classification and spurious correlations. We also conduct ablation studies and report the results in Appendix E.3.

4.2 Imbalanced classification

For imbalanced classification, we designate the samples with label 1 as the majority group, and those with label 0 as the minority group. When generating the synthetic data, we select a balanced subset of the raw data to serve as the seed data to feed into GPT-4. For instance, for the Diabetes dataset, the seed data consists of 10 samples from the majority group and 10 from the minority group.

Figure 2 reports the misclassification error rate in graphs based on 5 data replications with random forest. In Appendix E.4, Figure 5 and Figure 6 report the results with logistic regression and CatBoost, which show similar qualitative patterns. In addition, Table 4 reports the corresponding numeric results in tabular forms. We see that, our OPAL outperforms both duplication and SMOTE considerably across all datasets and classifiers, while the improvement increases as more synthetic data is added for the classifier training. For instance, OPAL outperforms SMOTE up to 18.4%, 17.5%, and 5.2% in Diabetes, HeartFailure, and Gender when $\text{syn/raw} = 1$. Meanwhile, our method also improves the standard error for HeartFailure and Gender data.

4.3 Spurious correlations

For spurious correlations, it involves imbalanced data in the pair (y, a) , where y represents the class label and a is the spurious attribute. The attribute a is considered spurious because its correlation with y in the training set may compromise fairness and under-represent the minority group. In our experiment, we artificially induce spurious correlations in the Diabetes, Heart Failure, and Gender datasets. For Diabetes, we select 'Triceps skin fold thickness' (`skin`) as the spurious attribute, paired with the binary diabetes indicator (`class`); that is, $(y, a) = (\text{class}, \text{skin})$. Here `skin` is positive if the thickness is measured and zero otherwise. The majority group in the raw data comprises samples with positive correlations between y and a : $\{\text{class} = 1, \text{skin} > 0\}$ and $\{\text{class} = 0, \text{skin} = 0\}$. The minority group includes samples with negative correlations between y and a : $\{\text{class} = 1, \text{skin} = 0\}$ and $\{\text{class} = 0, \text{skin} > 0\}$. For Heart Failure, the spurious pair (y, a) is $(\text{death event}, \text{sex})$, where the majority group exhibits a positive correlation between `death` and `sex`. In the

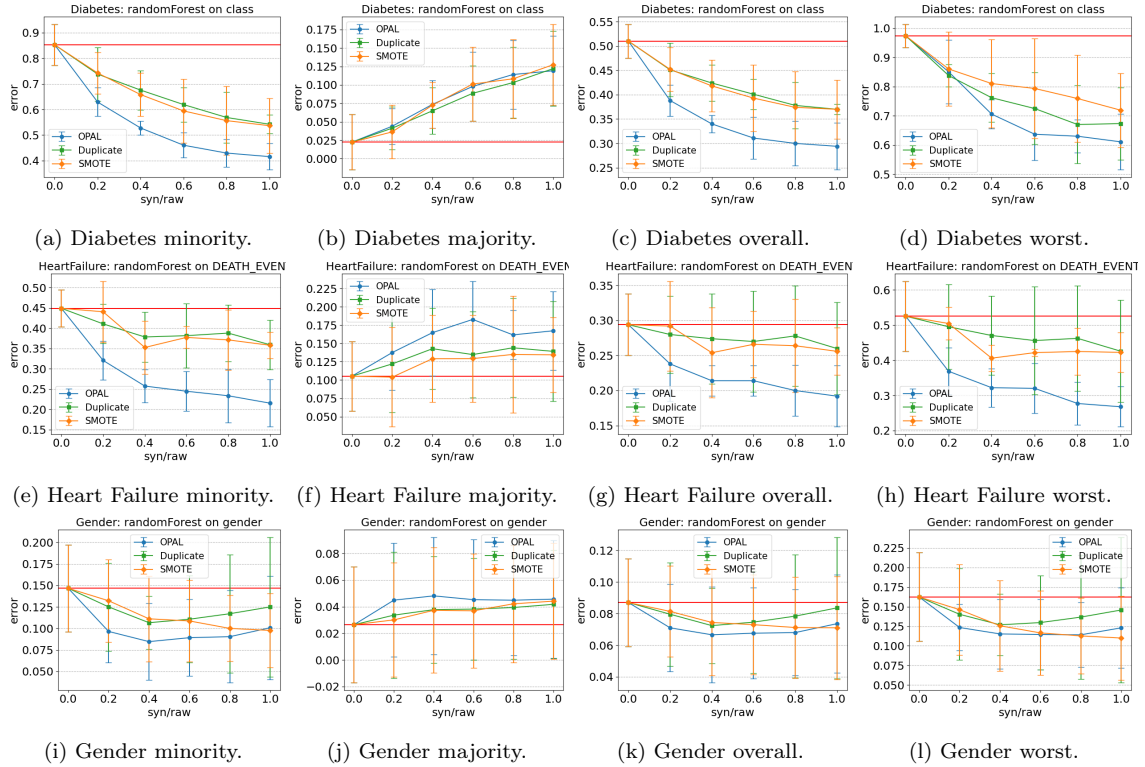


Figure 3: Spurious correlations: comparison of OPAL, SMOTE, and duplication, with three datasets, Diabetes, Heart Failure, Gender, and the random forest classifier. The red line represents the mean error of the classifier trained with the raw data.

Gender dataset, the spurious pair (y, a) is $(\text{gender}, \text{long hair})$, with **long hair** indicating whether an individual has long hair, again showing a positive correlation in the majority group. We choose these artificial correlations due to their implications in practice and their correlations in the datasets; see a more detailed discussion in Appendix E.2.

Figure 3 reports the misclassification error rate in graphs based on 5 data replications with random forest for four different groups: the minority group, the majority group, the overall group with all samples, and the worst group, respectively. More information about these four groups are given in Appendix E.2. In Appendix E.4, Figure 7 and Figure 8 report the results with logistic regression and CatBoost, which again show similar qualitative patterns. In addition, Table 5, Table 6 and Table 7 report the corresponding numeric results in tabular forms. We see that, our OPAL outperforms both duplication and SMOTE considerably in the minority, overall, and worst groups in all datasets. For instance, for the minority group of the HeartFailure data, OPAL reduces the misclassification error by 23.4% when $\text{syn/raw} = 1$, while duplication and SMOTE only decrease the error by 9.0% and 9.1%, respectively. For the majority group, we observe an increase in misclassification error across all oversampling methods. This trend arises because the oversampling approach downweights the role of the majority group during the training. By doing so, it inadvertently filters out some features that are particularly beneficial for accurate classification in the majority group, leading to an elevated error rate.

To further show our method can enhance fairness as well, we report the maximum absolute difference among all groups in Table 8 in Appendix E.4. We see that OPAL reduces the group-wise difference in accuracy across all datasets more effectively compared to the duplication and SMOTE.

5 Conclusions, Limitations, and Future Directions

In this article, we introduced OPAL, a systematic oversampling approach to address data imbalance by leveraging the generative capacity of large language models. We have provided a new theoretical framework to explicitly quantify the bias introduced by oversampling with the LLM-generated synthetic data, and to demonstrate that pre-trained language models can indeed generate high-quality data. Our empirical results have shown that our method outperforms traditional oversampling solutions such as duplication and SMOTE.

Meanwhile, there are some potential limitations with our method that leave room for further improvement. Theoretically, our theory requires a large token dimension, $O(r|\mathcal{M}|)$, because we use zeros in the input tokens as temporal memory to store computed results. Operationally, our implementation now hinges on GPT-4, which has a token limit, resulting in a small data scale, even though GPT-4 still demonstrates the great potential of our method with a very limited sample size.

There are several promising future directions. First, while the focus of this article has been on tabular data, our methodologies can be adapted to other data types, for instance, images. Second, we can further explore the transfer learning scenarios. In many real-world applications, obtaining labeled data is expensive and challenging, whereas there is often an abundance of unlabeled data. By generating synthetic labeled data for these unlabeled samples using LLMs, we expect to enhance the model performance in the target domain.

References

- (2020). Heart Failure Clinical Records. UCI Machine Learning Repository. DOI: <https://doi.org/10.24432/C5Z89R>.
- Akyürek, E., Schuurmans, D., Andreas, J., Ma, T., and Zhou, D. (2022). What learning algorithm is in-context learning? investigations with linear models. *arXiv preprint arXiv:2211.15661*.
- An, J., Ying, L., and Zhu, Y. (2020). Why resampling outperforms reweighting for correcting sampling bias with stochastic gradients. *arXiv preprint arXiv:2009.13447*.
- Arjovsky, M., Bottou, L., Gulrajani, I., and Lopez-Paz, D. (2019). Invariant risk minimization. *arXiv preprint arXiv:1907.02893*.
- Arora, S., Li, Y., Liang, Y., Ma, T., and Risteski, A. (2015). A latent variable model approach to pmi-based word embeddings. *arXiv preprint arXiv:1502.03520*.
- Arora, S., Liang, Y., and Ma, T. (2017). A simple but tough-to-beat baseline for sentence embeddings. In *International conference on learning representations*.
- Bai, Y., Chen, F., Wang, H., Xiong, C., and Mei, S. (2023). Transformers as statisticians: Provable in-context learning with in-context algorithm selection. *arXiv preprint arXiv:2306.04637*.
- Borisov, V., Seßler, K., Leemann, T., Pawelczyk, M., and Kasneci, G. (2023). Language models are realistic tabular data generators.
- Breiman, L. (2001). Random forests. *Machine learning*, 45:5–32.
- Buda, M., Maki, A., and Mazurowski, M. A. (2018). A systematic study of the class imbalance problem in convolutional neural networks. *Neural Networks*, 106:249–259.
- Bunkhumpornpat, C., Sinapiromsaran, K., and Lursinsap, C. (2009). Safe-level-smote: Safe-level-synthetic minority over-sampling technique for handling the class imbalanced problem. In *Advances in Knowledge Discovery and Data Mining: 13th Pacific-Asia Conference, PAKDD 2009 Bangkok, Thailand, April 27-30, 2009 Proceedings 13*, pages 475–482. Springer.
- Byrd, J. and Lipton, Z. (2019). What is the effect of importance weighting in deep learning? In *International conference on machine learning*, pages 872–881. PMLR.
- Chatterji, N. S., Haque, S., and Hashimoto, T. (2022). Undersampling is a minimax optimal robustness intervention in nonparametric classification. *arXiv preprint arXiv:2205.13094*.
- Chaudhuri, K., Ahuja, K., Arjovsky, M., and Lopez-Paz, D. (2023). Why does throwing away data improve worst-group error? In *International Conference on Machine Learning*, pages 4144–4188. PMLR.
- Chawla, N. V., Bowyer, K. W., Hall, L. O., and Kegelmeyer, W. P. (2002). Smote: Synthetic minority over-sampling technique. *Journal of Artificial Intelligence Research*, 16:321–357.
- Chawla, N. V., Japkowicz, N., and Kotcz, A. (2004). Special issue on learning from imbalanced data sets. *ACM SIGKDD explorations newsletter*, 6(1):1–6.

- Douzias, G. and Bacao, F. (2018). Effective data generation for imbalanced learning using conditional generative adversarial networks. *Expert Systems with applications*, 91:464–471.
- Douzias, G., Bacao, F., and Last, F. (2018). Improving imbalanced learning through a heuristic oversampling method based on k-means and smote. *Information sciences*, 465:1–20.
- Fernández, A., García, S., Galar, M., Prati, R. C., Krawczyk, B., and Herrera, F. (2018). *Learning from imbalanced data sets*, volume 10. Springer.
- Garg, S., Tsipras, D., Liang, P. S., and Valiant, G. (2022). What can transformers learn in-context? a case study of simple function classes. *Advances in Neural Information Processing Systems*, 35:30583–30598.
- Goodfellow, I., Pouget-Abadie, J., Mirza, M., Xu, B., Warde-Farley, D., Ozair, S., Courville, A., and Bengio, Y. (2014). Generative adversarial nets. *Advances in neural information processing systems*, 27.
- Gosain, A. and Sardana, S. (2017). Handling class imbalance problem using oversampling techniques: A review. In *2017 international conference on advances in computing, communications and informatics (ICACCI)*, pages 79–85. IEEE.
- Gulati, M. S. and Roysdon, P. F. (2023). Tabmt: Generating tabular data with masked transformers.
- Haixiang, G., Yijing, L., Shang, J., Mingyun, G., Yuanyue, H., and Bing, G. (2017). Learning from class-imbalanced data: Review of methods and applications. *Expert Systems with Applications*, 73:220–239.
- Han, H., Wang, W.-Y., and Mao, B.-H. (2005). Borderline-smote: a new over-sampling method in imbalanced data sets learning. In *International conference on intelligent computing*, pages 878–887. Springer.
- He, H., Bai, Y., Garcia, E. A., and Li, S. (2008). Adasyn: Adaptive synthetic sampling approach for imbalanced learning. In *2008 IEEE international joint conference on neural networks (IEEE world congress on computational intelligence)*, pages 1322–1328. Ieee.
- Huang, D., Wang, F., Rubin, D. B., and Kou, S. (2022). Catalytic priors: Using synthetic data to specify prior distributions in bayesian analysis. *arXiv preprint arXiv:2208.14123*.
- Issadeen, J. (2020). gender. Accessed: 2023-12-21.
- Jain, A., Montanari, A., and Sasoglu, E. (2024). Scaling laws for learning with real and surrogate data. *arXiv preprint arXiv:2402.04376*.
- Jo, W. and Kim, D. (2022). Obgan: Minority oversampling near borderline with generative adversarial networks. *Expert Systems with Applications*, 197:116694.
- Johnson, J. M. and Khoshgoftaar, T. M. (2019). Survey on deep learning with class imbalance. *Journal of Big Data*, 6(1):1–54.
- Khalife, S., Gonçalves, D., Allouah, Y., and Liberti, L. (2021). Further results on latent discourse models and word embeddings. *Journal of Machine Learning Research*, 22(270):1–36.

- Krawczyk, B. (2016). Learning from imbalanced data: open challenges and future directions. *Progress in Artificial Intelligence*, 5(4):221–232.
- Laurent, B. and Massart, P. (2000). Adaptive estimation of a quadratic functional by model selection. *Annals of statistics*, pages 1302–1338.
- Lemaître, G., Nogueira, F., and Aridas, C. K. (2017). Imbalanced-learn: A python toolbox to tackle the curse of imbalanced datasets in machine learning. *Journal of Machine Learning Research*.
- Li, R., Zhao, X., and Moens, M.-F. (2022). A brief overview of universal sentence representation methods: A linguistic view. *ACM Computing Surveys (CSUR)*, 55(3):1–42.
- Loyola-González, O., Martínez-Trinidad, J. F., Carrasco-Ochoa, J. A., and García-Borroto, M. (2016). Study of the impact of resampling methods for contrast pattern based classifiers in imbalanced databases. *Neurocomputing*, 175:935–947.
- Mnih, A. and Hinton, G. (2007). Three new graphical models for statistical language modelling. In *Proceedings of the 24th international conference on Machine learning*, pages 641–648.
- Oh, J.-H., Hong, J. Y., and Baek, J.-G. (2019). Oversampling method using outlier detectable generative adversarial network. *Expert Systems with Applications*, 133:1–8.
- Prokhorenkova, L., Gusev, G., Vorobev, A., Dorogush, A. V., and Gulin, A. (2018). Catboost: unbiased boosting with categorical features. *Advances in neural information processing systems*, 31.
- Sagawa, S., Koh, P. W., Hashimoto, T. B., and Liang, P. (2019). Distributionally robust neural networks for group shifts: On the importance of regularization for worst-case generalization. *arXiv preprint arXiv:1911.08731*.
- Sagawa, S., Raghunathan, A., Koh, P. W., and Liang, P. (2020). An investigation of why overparameterization exacerbates spurious correlations. In *International Conference on Machine Learning*, pages 8346–8356. PMLR.
- Seedat, N., Huynh, N., van Breugel, B., and van der Schaar, M. (2024). Curated llm: Synergy of llms and data curation for tabular augmentation in ultra low-data regimes.
- Shi, B., Lam, W., Jameel, S., Schockaert, S., and Lai, K. P. (2017). Jointly learning word embeddings and latent topics. In *Proceedings of the 40th international ACM SIGIR conference on research and development in information retrieval*, pages 375–384.
- Shimodaira, H. (2000). Improving predictive inference under covariate shift by weighting the log-likelihood function. *Journal of statistical planning and inference*, 90(2):227–244.
- Sigillito, V. (2014). diabetes. Accessed: 2023-12-01.
- Solatorio, A. V. and Dupriez, O. (2023). Realtabformer: Generating realistic relational and tabular data using transformers.
- Van der Vaart, A. W. (2000). *Asymptotic statistics*, volume 3. Cambridge university press.
- Viloria, A., Lezama, O. B. P., and Mercado-Caruzo, N. (2020). Unbalanced data processing using oversampling: machine learning. *Procedia Computer Science*, 175:108–113.

- Von Oswald, J., Niklasson, E., Randazzo, E., Sacramento, J., Mordvintsev, A., Zhmoginov, A., and Vladymyrov, M. (2023). Transformers learn in-context by gradient descent. In *International Conference on Machine Learning*, pages 35151–35174. PMLR.
- Xie, S. M., Raghunathan, A., Liang, P., and Ma, T. (2021). An explanation of in-context learning as implicit bayesian inference. *arXiv preprint arXiv:2111.02080*.
- Xu, L., Skoularidou, M., Cuesta-Infante, A., and Veeramachaneni, K. (2019). Modeling tabular data using conditional gan. In *Advances in Neural Information Processing Systems*.
- Ye, H., Zou, J., and Zhang, L. (2023). Freeze then train: Towards provable representation learning under spurious correlations and feature noise. In *International Conference on Artificial Intelligence and Statistics*, pages 8968–8990. PMLR.
- Ye, W., Zheng, G., Cao, X., Ma, Y., Hu, X., and Zhang, A. (2024). Spurious correlations in machine learning: A survey. *arXiv preprint arXiv:2402.12715*.
- Zhang, R., Frei, S., and Bartlett, P. L. (2023a). Trained transformers learn linear models in-context. *arXiv preprint arXiv:2306.09927*.
- Zhang, T., Wang, S., Yan, S., Li, J., and Liu, Q. (2023b). Generative table pre-training empowers models for tabular prediction. *arXiv preprint arXiv:2305.09696*.
- Zhao, Z., Birke, R., and Chen, L. (2023). Tabula: Harnessing language models for tabular data synthesis.

A More Details for Theoretical Analysis

In this section, we provide more details regarding the theoretical analysis in Section 3.

A.1 Notations

For two sequences of positive numbers $(a_k)_k$ and $(b_k)_k$ indexed by $k \in \mathcal{K}$, we write $a_k \lesssim b_k$ if and only if there exists a constant $C > 0$ independent of the index k such that $\sup_{k \in \mathcal{K}} a_k/b_k < C$ holds. For any matrix A , let $\|A\|$ and $\|A\|_F$ denote the operator norm and Frobenius norm of A , respectively. $\mathcal{O}_{d,r} \triangleq \{O \in \mathbb{R}^{r \times d} : O^\top O = I_r\}$ is a set of orthogonal matrices of order $d \times r$. For any positive integer I , let $[I] = \{1, 2, \dots, I\}$. We write $a \vee b$ and $a \wedge b$ to denote $\max(a, b)$ and $\min(a, b)$, respectively. When the right singular vectors are not unique, we choose arbitrary singular vectors. For any matrix A , let $\lambda_{\min}(A)$ be the minimum singular value of A . For a vector $\mathbf{a} = (a_1, \dots, a_D)^\top \in \mathbb{R}^D$, we write $(\mathbf{a})_i = a_i$, $(\mathbf{a})_{n_1:n_2} = (a_{n_1+1}, a_{n_1+2}, \dots, a_{n_2})^\top \in \mathbb{R}^{n_2-n_1}$. For a matrix $A = [\mathbf{a}_1; \dots; \mathbf{a}_D]$, we write $(A)_i = \mathbf{a}_i$. Denote a ball in \mathbb{R}^D with radius $R > 0$ centered at $\mathbf{0}_D$ by $\mathbb{B}_D(R)$. For a finite set A , let $\text{conv}(A)$ be the convex hull of A . Hereafter we call an event \mathcal{E} occurs with high probability when $\mathbb{P}(\mathcal{E}) = 1 - \exp(-\Omega(\log^2 d))$.

A.2 Data generating process

As assumed in the literature on word representations Arora et al. (2015), we consider a Bayesian setting for the token embeddings; $\mathbf{u}_1, \dots, \mathbf{u}_d \in \mathbb{R}^r$ are modeled as i.i.d. realizations of $N(0, (1/r)I_r)$. Let $U = [\mathbf{u}_1, \dots, \mathbf{u}_d]^\top$. We assume that X_i and Y_i take values in a finite set $\mathcal{X} = [d]$. This assumption reflects the fact that tabular data is treated as a collection of finite tokens for language models. We define a ‘‘subject’’ as any background information that provides context for each tabular data. For example, data on heart failure rates is specified by the subject ‘‘heart failure’’.

We then formally introduce data generating process for tabular data: generative models for covariates and discriminative models for labels. More specifically, $(X_i, Y_i) \in \mathcal{X}^2$ given subject $T = t$ and discriminative function index $M = m$ follows multinomial distribution defined by:

$$\begin{aligned} \mathbb{P}(X_i = x; T = t, U, \eta) &\propto \exp\left(\eta^{-1} \langle \mathbf{z}^{(t)}, \mathbf{u}_x \rangle\right), \\ \mathbb{P}(Y_i = y | X_i = x; M = m, U, \eta) &\propto \exp\left(\eta^{-1} \langle f^{(m)}(\mathbf{u}_x), \mathbf{u}_y \rangle\right), \end{aligned} \quad (4)$$

where $t \in \mathcal{T}$, $m \in \mathcal{M}$ are possible indices of subjects and discriminative function indices, $\eta > 0$ is a parameter, $\mathbf{u}_x \in \mathbb{R}^r$ is the embedding of the token $x \in \mathcal{X}$, $\mathbf{z}^{(t)} \in \mathbb{R}^r$ is the representation of subject t , and $f^{(m)} : \mathbb{R}^r \rightarrow \mathbb{R}^r$ is a discriminative function with index m . We consider the case where $|\mathcal{M}| \geq |\mathcal{T}|$ for simplicity. A similar model has been proposed and used in language modeling literature Mnih and Hinton (2007); Arora et al. (2015, 2017); Shi et al. (2017); Khalife et al. (2021).

We assume that \mathcal{T} and \mathcal{M} are finite. We allow η to vary on the interval $[(1/\sqrt{r}) \log d, \infty)$, while assume $\|\mathbf{z}^{(t)}\| = 1$ for any $t \in \mathcal{T}$ and $\sup_{\mathbf{u} \in \mathbb{B}_r(\log d)} \|f^{(m)}(\mathbf{u})\| \leq 1$ for identifiability. The lower bound $(1/\sqrt{r}) \log d$ of η is due to the limitation of our theory; when η is too small, we cannot derive the concentration for the normalizing constant of $\mathbb{P}(X_i = x; T = t, U, \eta)$.

Denote the joint distribution of X_1 and Y_1 by $P_{X_1, Y_1; T=t, M=m, U, \eta}$ and (conditional) distributions of X_1 and $Y_1 | X_1$ under model 4 by $P_{X_1; T=t, U, \eta}$ and $P_{Y_1 | X_1; M=m, U, \eta}$, respectively.

We remark that, the probability mass of X_i given Z has mode at $\arg \max_{x \in \mathcal{X}} Z^\top \mathbf{u}_x$. This implies that tokens similar to the subject embedding are likely to be generated. If η is

sufficiently large, the distribution of X given Z becomes closer to uniform distribution on \mathcal{X} almost independent of Z . Henceforth, the parameter η is responsible for the observation error of X and Y .

Finite known candidates of subject embeddings and functions Based on the intuition that transformers are pre-trained on vast amount of data, we further assume that the transformer knows the candidate of subject embeddings $\{\mathbf{z}^{(t)}\}_{t \in \mathcal{T}}$ and candidate of functions $\{f^{(m)}\}_{m \in \mathcal{M}} \subset \mathcal{F}(L_0, r_0) \subset \{\text{FFN}_{\nu_{\text{pre}, L_0}} \circ \text{FFN}_{\nu_{\text{pre}, L_0-1}} \circ \dots \circ \text{FFN}_{\nu_{\text{pre}, 1}} : \nu_{\text{pre}, \ell} \in \mathbb{R}^{r_0 \times r} \times \mathbb{R}^{r \times r_0} \text{ for } \ell \in [L_0]\}$ with $L_0, r_0 \in \mathbb{N}^+$.

A.3 Details of transformers

Input tokens for tabular data We assume that tokens $(\mathbf{h}_i^Y)_{i \in [n]}$ corresponds to $(Y_i)_{i \in [n]}$ and $(\mathbf{h}_i^X)_{i \in [n]}$ corresponds to $(X_i)_{i \in [n]}$. The input of the transformer is given by

$$H_n = [\mathbf{h}_1^X; \mathbf{h}_1^Y; \mathbf{h}_2^X; \mathbf{h}_2^Y; \dots; \mathbf{h}_n^X; \mathbf{h}_n^Y]. \quad (5)$$

We consider the composite type positional encoding, that is, the forms of \mathbf{h}_i^X and \mathbf{h}_i^Y are given by $\mathbf{h}_i^X = (\mathbf{u}_{X_i}^\top, \mathbf{0}^\top, \mathbf{p}_{2i-1, n}^\top)^\top$ and $\mathbf{h}_i^Y = (\mathbf{u}_{X_i}^\top, \mathbf{0}^\top, \mathbf{p}_{2i, n}^\top)^\top$, respectively. Note that this differs from practical additive positional encoding. Specifically for $i \in [n]$, the positional encoding $\mathbf{p}_{s, n} \in \mathbb{R}^4$ is defined as

$$\mathbf{p}_{s, n} = (\lceil s/2 \rceil, (s \bmod 2), 2n, 1)^\top,$$

where the first coordinate specifies the index of the current token, and the second coordinate indicates whether the current token corresponds to X_i or Y_i . The third coordinate takes the length of the given tokens. The last coordinate is a constant added for technical convenience.

Output distribution Given the initial input tokens $H_n \in \mathbb{R}^{D \times 2n}$ in equation 5, a transformer parameterized by Ψ sequentially outputs $\mathbf{h}_{2n+1}, \mathbf{h}_{2n+2}, \dots$ corresponding to synthetic data from categorical distribution given last output from the transformer layers. At each step $\ell \in \mathbb{N}^+$, given all previous tokens H_n and $\mathbf{h}_{2n+1}, \mathbf{h}_{2n+2}, \dots, \mathbf{h}_{2n+\ell-1}$, the next token $\mathbf{h}_{2n+\ell}$ is given by $\mathbf{h}_{2n+\ell} = (\mathbf{v}_{2n+\ell}^\top, \mathbf{0}^\top, \mathbf{p}_{2n+\ell, n}^\top)^\top$, where $\mathbf{v}_{2n+\ell} \in \mathbb{R}^r$ is drawn from a categorical distribution with softmax probability over all possible tokens $\mathbf{u}_1, \dots, \mathbf{u}_d \in \mathbb{R}^r$:

$$\mathbb{P}(\mathbf{v}_{2n+\ell} = \mathbf{u}_x) \propto \exp\left(\tau^{-1} \langle \mathbf{u}_x, (\tilde{\mathbf{h}}_{2n+\ell-1})_{1:r} \rangle\right), \quad (6)$$

where $\tilde{\mathbf{h}}_{2n+\ell-1} := (\text{TF}_\Psi([H_n, \mathbf{h}_{2n+1}, \mathbf{h}_{2n+2}, \dots, \mathbf{h}_{2n+\ell-1}]))_{2n+\ell-1}$ and $\tau > 0$ is the temperature parameter. Since we expect the outputs $\mathbf{h}_{2n+1}, \mathbf{h}_{2n+2}, \mathbf{h}_{2n+3}, \mathbf{h}_{2n+4}, \dots$ from a transformer TF_Ψ correspond to $\tilde{X}_1, \tilde{Y}_1, \tilde{X}_2, \tilde{Y}_2, \dots$, we write the joint distribution of $\mathbf{v}_{2n+2s-1}$ and \mathbf{v}_{2n+2s} as

$$Q_{\tilde{X}_s, \tilde{Y}_s; \Psi, \tau, \mathcal{D}_n}(x, y) := \mathbb{P}(\mathbf{v}_{2n+2s-1} = \mathbf{u}_x, \mathbf{v}_{2n+2s} = \mathbf{u}_y).$$

We similarly denote the marginal and conditional distributions of \tilde{X}_s and $\tilde{Y}_s | \tilde{X}_s$ by $Q_{\tilde{X}_s; \Psi, \tau, \mathcal{D}_n}(x)$ and $Q_{\tilde{Y}_s | \tilde{X}_s; \Psi, \tau, \mathcal{D}_n}(y)$. Table 2 shows the overview of the input and output tokens sequentially input to transformers.

	Input							Output			
Index s	1	2	3	4	\dots	$2n-1$	$2n$	\dots	$2n+2s-1$	$2n+2s$	\dots
Token	\mathbf{h}_1^X	\mathbf{h}_1^Y	\mathbf{h}_2^X	\mathbf{h}_2^Y	\dots	\mathbf{h}_n^X	\mathbf{h}_n^Y	\dots	$\mathbf{h}_{2n+2s-1}$	\mathbf{h}_{2n+2s}	\dots
Datum	X_1	Y_1	X_2	Y_2	\dots	X_n	Y_n	\dots	\tilde{X}_s	\tilde{Y}_s	\dots
$(\mathbf{p}_{s,n})_1$	1	1	2	2	\dots	n	n	\dots	$n+s$	$n+s$	\dots
$(\mathbf{p}_{s,n})_2$	0	1	0	1	\dots	0	1	\dots	0	1	\dots

Table 2: An overview of the input and output tokens.

B Proofs for Section 3.1

In this section, we restate the theoretical results for oversampling in Section 3.1 in a more rigorous way, then provide the detailed proofs.

B.1 General theory for oversampling

We first see how oversampling improves the performance on minority group in general. Let n_g be the number of raw samples observed for group $g \in \mathcal{G}$. For each group g , we generate m_g synthetic data m_g . Denote $n_{\text{total}} := \sum_g n_g$ and $m_{\text{total}} := \sum_g m_g$ by the total number of raw data and the total number of synthetic data, respectively.

Denote the observed raw data as $\{(\mathbf{x}_1, \dots, \mathbf{x}_{n_g})\}_{g \in \mathcal{G}}$ and generated synthetic data as $\{(\tilde{\mathbf{x}}_1, \dots, \tilde{\mathbf{x}}_{m_g})\}_{g \in \mathcal{G}}$. We assume the independence between raw data and synthetic data. When directly using raw data as a reference to synthetic data, the independence does not hold. However, we can always split the raw data, with one half used as raw data, and the other half used as a reference. Given a loss function $\ell(\boldsymbol{\theta}; x, y) \in \mathbb{R}$ we define the empirical risk with raw and synthetic data as follows

$$\widehat{\mathcal{R}}_{\text{syn}}(\boldsymbol{\theta}) = \frac{1}{n_{\text{total}} + m_{\text{total}}} \sum_{g \in \mathcal{G}} \sum_{i \in [n_g]} \ell(\boldsymbol{\theta}; \mathbf{x}_i^{(g)}, y_i^{(g)}) + \frac{1}{n_{\text{total}} + m_{\text{total}}} \sum_{g \in \mathcal{G}} \sum_{i \in [m_g]} \ell(\boldsymbol{\theta}; \tilde{\mathbf{x}}_i^{(g)}, \tilde{y}_i^{(g)}).$$

Let $\mathcal{R}_{\text{syn}}(\boldsymbol{\theta}) = \mathbb{E}[\widehat{\mathcal{R}}_{\text{syn}}(\boldsymbol{\theta})]$ be the population version of $\widehat{\mathcal{R}}_{\text{syn}}$. We also define the balanced risk

$$\mathcal{R}_{\text{bal}}(\boldsymbol{\theta}) = \frac{1}{|\mathcal{G}|} \sum_{g \in \mathcal{G}} \mathcal{R}_g(\boldsymbol{\theta}),$$

where $\mathcal{R}_g(\boldsymbol{\theta}) = \mathbb{E}[\ell(\boldsymbol{\theta}; \mathbf{x}_1^{(g)}, y_1^{(g)})]$ is the group specific risk. Let the minimizers of $\widehat{\mathcal{R}}_{\text{syn}}$, \mathcal{R}_{syn} , and \mathcal{R}_{bal} be $\widehat{\boldsymbol{\theta}}_{\text{syn}}$, $\boldsymbol{\theta}_{\text{syn}}$, $\boldsymbol{\theta}_{\text{bal}}$ respectively. Define the bias term for group g as

$$\mathcal{B}_g(\boldsymbol{\theta}) := \mathbb{E}[\ell(\boldsymbol{\theta}; \tilde{\mathbf{x}}_1^{(g)}, \tilde{y}_1^{(g)})] - \mathbb{E}[\ell(\boldsymbol{\theta}; \mathbf{x}_1^{(g)}, y_1^{(g)})].$$

Note that $\boldsymbol{\theta}_{\text{bal}}$ is the ideal estimator, balancing out the parameters over all groups present in the dataset.

Our goal is to see the effect of bias present in the synthetic data to the estimator $\widehat{\boldsymbol{\theta}}_{\text{syn}}$ by measuring the risk of group g :

$$\mathcal{R}_g(\widehat{\boldsymbol{\theta}}_{\text{syn}}) - \mathcal{R}_g(\boldsymbol{\theta}_{\text{bal}}).$$

Here we formally introduce standard assumptions that are commonly used in asymptotic theory Van der Vaart (2000).

Assumption B.1. Assume that $\sup_{\boldsymbol{\theta} \in \Theta} |\mathcal{B}_g(\boldsymbol{\theta})| \vee \|\nabla \mathcal{B}_g(\boldsymbol{\theta})\| = o(1)$ for all $g \in \mathcal{G}$.

Assumption B.2. Assume that

$$\sup_{\boldsymbol{\theta} \in \Theta} |\widehat{\mathcal{R}}_{\text{syn}}(\boldsymbol{\theta}) - \mathcal{R}_{\text{syn}}(\boldsymbol{\theta})| = o_p(1),$$

Assumption B.3 (Identifiability of $\boldsymbol{\theta}_{\text{syn}}$). Assume that

$$\inf_{\boldsymbol{\theta}: \|\boldsymbol{\theta} - \boldsymbol{\theta}_{\text{syn}}\| \geq \epsilon} \mathcal{R}_{\text{syn}}(\boldsymbol{\theta}) > \mathcal{R}_{\text{syn}}(\boldsymbol{\theta}_{\text{syn}})$$

and

$$\inf_{\boldsymbol{\theta}: \|\boldsymbol{\theta} - \boldsymbol{\theta}_{\text{bal}}\| \geq \epsilon} \mathcal{R}_{\text{bal}}(\boldsymbol{\theta}) > \mathcal{R}_{\text{bal}}(\boldsymbol{\theta}_{\text{bal}}).$$

Assumption B.4. \mathcal{B}_g and \mathcal{R}_g are twice differentiable around $\boldsymbol{\theta}_{\text{bal}}$ with bounded Lipschitz Hessian, and $\sum_g \nabla^2 \mathcal{R}_g(\boldsymbol{\theta})$ is strictly positive definite around $\boldsymbol{\theta}_{\text{bal}}$.

Assumption B.5. Assume that $\ell(\boldsymbol{\theta}; \mathbf{x}, y)$ and $\ell(\boldsymbol{\theta}; \tilde{\mathbf{x}}, \tilde{y})$ are differentiable around $\boldsymbol{\theta}_{\text{bal}}$ almost surely under the distributions for raw data (\mathbf{x}, y) and synthetic data $(\tilde{\mathbf{x}}, \tilde{y})$. Also assume that Σ_g and $\tilde{\Sigma}_g$ are Lipschitz around $\boldsymbol{\theta}_{\text{bal}}$, and $\sup_{\boldsymbol{\theta} \in \Theta} \|\Sigma_g(\boldsymbol{\theta}) - \tilde{\Sigma}_g(\boldsymbol{\theta})\| = o(1)$.

Denote the covariance matrices of gradients for each group $g \in \mathcal{G}$ by

$$\begin{aligned} \Sigma_g(\boldsymbol{\theta}) &= \mathbb{E} \left[\left(\nabla \ell(\boldsymbol{\theta}; \mathbf{x}_1^{(g)}, y_1^{(g)}) \right) \left(\nabla \ell(\boldsymbol{\theta}; \mathbf{x}_1^{(g)}, y_1^{(g)}) \right)^\top \right], \\ \tilde{\Sigma}_g(\boldsymbol{\theta}) &= \mathbb{E} \left[\left(\nabla \ell(\boldsymbol{\theta}; \tilde{\mathbf{x}}_1^{(g)}, \tilde{y}_1^{(g)}) \right) \left(\nabla \ell(\boldsymbol{\theta}; \tilde{\mathbf{x}}_1^{(g)}, \tilde{y}_1^{(g)}) \right)^\top \right]. \end{aligned}$$

Theorem B.1 (Restatement of Theorem 3.1). *Under Assumptions B.1-B.5, for any $g \in \mathcal{G}$,*

$$\begin{aligned} \mathcal{R}_g(\widehat{\boldsymbol{\theta}}_{\text{syn}}) &= \mathcal{R}_g(\boldsymbol{\theta}_{\text{bal}}) - \sum_{g' \in \mathcal{G}} \frac{m_{g'}}{n_{\text{total}} + m_{\text{total}}} b_{g,g'} \\ &\quad + O_p \left(\frac{1}{\sqrt{n_{\text{total}} + m_{\text{total}}}} v_g + \frac{1}{m_{\text{total}} \wedge n_{\text{total}}} + \left\| \sum_{g' \in \mathcal{G}} \frac{m_{g'}}{n_{\text{total}} + m_{\text{total}}} \nabla \mathcal{B}_{g'}(\boldsymbol{\theta}_{\text{bal}}) \right\|^2 \right), \end{aligned}$$

where v_g and $b_{g,g'}$ are defined as

$$v_g^2 := \{ \nabla \mathcal{R}_g(\boldsymbol{\theta}_{\text{bal}}) \}^\top \{ \nabla^2 \mathcal{R}_{\text{bal}}(\boldsymbol{\theta}_{\text{bal}}) \}^{-1} \left(\frac{1}{G} \sum_{g' \in \mathcal{G}} \Sigma_{g'}(\boldsymbol{\theta}_{\text{bal}}) \right) \{ \nabla^2 \mathcal{R}_{\text{bal}}(\boldsymbol{\theta}_{\text{bal}}) \}^{-1} \nabla \mathcal{R}_g(\boldsymbol{\theta}_{\text{bal}}), \quad (7)$$

$$b_{g,g'} := \{ \nabla \mathcal{R}_g(\boldsymbol{\theta}_{\text{bal}}) \}^\top \{ \nabla^2 \mathcal{R}_{\text{bal}}(\boldsymbol{\theta}_{\text{bal}}) \}^{-1} \nabla \mathcal{B}_{g'}(\boldsymbol{\theta}_{\text{bal}}). \quad (8)$$

Proof of Theorem B.1. To ease notation we define $H_{\text{syn}} = \nabla^2 \mathcal{R}_{\text{syn}}(\boldsymbol{\theta}_{\text{syn}})$ and $H_{\text{bal}} = \nabla^2 \mathcal{R}_{\text{bal}}(\boldsymbol{\theta}_{\text{bal}})$. We note that

$$\mathcal{R}_{\text{syn}}(\boldsymbol{\theta}) = \mathcal{R}_{\text{bal}}(\boldsymbol{\theta}) + \sum_{g \in \mathcal{G}} \frac{m_g}{n_{\text{total}} + m_{\text{total}}} \mathcal{B}_g(\boldsymbol{\theta}). \quad (9)$$

We divide the proof into two parts. In the first part we derive the bias between $\boldsymbol{\theta}_{\text{bal}}$ and $\boldsymbol{\theta}_{\text{syn}}$. In the second part we show the convergence of $\widehat{\boldsymbol{\theta}}_{\text{syn}}$ to $\boldsymbol{\theta}_{\text{syn}}$.

Part 1. Note that $\sup_{\boldsymbol{\theta}} |\mathcal{R}_{\text{syn}}(\boldsymbol{\theta}) - \mathcal{R}_{\text{bal}}(\boldsymbol{\theta})| = o_p(1)$ follows from Assumption B.1 and equation 9. Then, the convergence $\|\boldsymbol{\theta}_{\text{syn}} - \boldsymbol{\theta}_{\text{bal}}\| = o(1)$ follows by a standard Taylor expansion argument, using Assumption B.3. (See, for example, Theorem 5.7 of Van der Vaart (2000).) From equation 9, we obtain

$$\nabla \mathcal{R}_{\text{syn}}(\boldsymbol{\theta}_{\text{bal}}) = \sum_{g' \in \mathcal{G}} \nabla \mathcal{R}_{g'}(\boldsymbol{\theta}_{\text{bal}}) + \sum_{g' \in \mathcal{G}} \frac{m_{g'}}{n_{\text{total}} + m_{\text{total}}} \nabla \mathcal{B}_{g'}(\boldsymbol{\theta}_{\text{bal}}) \quad (10)$$

$$= \sum_{g' \in \mathcal{G}} \frac{m_{g'}}{n_{\text{total}} + m_{\text{total}}} \nabla \mathcal{B}_{g'}(\boldsymbol{\theta}_{\text{bal}}), \quad (11)$$

where we used $\sum_{g'} \nabla \mathcal{R}_{g'}(\boldsymbol{\theta}_{\text{bal}}) = 0$. By Taylor expansion, there exists some $\boldsymbol{\theta}'$ in a line segment between $\boldsymbol{\theta}_{\text{bal}}$ and $\boldsymbol{\theta}_{\text{syn}}$ such that

$$\nabla \mathcal{R}_{\text{syn}}(\boldsymbol{\theta}_{\text{bal}}) = \underbrace{\nabla \mathcal{R}_{\text{syn}}(\boldsymbol{\theta}_{\text{syn}})}_{=0} + \nabla^2 \mathcal{R}_{\text{syn}}(\boldsymbol{\theta}')(\boldsymbol{\theta}_{\text{bal}} - \boldsymbol{\theta}_{\text{syn}}). \quad (12)$$

This yields

$$\{\nabla \mathcal{R}_{\text{syn}}(\boldsymbol{\theta}_{\text{bal}})\}^\top (\boldsymbol{\theta}_{\text{bal}} - \boldsymbol{\theta}_{\text{syn}}) = (\boldsymbol{\theta}_{\text{bal}} - \boldsymbol{\theta}_{\text{syn}})^\top \nabla^2 \mathcal{R}_{\text{syn}}(\boldsymbol{\theta}')(\boldsymbol{\theta}_{\text{bal}} - \boldsymbol{\theta}_{\text{syn}}).$$

Since $\|\boldsymbol{\theta}_{\text{bal}} - \boldsymbol{\theta}_{\text{syn}}\| = o(1)$, and $\nabla^2 \mathcal{R}_{\text{syn}}(\boldsymbol{\theta})$ is Lipschitz continuous around $\boldsymbol{\theta}_{\text{bal}}$ with its smallest eigenvalue bounded below, we have

$$\begin{aligned} \|\boldsymbol{\theta}_{\text{bal}} - \boldsymbol{\theta}_{\text{syn}}\| &\leq \frac{1}{\lambda_{\min}(\nabla^2 \mathcal{R}_{\text{syn}}(\boldsymbol{\theta}_{\text{bal}})) + o(1)} \|\nabla \mathcal{R}_{\text{syn}}(\boldsymbol{\theta}_{\text{bal}})\| \\ &\lesssim \|\nabla \mathcal{R}_{\text{syn}}(\boldsymbol{\theta}_{\text{bal}})\|. \end{aligned}$$

Using equation 11 and equation 12, we have

$$\begin{aligned} \boldsymbol{\theta}_{\text{bal}} - \boldsymbol{\theta}_{\text{syn}} &= \{\nabla^2 \mathcal{R}_{\text{syn}}(\boldsymbol{\theta}')\}^{-1} \nabla \mathcal{R}_{\text{syn}}(\boldsymbol{\theta}_{\text{bal}}) \\ &= H_{\text{syn}}^{-1} \nabla \mathcal{R}_{\text{syn}}(\boldsymbol{\theta}_{\text{bal}}) + R_1 \\ &= \sum_{g' \in \mathcal{G}} \frac{m_{g'}}{n_{\text{total}} + m_{\text{total}}} H_{\text{syn}}^{-1} \nabla \mathcal{B}_{g'}(\boldsymbol{\theta}_{\text{bal}}) + R_1, \end{aligned}$$

where $\|R_1\| = O(\|\nabla \mathcal{R}_{\text{syn}}(\boldsymbol{\theta}_{\text{bal}})\|^2)$.

Part 2. The consistency $\|\widehat{\boldsymbol{\theta}}_{\text{syn}} - \boldsymbol{\theta}_{\text{syn}}\| = o_p(1)$ follows by a standard argument of M -estimators combined with Assumptions B.2 and B.3. (Theorem 5.7 in Van der Vaart (2000).) We follow the argument in the proof of Proposition 3.1 of Jain et al. (2024). By a modification to Theorem 5.23 in Van der Vaart (2000) combined with Assumptions B.4 and B.5, and $\|\boldsymbol{\theta}_{\text{bal}} - \boldsymbol{\theta}_{\text{syn}}\| = o(1)$, we have

$$\widehat{\boldsymbol{\theta}}_{\text{syn}} = \boldsymbol{\theta}_{\text{syn}} - H_{\text{syn}}^{-1} \nabla \widehat{\mathcal{R}}_{\text{syn}}(\boldsymbol{\theta}_{\text{syn}}) + R_2,$$

where $\|R_2\| = O_p(1/m + 1/n)$.

Part 3. Combining the results from Part 1 and Part 2, we have

$$\widehat{\boldsymbol{\theta}}_{\text{syn}} - \boldsymbol{\theta}_{\text{bal}} = -H_{\text{syn}}^{-1} \nabla \widehat{\mathcal{R}}_{\text{syn}}(\boldsymbol{\theta}_{\text{syn}}) - \sum_{g' \in \mathcal{G}} \frac{m_{g'}}{n_{\text{total}} + m_{\text{total}}} H_{\text{syn}}^{-1} \nabla \mathcal{B}_{g'}(\boldsymbol{\theta}_{\text{bal}}) + R_3,$$

where

$$\|R_3\| = O_p\left(\frac{1}{m} + \frac{1}{n} + \|\nabla\mathcal{R}_{\text{syn}}(\boldsymbol{\theta}_{\text{bal}})\|^2\right).$$

Now we measure the performance of $\widehat{\boldsymbol{\theta}}_{\text{syn}}$ for group g . From Assumption B.4, $\|\nabla^2\mathcal{R}_g(\boldsymbol{\theta}')\| = O(1)$ for any $\boldsymbol{\theta}'$ in the line segment between $\boldsymbol{\theta}_{\text{syn}}$ and $\boldsymbol{\theta}_{\text{bal}}$, since $\|\boldsymbol{\theta}_{\text{bal}} - \boldsymbol{\theta}_{\text{syn}}\| = o(1)$ by Part 1. Using Taylor expansion, we have

$$\begin{aligned} & \mathcal{R}_g(\widehat{\boldsymbol{\theta}}_{\text{syn}}) - \mathcal{R}_g(\boldsymbol{\theta}_{\text{bal}}) \\ &= \{\nabla\mathcal{R}_g(\boldsymbol{\theta}_{\text{bal}})\}^\top (\widehat{\boldsymbol{\theta}}_{\text{syn}} - \boldsymbol{\theta}_{\text{bal}}) + O(\|\widehat{\boldsymbol{\theta}}_{\text{syn}} - \boldsymbol{\theta}_{\text{bal}}\|^2) \\ &=: -\{\nabla\mathcal{R}_g(\boldsymbol{\theta}_{\text{bal}})\}^\top H_{\text{syn}}^{-1} \nabla\widehat{\mathcal{R}}_{\text{syn}}(\boldsymbol{\theta}_{\text{syn}}) - \sum_{g' \in \mathcal{G}} \frac{m_{g'}}{n_{\text{total}} + m_{\text{total}}} \{\nabla\mathcal{R}_g(\boldsymbol{\theta}_{\text{bal}})\}^\top H_{\text{syn}}^{-1} \nabla\mathcal{B}_{g'}(\boldsymbol{\theta}_{\text{bal}}) + R, \end{aligned}$$

where

$$\begin{aligned} R &= O_p\left(\frac{1}{m_{\text{total}}} + \frac{1}{n_{\text{total}}} + \|\nabla\mathcal{R}_{\text{syn}}(\boldsymbol{\theta}_{\text{bal}})\|^2 + \|\nabla\widehat{\mathcal{R}}_{\text{syn}}(\boldsymbol{\theta}_{\text{syn}})\|^2\right) \\ &= O_p\left(\frac{1}{m_{\text{total}}} + \frac{1}{n_{\text{total}}} + \|\nabla\mathcal{R}_{\text{syn}}(\boldsymbol{\theta}_{\text{bal}})\|^2\right). \end{aligned}$$

Recall that v_g and $b_{g,g'}$ are defined as

$$\begin{aligned} v_g^2 &= \{\nabla\mathcal{R}_g(\boldsymbol{\theta}_{\text{bal}})\}^\top H_{\text{bal}}^{-1} \left(\frac{1}{G} \sum_{g' \in \mathcal{G}} \Sigma_{g'}(\boldsymbol{\theta}_{\text{bal}})\right) H_{\text{bal}}^{-1} \nabla\mathcal{R}_g(\boldsymbol{\theta}_{\text{bal}}), \\ b_{g,g'} &= \{\nabla\mathcal{R}_g(\boldsymbol{\theta}_{\text{bal}})\}^\top H_{\text{bal}}^{-1} \nabla\mathcal{B}_{g'}(\boldsymbol{\theta}_{\text{bal}}). \end{aligned}$$

Again from Assumptions B.4 and B.5, we have $\|H_{\text{syn}} - H_{\text{bal}}\| = O(\|\boldsymbol{\theta}_{\text{syn}} - \boldsymbol{\theta}_{\text{bal}}\|)$, $\|\tilde{\Sigma}_g(\boldsymbol{\theta}_{\text{syn}}) - \Sigma_g(\boldsymbol{\theta}_{\text{syn}})\| = o(1)$ and $\|\Sigma_g(\boldsymbol{\theta}_{\text{syn}}) - \Sigma_g(\boldsymbol{\theta}_{\text{bal}})\| = o(1)$. Therefore, we have

$$\begin{aligned} \mathcal{R}_g(\widehat{\boldsymbol{\theta}}_{\text{syn}}) - \mathcal{R}_g(\boldsymbol{\theta}_{\text{bal}}) &= - \sum_{g' \in \mathcal{G}} \frac{m_{g'}}{n_{\text{total}} + m_{\text{total}}} b_{g,g'} \\ &+ O_p\left(\frac{1}{\sqrt{n_{\text{total}} + m_{\text{total}}}} v_g + \frac{1}{m_{\text{total}} \wedge n_{\text{total}}} + \|\nabla\mathcal{R}_{\text{syn}}(\boldsymbol{\theta}_{\text{bal}})\|^2\right), \end{aligned}$$

where O_p hides constants in the assumption. The conclusion follows from equation 11, which completes the proof of Theorem B.1. \square

B.2 Imbalanced Data

We specifically consider the binary classification task with the label set $\mathcal{Y} = \{0, 1\}$. Let $\mathcal{G} = \mathcal{Y}$. Here group 0 is the minority group and group 1 is the majority group. For imbalanced data classification, we add synthetic data only to minority group $g = 0$ such that the total number of samples for each group becomes equal, i.e., $n_0 + m_0 = n_1$.

Corollary B.1 (Restatement of Corollary 3.1). *Under Assumptions B.1-B.5, if there exists some constant $c \in (0, 1)$ such that $n_0/n_1 \leq c$ holds, then,*

$$\mathcal{R}_0(\widehat{\boldsymbol{\theta}}_{\text{syn}}) = \mathcal{R}_0(\boldsymbol{\theta}_{\text{bal}}) - \frac{n_1 - n_0}{2n_1} b_{0,0} + O_p\left(\frac{1}{\sqrt{n_1}} v_0 + \|\nabla\mathcal{B}_0(\boldsymbol{\theta}_{\text{bal}})\|^2\right),$$

where

$$v_0^2 := \{\nabla \mathcal{R}_0(\boldsymbol{\theta}_{\text{bal}})\}^\top \{\nabla^2 \mathcal{R}_{\text{bal}}(\boldsymbol{\theta}_{\text{bal}})\}^{-1} \frac{\Sigma_0(\boldsymbol{\theta}_{\text{bal}}) + \Sigma_1(\boldsymbol{\theta}_{\text{bal}})}{2} \{\nabla^2 \mathcal{R}_{\text{bal}}(\boldsymbol{\theta}_{\text{bal}})\}^{-1} \nabla \mathcal{R}_0(\boldsymbol{\theta}_{\text{bal}}), \quad (13)$$

$$b_{0,0} := \{\nabla \mathcal{R}_0(\boldsymbol{\theta}_{\text{bal}})\}^\top \{\nabla^2 \mathcal{R}_{\text{bal}}(\boldsymbol{\theta}_{\text{bal}})\}^{-1} \nabla \mathcal{B}_0(\boldsymbol{\theta}_{\text{bal}}). \quad (14)$$

Proof of Corollary B.1. Directly applying Theorem B.1 completes the proof of Corollary B.1. \square

B.3 Spurious Correlation

Let $\mathcal{G} = \mathcal{Y} \times \mathcal{A}$. We specifically consider binary label and discrete spurious features, $\mathcal{Y} = \{-1, 1\}$ and $\mathcal{A} = \{-\gamma, \gamma\}$ with some $\gamma \in \mathbb{R}^q$. We observe $\mathbf{x}_i = (\mathbf{z}_i, \mathbf{a}_i)$ and y_i , $\mathbf{z}_i \in \mathbb{R}^p$ is the core feature and $\mathbf{a}_i \in \mathcal{A}$ is the spurious feature. We assume the conditional independence of \mathbf{a}_i and \mathbf{z}_i given y_i . For simplicity, assume $n_{(-1, \gamma)} = n_{(1, -\gamma)} = n_{\min} < n_{\text{maj}} = n_{(1, \gamma)} = n_{(-1, -\gamma)}$ so that groups $(-1, -\gamma)$ and $(1, \gamma)$ are the majority groups. We choose the synthetic data size for group $g = (y, a) \in \mathcal{G}$ by $m_{(y,a)} = (n_{\text{maj}} - n_{\min}) \mathbb{1}\{y = a\}$ to equalize the raw and synthetic data size for each group. Define the reweighted risk as

$$\mathcal{R}_{\text{rw}}(\boldsymbol{\theta}) := \frac{1}{2} \sum_y \mathbb{E}[\ell(\boldsymbol{\theta}; \mathbf{x}'_i, y_i) | y_i = y].$$

where $\mathbf{x}'_i = (\mathbf{z}_i, \mathbf{a}'_i)$ with $\mathbf{a}'_i \sim \text{Unif}(\{-\gamma, \gamma\})$ independent of y_i .

We are interested in the performance of $\widehat{\boldsymbol{\theta}}_{\text{syn}}$ against the minimizer $\boldsymbol{\theta}_{\text{rw}}$ of \mathcal{R}_{rw} , measured in minority group risk $\mathcal{R}_{(-1,1)}(\boldsymbol{\theta}) := \mathbb{E}[\ell(\boldsymbol{\theta}; (\mathbf{z}_1, \mathbf{a}_1), \mathbf{y}_1) | y_1 = -1, \mathbf{a}_1 = \gamma]$.

Corollary B.2 (Restatement of Corollary 3.2). *Under Assumptions B.1-B.5, if $n_{\min}/n_{\text{maj}} \leq c$ holds for some constant $c \in (0, 1)$, then,*

$$\begin{aligned} \max_{g \in \mathcal{G}} \mathcal{R}_g(\widehat{\boldsymbol{\theta}}_{\text{syn}}) &= \max_{g \in \mathcal{G}} \mathcal{R}_g(\boldsymbol{\theta}_{\text{rw}}) \\ &+ O_p\left(\frac{n_{\text{maj}} - n_{\min}}{n_{\text{maj}}} (\|\nabla \mathcal{B}_{(1, -\gamma)}(\boldsymbol{\theta}_{\text{rw}})\| + \|\nabla \mathcal{B}_{(-1, \gamma)}(\boldsymbol{\theta}_{\text{rw}})\|) + \frac{1}{\sqrt{n_{\text{maj}}}} \max_{g \in \mathcal{G}} v_g\right), \end{aligned}$$

where

$$v_g^2 := \{\nabla \mathcal{R}_g(\boldsymbol{\theta}_{\text{rw}})\}^\top \{\nabla^2 \mathcal{R}_{\text{rw}}(\boldsymbol{\theta}_{\text{rw}})\}^{-1} \left(\frac{1}{4} \sum_{g' \in \mathcal{G}} \Sigma_{g'}(\boldsymbol{\theta}_{\text{rw}}) \right) \{\nabla^2 \mathcal{R}_{\text{rw}}(\boldsymbol{\theta}_{\text{rw}})\}^{-1} \nabla \mathcal{R}_g(\boldsymbol{\theta}_{\text{rw}}). \quad (15)$$

Proof of Corollary B.2. We first show that $\boldsymbol{\theta}_{\text{bal}} = \boldsymbol{\theta}_{\text{rw}}$. Let \mathbf{a}'_i be an independent copy of \mathbf{a}_i independent of \mathbf{z}_i . The conditional independence between \mathbf{z}_i and \mathbf{a}_i given y_i yields

$$\begin{aligned} \mathcal{R}_{\text{bal}}(\boldsymbol{\theta}) &= \frac{1}{4} \sum_{y, a} \mathbb{E}[\ell(\boldsymbol{\theta}; (\mathbf{z}_i, \mathbf{a}'_i)^\top, y_i)] \\ &= \frac{1}{4} \sum_{y, a} \mathbb{E}[\ell(\boldsymbol{\theta}; (\mathbf{z}_i, \mathbf{a}_i)^\top, y_i) | y_i = y, \mathbf{a}_i = \mathbf{a}] \\ &= \frac{1}{2} \sum_y \mathbb{E}[\ell(\boldsymbol{\theta}; (\mathbf{z}_i, \mathbf{a}'_i)^\top, y_i) | y_i = y] = \mathcal{R}_{\text{rw}}(\boldsymbol{\theta}). \end{aligned}$$

Thus $\boldsymbol{\theta}_{\text{bal}} = \boldsymbol{\theta}_{\text{rw}}$ by definition. For any $g \in \mathcal{G}$, Theorem B.1 gives

$$\begin{aligned} \mathcal{R}_g(\widehat{\boldsymbol{\theta}}_{\text{syn}}) &= \mathcal{R}_g(\boldsymbol{\theta}_{\text{rw}}) - \sum_{g' \in \mathcal{G}} \frac{m_{g'}}{n_{\text{total}} + m_{\text{total}}} b_{g,g'} \\ &\quad + O_p \left(\frac{1}{\sqrt{n_{\text{total}} + m_{\text{total}}}} v_g + \frac{1}{m_{\text{total}} \wedge n_{\text{total}}} + \left\| \sum_{g' \in \mathcal{G}} \frac{m_{g'}}{n_{\text{total}} + m_{\text{total}}} \nabla \mathcal{B}_{g'}(\boldsymbol{\theta}_{\text{rw}}) \right\|^2 \right). \end{aligned}$$

Since $|\mathcal{G}| = 4$, using $|\max(a, b) - \max(a, c)| \leq |b - c|$ for any $a, b, c \in \mathbb{R}$ repeatedly, we obtain

$$\begin{aligned} & \left| \max_{g \in \mathcal{G}} \mathcal{R}_g(\widehat{\boldsymbol{\theta}}_{\text{syn}}) - \max_{g \in \mathcal{G}} \mathcal{R}_g(\boldsymbol{\theta}_{\text{rw}}) \right| \\ &= O_p \left(\max_{g \in \mathcal{G}} \sum_{g' \in \mathcal{G}} \frac{m_{g'}}{n_{\text{total}} + m_{\text{total}}} b_{g,g'} + \max_{g \in \mathcal{G}} \frac{1}{\sqrt{n_{\text{total}} + m_{\text{total}}}} v_g \right. \\ &\quad \left. + \frac{1}{m_{\text{total}} \wedge n_{\text{total}}} + \left\| \sum_{g' \in \mathcal{G}} \frac{m_{g'}}{n_{\text{total}} + m_{\text{total}}} \nabla \mathcal{B}_{g'}(\boldsymbol{\theta}_{\text{rw}}) \right\|^2 \right) \\ &= O_p \left(\frac{n_{\text{maj}} - n_{\text{min}}}{n_{\text{maj}}} (\|\nabla \mathcal{B}_{(1,-\gamma)}(\boldsymbol{\theta}_{\text{rw}})\| + \|\nabla \mathcal{B}_{(-1,\gamma)}(\boldsymbol{\theta}_{\text{rw}})\|) + \frac{1}{\sqrt{n_{\text{maj}}}} \max_{g \in \mathcal{G}} v_g \right), \end{aligned}$$

where the last inequality follows since $n_1 \leq cn_2$ for some $c < 1$, and $|b_{g,g'}| \leq \|\nabla \mathcal{B}_{g'}(\boldsymbol{\theta}_{\text{rw}})\|$. This completes the proof of Corollary B.2. \square

C Proofs for Section 3.2

In this section, we prove the results for transformers in Section 3.2.

Recall that $\eta \geq (1/\sqrt{r}) \log d$. Assume that $\|\mathbf{z}^{(t)}\| = 1$ for all $t \in \mathcal{T}$, $|\mathcal{F}| \lesssim d^\alpha$ for some positive constant $\alpha = O(1)$, and $\sup_{\mathbf{u} \in \mathbb{B}_r(\log d)} \|f^{(m)}(\mathbf{u})\| \leq 1$. We introduce several assumptions. Note that in the main body we only use Assumption C.3, which is weaker than Assumptions C.1 and C.2.

Assumption C.1. Assume that $\mathbb{E}[\|f^{(m)}(\mathbf{u}_{X_1})\|^2 | T = t, U, \eta] = N_{t,U,\eta}^2$ for all $m \in \mathcal{M}$ for some $N_{t,U,\eta} > 0$ allowed to be dependent on $t \in \mathcal{T}$, U , and η .

This assumption can be easily satisfied when functions $(f^{(m)})_{m \in \mathcal{M}}$ take values on the same sphere in \mathbb{R}^r on average.

Define $\xi_{\mathcal{T}}$ and $\xi_{\mathcal{M}}$ as

$$\begin{aligned} \xi_{\mathcal{T}} &:= 1 - \max_{t \neq t'} \langle \mathbf{z}^{(t)}, \mathbf{z}^{(t')} \rangle, \\ \xi_{\mathcal{M}}(U) &:= \min_{m \neq m'} \mathbb{E} [D_{\text{KL}}(\mathbb{P}(Y_i | X_i, M = m, U, \eta) \| \mathbb{P}(Y_i | X_i, M = m', U, \eta)) | T = t, U, \eta]. \end{aligned} \quad (16)$$

Note that $\xi_{\mathcal{T}}$ measures the smallest cosine dissimilarity between different subject embeddings, and $\xi_{\mathcal{M}}(U)$ is the KL divergence between distributions of Y_i given different M . We introduce the following identifiability condition for $(\mathbf{z}^{(t)})_{t \in \mathcal{T}}$ and $(f^{(m)})_{m \in \mathcal{M}}$, which is used to prove the perfect recovery of distribution. Recall that $\xi_{\mathcal{T}}$ and $\xi_{\mathcal{M}}$ defined in equation 16 are responsible for the identifiability.

Assumption C.2. Assume that there exist sufficiently large constants $C_{\mathcal{T}}$ and $C_{\mathcal{M}}$ such that

$$\xi_{\mathcal{T}} \geq C_{\mathcal{T}} \frac{\eta r}{\min_{t \in \mathcal{T}} \|\mathbf{z}^{(t)}\|} \left(\frac{\log^2 d}{\sqrt{nr}} + \frac{\log d}{\sqrt{dr}} \right),$$

$$\mathbb{P}\left(\xi_{\mathcal{M}}(U) \geq C_M \left(\frac{\log^2 d}{\eta\sqrt{nr}} + \frac{\log d}{\sqrt{d}} \right)\right) = 1 - \exp(-\Omega(\log^2 d)),$$

where the probability is taken with respect to U .

We introduce another identifiability condition for the function class \mathcal{F} .

Assumption C.3. There exists a constant $C > 0$ and $\epsilon > 0$ such that for any $\epsilon' \leq \epsilon$ and $m, m' \in \mathcal{M}$, if $|\mathbb{E}[f^{(m')}(\mathbf{u}_{X_1})^\top f^{(m)}(\mathbf{u}_{X_1}) | T = t, U, \eta] - \mathbb{E}[\|f^{(m)}(\mathbf{u}_{X_1})\|^2 | T = t, U, \eta]| \leq \epsilon'$, then $|\mathbb{E}[\|f^{(m')}(\mathbf{u}_{X_1}) - f^{(m)}(\mathbf{u}_{X_1})\|^2 | T = t, U, \eta]| \leq C\epsilon'$ holds with high probability with respect to U .

We then provide Lemmas C.1 and C.2 to show that selecting the subject or function embeddings by maximizing the cosine similarity gives the ground-truth subject or function with high probability.

C.1 A Lemma for generative capacity of LLMs

Given observed covariates $(X_i)_{i \in [n]}$ and token embeddings U , we define the estimator of T as

$$\hat{T} = \arg \max_{t' \in \mathcal{T}} \frac{1}{n} \sum_{i \in [n]} \langle \mathbf{z}^{(t')}, \mathbf{u}_{X_i} \rangle. \quad (17)$$

Lemma C.1. For any $t \in \mathcal{T}$ and $\eta \geq (1/\sqrt{r}) \log d$, it holds that

$$\mathbb{P}\left(\max_{t' \in \mathcal{T}} \left| \mathbf{z}^{(t')\top} \left(\frac{1}{n} \sum_{i \in [n]} \mathbf{u}_{X_i} \right) - \frac{1}{\eta r} \mathbf{z}^{(t')\top} \mathbf{z}^{(t)} \right| \lesssim \frac{\log^2 d}{\sqrt{nr}} + \frac{\log d}{\sqrt{dr}} \middle| T = t, U, \eta \right) = 1 - \exp(-\Omega(\log^2 d)).$$

Furthermore, under Assumption C.2,

$$\begin{aligned} \mathbb{P}(\hat{T} \neq t | T = t, U, \eta) &= \exp(-\Omega(\log^2 d)), \\ \mathbb{P}\left(\frac{1}{n} \sum_{i \in [n]} \langle \mathbf{z}^{(\hat{T})}, \mathbf{u}_{X_i} \rangle - \max_{t' \neq \hat{T}} \frac{1}{n} \sum_{i \in [n]} \langle \mathbf{z}^{(t')}, \mathbf{u}_{X_i} \rangle \leq \frac{\xi_{\mathcal{T}}}{2\eta r} \middle| T = t, U, \eta \right) &= \exp(-\Omega(\log^2 d)) \end{aligned}$$

hold with high probability with respect to U . Here Ω 's do not depend on t .

Proof of Lemma C.1. Define $E_i^{(t')} := \sum_{x \in \mathcal{X}} \mathbf{z}^{(t')\top} \mathbf{u}_x \mathbb{1}\{X_i = x\}$. From Lemma D.1, there exists an event \mathcal{E} for a random matrix $U = [\mathbf{u}_1; \dots; \mathbf{u}_d]^\top$ with $\mathbb{P}(\mathcal{E}) = 1 - \exp(-\Omega(\log^2 d))$ such that on this event,

$$\max_{T \in \mathcal{T}, x \in \mathcal{X}} |\mathbf{z}^{(T)\top} \mathbf{u}_x| \lesssim \frac{1}{\sqrt{r}} \log d, \quad \max_{t \in \mathcal{T}} \left| \frac{d\mathbb{E}[C_x^{(t)}]}{\sum_{x \in \mathcal{X}} C_x^{(t)}} - 1 \right| \lesssim \frac{1}{\sqrt{d}} \log d, \quad (18)$$

$$\max_{t, t' \in \mathcal{T}} \left| \sum_{x \in \mathcal{X}} (D_x^{(t, t')} - \mathbb{E}[D_x^{(t, t')}]) \right| \lesssim \sqrt{\frac{d}{r}} \log d \quad (19)$$

$$\max_{t, t' \in \mathcal{T}} \left| \sum_{x \in \mathcal{X}} \frac{D_x^{(t, t')}}{\sum_{x' \in \mathcal{X}} C_{x'}^{(t)}} - \frac{\mathbb{E}[D_x^{(t, t')}]}{\mathbb{E}[C_x^{(t)}]} \right| \lesssim \frac{1}{\sqrt{dr}} \log d, \quad (20)$$

hold, where $C_x^{(t)} = \sum_{x \in \mathcal{X}} \exp(\eta^{-1} \mathbf{z}^{(t)\top} \mathbf{u}_x)$ and $D_x^{(t, t')} = \sum_{x \in \mathcal{X}} \mathbf{z}^{(t')\top} \mathbf{u}_x \exp(\eta^{-1} \mathbf{z}^{(t)\top} \mathbf{u}_x)$. For now we fix any U satisfying equation 18 and equation 19. We also fix any $t \in \mathcal{T}$

and $\eta \geq (1/\sqrt{r}) \log d$. Then, there exists some constant $C > 0$ such that $|E_i^{(t')}| \leq \max_{x \in \mathcal{X}} |\mathbf{z}^{(t')\top} \mathbf{u}_x| \leq (C/\sqrt{r}) \log d$ holds. From Hoeffding's inequality, it follows that

$$\mathbb{P} \left(\left| \sum_{i \in [n]} (E_i^{(t')} - \mathbb{E}[E_i^{(t')} | U, T = t, \eta]) \right| \geq \epsilon \middle| U, T = t, \eta \right) \leq 2 \exp \left(-\frac{r\epsilon^2}{2C^2 n \log^2 d} \right).$$

Choosing $\epsilon \leftarrow \sqrt{n/r} \log^2 d$, and using $(1/n) \sum_{i \in [n]} \mathbf{z}^{(t')\top} \mathbf{u}_{X_i} = (1/n) \sum_{i \in [n]} E_i^{(t')}$, we have

$$\mathbb{P} \left(\left| \mathbf{z}^{(t')\top} \left(\frac{1}{n} \sum_{i \in [n]} \mathbf{u}_{X_i} \right) - \sum_{x \in \mathcal{X}} \frac{D_x^{(t,t')}}{\sum_{x' \in \mathcal{X}} C_{x'}^{(t)}} \right| \leq \frac{\log^2 d}{\sqrt{nr}} \middle| U, T = t, \eta \right) = 1 - \exp(-\Omega(\log^2 d)),$$

where we used

$$\mathbb{E}[E_i^{(t')} | U, T = t, \eta] = \sum_{x \in \mathcal{X}} \mathbf{z}^{(t')\top} \mathbf{u}_x \mathbb{P}(X_i = x | U, T = t, \eta) = \frac{\sum_{x \in \mathcal{X}} D_x^{(t,t')}}{\sum_{x' \in \mathcal{X}} C_{x'}^{(t)}}.$$

By a union bound argument,

$$\mathbb{P} \left(\max_{t' \in \mathcal{T}} \left| \mathbf{z}^{(t')\top} \left(\frac{1}{n} \sum_{i \in [n]} \mathbf{u}_{X_i} \right) - \sum_{x \in \mathcal{X}} \frac{D_x^{(t,t')}}{\sum_{x' \in \mathcal{X}} C_{x'}^{(t)}} \right| \leq \frac{\log^2 d}{\sqrt{nr}} \middle| U, T = t, \eta \right) = 1 - \exp(-\Omega(\log^2 d)). \quad (21)$$

Notice that equation 64 and $\mathbb{E}[C_{x'}^{(t)}] = \exp(\|\mathbf{z}^{(t)}\|^2/(2\eta^2 r))$ yield

$$\frac{\mathbb{E}[D_x^{(t,t')}]}{\mathbb{E}[C_x^{(t)}]} = \frac{1}{\eta r} \mathbf{z}^{(t')\top} \mathbf{z}^{(t)}.$$

Therefore, combining equation 21 and equation 20, we have

$$\mathbb{P} \left(\max_{t' \in \mathcal{T}} |\Delta^{(t,t')}| \lesssim \frac{\log^2 d}{\sqrt{nr}} + \frac{\log d}{\sqrt{dr}} \middle| U, T = t, \eta \right) = 1 - \exp(-\Omega(\log^2 d)), \quad (22)$$

where $\Delta^{(t,t')} := (1/n) \sum_{i \in [n]} \mathbf{z}^{(t')\top} \mathbf{u}_{X_i} - (1/\eta r) \mathbf{z}^{(t')\top} \mathbf{z}^{(t)}$. This gives the first claim. The second claim follows since

$$\mathbb{P}(\widehat{T} \neq t | T = t, U, \eta) = \mathbb{P} \left(\frac{1}{n} \sum_{i \in [n]} \mathbf{z}^{(t)\top} \mathbf{u}_{X_i} < \max_{t': t' \neq t} \frac{1}{n} \sum_{i \in [n]} \mathbf{z}^{(t')\top} \mathbf{u}_{X_i} \middle| T = t, U, \eta \right) \quad (23)$$

$$\leq \mathbb{P} \left(\frac{1}{\eta r} < \max_{t': t' \neq t} \frac{\mathbf{z}^{(t')\top} \mathbf{z}^{(t)}}{\eta r} + 2 \max_{t' \in \mathcal{T}} |\Delta^{(t,t')}| \middle| T = t, U, \eta \right) \quad (24)$$

$$= \mathbb{P} \left(\max_{t' \in \mathcal{T}} |\Delta^{(t,t')}| > \frac{\xi_{\mathcal{T}}}{2\eta r} \middle| T = t, U, \eta \right) \quad (25)$$

$$= \exp(-\Omega(\log^2 d)), \quad (26)$$

where the last equality follows from equation 22 and by assumption for $\xi_{\mathcal{T}}$.

Next we prove the third claim. We already know that $\max_{t \in \mathcal{T}} \mathbb{P}(\widehat{T} \neq t | T = t, U, \eta) = 1 - \exp(-\Omega(\log^2 d))$. Thus by a union bound argument we only need to bound

$$\delta_n^{(t)} := \frac{1}{n} \sum_{i \in [n]} \langle \mathbf{z}^{(t)}, \mathbf{u}_{X_i} \rangle - \max_{t': t' \neq t} \frac{1}{n} \sum_{i \in [n]} \langle \mathbf{z}^{(t')}, \mathbf{u}_{X_i} \rangle \quad (27)$$

given $T = t$ and U . By the same argument as in equation 26,

$$\mathbb{P}\left(\delta_n^{(t)} < \delta' \middle| T = t, U, \eta\right) \leq \mathbb{P}\left(\frac{1}{\eta r} < \max_{t': t' \neq t} \frac{\mathbf{z}^{(t')\top} \mathbf{z}^{(t)}}{\eta r} + 2 \max_{t' \in \mathcal{T}} |\Delta^{(t, t')}| + \delta' \middle| T = t, U, \eta\right) \quad (28)$$

$$= \mathbb{P}\left(\max_{t' \in \mathcal{T}} |\Delta^{(t, t')}| > \frac{\xi_{\mathcal{T}}}{2\eta r} - \frac{\xi_{\mathcal{T}}}{4\eta r} \middle| T = t, U, \eta\right) \quad (29)$$

$$= \exp(-\Omega(\log^2 d)) \quad (30)$$

This completes the proof of Lemma C.1. \square

C.2 A Lemma for discriminative capacity of LLMs

Given observed pairs $(X_i, Y_i)_{i \in [n]}$, we define the estimator of M as

$$\widehat{M} := \arg \max_{m' \in \mathcal{M}} \frac{1}{n} \sum_{i \in [n]} \langle f^{(m')}(\mathbf{u}_{X_i}), \mathbf{u}_{Y_i} \rangle. \quad (31)$$

We first provide a lemma stating that M can be estimated perfectly with high probability under the identifiability condition on $\xi_{\mathcal{M}}$.

Lemma C.2. *For any $m \in \mathcal{M}$, $t \in \mathcal{T}$ and $\eta \geq (1/\sqrt{r}) \log d$, it holds that*

$$\begin{aligned} & \mathbb{P}\left(\max_{m' \in \mathcal{M}} \left| \frac{1}{n} \sum_{i \in [n]} \langle f^{(m')}(\mathbf{u}_{X_i}), \mathbf{u}_{Y_i} \rangle - \mathbb{E}\left[\langle f^{(m')}(\mathbf{u}_{X_1}), \mathbf{u}_{Y_1} \rangle \middle| M = m, T = t, U, \eta\right] \right| \right. \\ & \quad \left. > \frac{\log^2 d}{\sqrt{nr}} \middle| M = m, T = t, U, \eta\right) \\ & = \exp(-\Omega(\log^2 d)). \end{aligned}$$

with high probability. Furthermore, under Assumptions C.1 and C.2,

$$\begin{aligned} & \mathbb{P}(\widehat{M} \neq m \middle| M = m, T = t, U, \eta) = \exp(-\Omega(\log^2 d)), \\ & \mathbb{P}\left(\frac{1}{n} \sum_{i \in [n]} \langle f^{(\widehat{M})}(\mathbf{u}_{X_i}), \mathbf{u}_{Y_i} \rangle - \max_{m' \neq \widehat{M}} \frac{1}{n} \sum_{i \in [n]} \langle f^{(m')}(\mathbf{u}_{X_i}), \mathbf{u}_{Y_i} \rangle \leq \frac{\eta \xi_{\mathcal{M}}}{2} \middle| M = m, T = t, U, \eta\right) \\ & = \exp(-\Omega(\log^2 d)). \end{aligned}$$

holds with high probability with respect to U .

Proof of Lemma C.2. To ease notation we let $p_x^{(t)} := \mathbb{P}(X_1 = x \mid T = t, U, \eta)$. We divide the proof into two parts.

Part 1. In this part we bound the quantity $\min_{m' \in \mathcal{M}} (\mathbb{E}[H_{X_1, Y_1}^{(m)} \mid M = m, T = t, U, \eta] - \mathbb{E}[H_{X_1, Y_1}^{(m')} \mid M = m, T = t, U, \eta])$. Note that for any $t \in \mathcal{T}$, $m \in \mathcal{M}$, U and η ,

$$\begin{aligned} & \mathbb{E}[\{f^{(m')}(\mathbf{u}_{X_1})\}^\top \mathbf{u}_{Y_1} \mid M = m, T = t, U, \eta] \\ & = \eta \sum_{x \in \mathcal{X}} p_x^{(t)} \sum_{y \in \mathcal{X}} \log \left(\frac{\exp(\eta^{-1} \{f^{(m')}(\mathbf{u}_x)\}^\top \mathbf{u}_y)}{\sum_{y' \in \mathcal{X}} \exp(\eta^{-1} \{f^{(m')}(\mathbf{u}_x)\}^\top \mathbf{u}_{y'})} \right) \frac{\exp(\eta^{-1} \{f^{(m)}(\mathbf{u}_x)\}^\top \mathbf{u}_y)}{\sum_{y' \in \mathcal{X}} \exp(\eta^{-1} \{f^{(m)}(\mathbf{u}_x)\}^\top \mathbf{u}_{y'})} \end{aligned}$$

$$+ \eta \sum_{x \in \mathcal{X}} p_x^{(t)} \log \left(\sum_{y' \in \mathcal{X}} C_{y'}(f^{(m')}(\mathbf{u}_x)) \right),$$

where $C_x(\mathbf{z}) := \exp(\eta^{-1} \mathbf{z}^\top \mathbf{u}_x)$. Then,

$$\begin{aligned} & \mathbb{E}[\{f^{(m)}(\mathbf{u}_{X_1})\}^\top \mathbf{u}_{Y_1} | M = m, T = t, U, \eta] - \mathbb{E}[\{f^{(m')}(\mathbf{u}_{X_1})\}^\top \mathbf{u}_{Y_1} | M = m, T = t, U, \eta] \\ &= \eta \mathbb{E}[D_{\text{KL}}(\mathbb{P}(Y_i | X_i, M = m, U) \| \mathbb{P}(Y_i | X_i, M = m', U)) | T = t, U, \eta] \\ &+ \eta \sum_{x \in \mathcal{X}} p_x^{(t)} \log \left(\frac{\sum_{y' \in \mathcal{X}} C_{y'}(f^{(m)}(\mathbf{u}_x))}{\sum_{y' \in \mathcal{X}} C_{y'}(f^{(m')}(\mathbf{u}_x))} \right). \end{aligned} \quad (32)$$

We first show that there exists a high probability event with respect to U such that the second term on the right hand side in equation 32 is small. Fix any $x \in \mathcal{X}$. Note that $\|\mathbf{u}_x\| \lesssim (1/\sqrt{r}) \log d$ holds with high probability from Lemma D.1. Thus $\max_{m \in [\bar{m}], x \in \mathcal{X}} \|f^{(m)}(\mathbf{u}_x)\| \leq 1$ holds with high probability by assumption. Again from Lemma D.1 with the choice $\mathcal{X} \leftarrow \mathcal{X} \setminus \{x\}$, we have

$$\max_{m \in \mathcal{M}} \left| \sum_{y \in \mathcal{X} \setminus \{x\}} \left\{ C_y(f^{(m)}(\mathbf{u}_x)) - \exp\left(\frac{\|f^{(m)}(\mathbf{u}_x)\|^2}{2\eta^2 r}\right) \right\} \right| \lesssim \sqrt{d} \log d$$

with high probability. By a union bound, we have

$$\max_{x \in \mathcal{X}} \max_{m \in \mathcal{M}} \left| \sum_{y \in \mathcal{X} \setminus \{x\}} \left\{ C_y(f^{(m)}(\mathbf{u}_x)) - \exp\left(\frac{\|f^{(m)}(\mathbf{u}_x)\|^2}{2\eta^2 r}\right) \right\} \right| \lesssim \sqrt{d} \log d$$

with probability $1 - d \exp(-\Omega(\log^2 d)) = 1 - \exp(-\Omega(\log^2 d))$. This gives

$$\begin{aligned} \log \left(\frac{\sum_{y' \in \mathcal{X}} C_{y'}(f^{(m)}(\mathbf{u}_x))}{\sum_{y' \in \mathcal{X}} C_{y'}(f^{(m')}(\mathbf{u}_x))} \right) &= \log \left(\frac{C_x(f^{(m)}(\mathbf{u}_x)) + \sum_{y' \neq x} C_{y'}(f^{(m)}(\mathbf{u}_x))}{C_x(f^{(m')}(\mathbf{u}_x)) + \sum_{y' \neq x} C_{y'}(f^{(m')}(\mathbf{u}_x))} \right) \\ &= \log \left(\frac{O(1) + O(\sqrt{d} \log d) + (d-1) \exp(\|f^{(m)}(\mathbf{u}_x)\|^2 / (2\eta^2 r))}{O(1) + O(\sqrt{d} \log d) + (d-1) \exp(\|f^{(m')}(\mathbf{u}_x)\|^2 / (2\eta^2 r))} \right) \\ &= \frac{\|f^{(m)}(\mathbf{u}_x)\|^2 - \|f^{(m')}(\mathbf{u}_x)\|^2}{2\eta^2 r} + O\left(\frac{\log d}{\sqrt{d}}\right) \end{aligned}$$

with high probability, where we used $C_x(f^{(m)}(\mathbf{u}_x)) = O(1)$ with high probability in the second equality. Here O 's do not depend on m, m' and x . To ease notation, we define $H_{x,y}^{(m)} := \langle f^{(m)}(\mathbf{u}_x), \mathbf{u}_y \rangle$. Then,

$$\begin{aligned} & \mathbb{E} \left[H_{X_1, Y_1}^{(m)} | M = m, T = t, U, \eta \right] - \mathbb{E} \left[H_{X_1, Y_1}^{(m')} | M = m, T = t, U, \eta \right] \\ &= \eta \mathbb{E} \left[D_{\text{KL}}(\mathbb{P}(Y_i | X_i, M = m, U) \| \mathbb{P}(Y_i | X_i, M = m', U)) | T = t, U, \eta \right] \\ &+ \eta \frac{\mathbb{E}[\|f^{(m)}(\mathbf{u}_{X_1})\|^2 - \|f^{(m')}(\mathbf{u}_{X_1})\|^2 | T = t, U, \eta]}{2\eta^2 r} + O\left(\frac{\eta \log d}{\sqrt{d}}\right) \\ &= \eta \mathbb{E} \left[D_{\text{KL}}(\mathbb{P}(Y_i | X_i, M = m, U) \| \mathbb{P}(Y_i | X_i, M = m', U)) | T = t, U, \eta \right] + O\left(\frac{\eta \log d}{\sqrt{d}}\right) \end{aligned}$$

holds with high probability, where the last equality follows by assumption that $\mathbb{E}[\|f^{(m)}(\mathbf{u}_{X_1})\|^2 | T = t, U, \eta] = N_{t,U,\eta}^2$ for all $m \in \mathcal{M}$. This gives

$$\min_{m' \in \mathcal{M}} \left(\mathbb{E} \left[H_{X_1, Y_1}^{(m)} | M = m, T = t, U, \eta \right] - \mathbb{E} \left[H_{X_1, Y_1}^{(m')} | M = m, T = t, U, \eta \right] \right) = \eta \xi_{\mathcal{M}} + O \left(\frac{\eta \log d}{\sqrt{d}} \right) \quad (33)$$

with high probability.

Part 2. Next we show the convergence of $(1/n) \sum_{i \in [n]} H_{X_i, Y_i}^{(m')}$ for all $m' \in \mathcal{M}$ given U . For now we fix any $m' \in \mathcal{M}$. We fix any $t \in \mathcal{T}$, $m \in \mathcal{M}$ and $\eta \geq (1/\sqrt{r}) \log d$. From Lemma D.1,

$$\max_{m' \in \mathcal{M}} \max_{x, y \in \mathcal{X}} |H_{x, y}^{(m')}| \leq \max_{y \in \mathcal{X}} \|\mathbf{u}_y\| \leq C(1/\sqrt{r}) \log d \quad (34)$$

holds for some constant $C > 0$. For any U satisfying equation 33 and equation 34, Hoeffding's inequality gives

$$\begin{aligned} & \mathbb{P} \left(\left| \sum_{i \in [n]} \left(H_{X_i, Y_i}^{(m')} - \mathbb{E} \left[H_{X_i, Y_i}^{(m')} | M = m, T = t, U, \eta \right] \right) \right| > \epsilon \middle| M = m, T = t, U, \eta \right) \\ & \leq 2 \exp \left(-\frac{r\epsilon^2}{2nC^2 \log^2 d} \right). \end{aligned}$$

Choosing $\epsilon \leftarrow \sqrt{n/r} \log^2 d$ and a union bound argument gives

$$\mathbb{P} \left(\max_{m' \in \mathcal{M}} \left| \frac{1}{n} \sum_{i \in [n]} H_{X_i, Y_i}^{(m')} - \mathbb{E} \left[H_{X_i, Y_i}^{(m')} | M = m, T = t, U, \eta \right] \right| > \frac{\log^2 d}{\sqrt{nr}} \middle| M = m, T = t, U, \eta \right) \quad (35)$$

$$\lesssim |\mathcal{M}| |\mathcal{T}| \exp(-\Omega(\log^2 d)) = \exp(-\Omega(\log^2 d)), \quad (36)$$

where we used $|\mathcal{M}| = d^\alpha$ for some constant $\alpha = O(1)$. This yields the first claim. Therefore,

$$\begin{aligned} & \mathbb{P}(\widehat{M} \neq m | M = m, T = t, U, \eta) \\ & = \mathbb{P} \left(\frac{1}{n} \sum_{i \in [n]} H_{X_i, Y_i}^{(m)} < \max_{m' \in \mathcal{M}} \frac{1}{n} \sum_{i \in [n]} H_{X_i, Y_i}^{(m')} \middle| M = m, T = t, U, \eta \right) \\ & \leq \mathbb{P} \left(\mathbb{E} \left[H_{X_1, Y_1}^{(m)} | M = m, T = t, U, \eta \right] - \max_{m' \in \mathcal{M}} \mathbb{E} \left[H_{X_1, Y_1}^{(m')} | M = m, T = t, U, \eta \right] \right. \\ & \quad \left. < 2 \max_{m' \in \mathcal{M}} \left| \frac{1}{n} \sum_{i \in [n]} H_{X_i, Y_i}^{(m')} - \mathbb{E} \left[H_{X_1, Y_1}^{(m')} | M = m, T = t, U, \eta \right] \right| \middle| M = m, T = t, U \right). \end{aligned}$$

Note that when $\xi_{\mathcal{M}} \gg (1/\sqrt{d}) \log d + (1/(\eta\sqrt{nr})) \log^2 d$,

$$\begin{aligned} & \mathbb{P} \left(\mathbb{E} \left[H_{X_1, Y_1}^{(m)} | M = m, T = t, U, \eta \right] - \max_{m' \in \mathcal{M}} \mathbb{E} \left[H_{X_1, Y_1}^{(m')} | M = m, T = t, U, \eta \right] \right. \\ & \quad \left. < 2 \max_{m' \in \mathcal{M}} \left| \frac{1}{n} \sum_{i \in [n]} H_{X_i, Y_i}^{(m')} - \mathbb{E} \left[H_{X_1, Y_1}^{(m')} | M = m, T = t, U, \eta \right] \right| \middle| M = m, T = t, U \right) \\ & \leq \mathbb{P} \left(\frac{\log^2 d}{\sqrt{nr}} < \max_{m' \in \mathcal{M}} \left| \frac{1}{n} \sum_{i \in [n]} H_{X_i, Y_i}^{(m')} - \mathbb{E} \left[H_{X_1, Y_1}^{(m')} | M = m, T = t, U, \eta \right] \right| \middle| M = m, T = t, U \right) \end{aligned}$$

$$= \exp(-\Omega(\log^2 d)),$$

where we used equation 36. In summary,

$$\mathbb{P}(\widehat{M} \neq m | M = m, T = t, U, \eta) = \exp(-\Omega(\log^2 d))$$

holds with high probability.

By the same argument as in the proof of Lemma C.1, we obtain

$$\mathbb{P}\left(\frac{1}{n} \sum_{i \in [n]} H_{X_i, Y_i}^{(m)} - \max_{m' \in \mathcal{M}} \frac{1}{n} \sum_{i \in [n]} H_{X_i, Y_i}^{(m')} < \frac{\eta \xi_{\mathcal{M}}}{2} \middle| M = m, T = t, U, \eta\right) = \exp(-\Omega(\log^2 d)),$$

This completes the proof of Lemma C.2. \square

C.3 Construction of transformer layers

In this section, we construct a transformer that outputs synthetic covariates or labels depending on the current task. We only consider the case where $|\mathcal{M}| \geq |\mathcal{T}|$. Otherwise the proof follows by a similar argument.

Before the proof, we define identity feed forward neural networks and transformers.

Definition C.1. Define the identity attention $\text{Attn}_{\mu_{\text{id}}}$ and identity feed forward neural network $\text{FFN}_{\nu_{\text{id}}}$ as $\mu_{\text{id}} = \{(O, O, O)\}$ and $\nu_{\text{id}} = \{O, O\}$.

We also introduce a useful function that combines the product and indicator functions. Define $\phi_B : \mathbb{R}^3 \rightarrow \mathbb{R}$ as

$$\begin{aligned} \phi_B(x; s, t) := & -4B\sigma\left(\frac{1}{4B}x + t - s + \frac{1}{2}\right) + 8B\sigma\left(\frac{1}{4B}x + t - s + \frac{1}{4}\right) \\ & - 8B\sigma\left(\frac{1}{4B}x + t - s - \frac{1}{4}\right) + 4B\sigma\left(\frac{1}{4B}x + t - s - \frac{1}{2}\right). \end{aligned} \quad (37)$$

We provide the following lemma without proof to help implement an attention layer that filters some input tokens.

Lemma C.3. For any $B > 0$ and $x \in [-B, B]$, and $s, t \in \mathbb{Z}$,

$$\phi_B(x; s, t) = x \mathbb{1}\{s = t\}.$$

We then introduce the notation to simplify the statement. We omit the second subscript n from $\mathbf{p}_{s,n}$ for the positional encoding. Define $\mathbf{h}_{2i-1} = \mathbf{h}_i^X$ and $\mathbf{h}_{2i} = \mathbf{h}_i^Y$ for all $i \in [n]$. Let $(\tilde{X}_s, \tilde{Y}_s)$ ($s \geq 1$) be the synthetic pair of data generated as the $(2s-1)$ -th and $(2s)$ -th output from the transformer. Let $X_{n+s} := \tilde{X}_s$ and $Y_{n+s} := \tilde{Y}_s$. Define

$$\mathbf{h}_{2n+2s-1} = \begin{pmatrix} \mathbf{u}_{X_{n+s}} \\ \mathbf{0} \\ \mathbf{p}_{2n+2s-1} \end{pmatrix}, \quad \mathbf{h}_{2n+2s} = \begin{pmatrix} \mathbf{u}_{Y_{n+s}} \\ \mathbf{0} \\ \mathbf{p}_{2n+2s} \end{pmatrix} \quad (38)$$

for $s \geq 1$. In summary, we have input tokens $H_n = [\mathbf{h}_1, \mathbf{h}_2, \dots, \mathbf{h}_{2n}]$ and previously generated tokens $[\mathbf{h}_{2n+1}, \mathbf{h}_{2n+2}, \dots, \mathbf{h}_{2n+\ell}]$ for some $\ell \in \{0\} \cup \mathbb{N}^+$.

Proposition C.1. Fix any $d, r, r_0, L_0 \in \mathbb{N}^+$, $\omega > 0$, $(\mathbf{z}^{(t)})_{t \in \mathcal{T}}$ and $(f^{(m)})_{m \in \mathcal{M}} \subset \mathcal{F}(L_0, r_0)$. Then, there exist transformer layers TF_{Ψ^*} with $\Psi^* = \Psi^*((\mathbf{z}^{(t)})_{t \in \mathcal{T}}, (f^{(m)})_{m \in \mathcal{M}}, d, r, \omega, L_0, r_0)$ such that

- the dimension of token embeddings is $r + r|\mathcal{M}| + |\mathcal{M}| + 4$,
- it consists of $L_0 + 9$ transformer layers with the width of FNN $O(|\mathcal{M}|^2 \vee |\mathcal{M}|r_0)$, and the number of heads of attention layers $O(|\mathcal{M}|)$,
- given inputs H_n and $\mathbf{h}_{2n+1}, \dots, \mathbf{h}_{2n+\ell}$ defined in equation 38, it outputs

$$\text{TF}_{\Psi^*}([H_n; \mathbf{h}_{2n+1}; \dots; \mathbf{h}_{2n+\ell}])_{2n+\ell} = \begin{cases} (\widehat{f}(\mathbf{u}_{X_{n+s}})^\top, \mathbf{0}^\top)^\top & \text{if } \ell = 2s - 1, \\ (\widehat{\mathbf{z}}^\top, \mathbf{0}^\top)^\top & \text{if } \ell = 2s, \end{cases}$$

for all $s \in \mathbb{N}^+$, where $\widehat{f}(\mathbf{u}_{X_{n+s}})$ and $\widehat{\mathbf{z}}$ satisfy

$$\begin{aligned} \widehat{f}(\mathbf{u}_{X_{n+s}}) &\in \text{conv} \left\{ f^{(m')}(\mathbf{u}_{X_{n+s}}) : m' \in \mathcal{M}, \frac{1}{n} \sum_{i \in [n]} \langle \mathbf{u}_{Y_i}, f^{(m')}(\mathbf{u}_{X_i}) \rangle \right. \\ &\quad \left. \geq \max_{m'' \in \mathcal{M}} \frac{1}{n} \sum_{i \in [n]} \langle \mathbf{u}_{Y_i}, f^{(m'')}(\mathbf{u}_{X_i}) \rangle - \frac{\omega}{n} \right\}, \\ \widehat{\mathbf{z}} &\in \text{conv} \left\{ \mathbf{z}^{(t')} : t' \in \mathcal{T}, \frac{1}{n} \sum_{i \in [n]} \langle \mathbf{u}_{X_i}, \mathbf{z}^{(t')} \rangle \geq \max_{t'' \in \mathcal{T}} \frac{1}{n} \sum_{i \in [n]} \langle \mathbf{u}_{X_i}, \mathbf{z}^{(t'')} \rangle - \frac{\omega}{n} \right\}. \end{aligned}$$

Theorem C.1. Suppose that Assumption C.3 holds. Fix any $d, r, r_0, L_0 \in \mathbb{N}^+$, $(\mathbf{z}^{(t)})_{t \in \mathcal{T}}$ and $(f^{(m)})_{m \in \mathcal{M}} \subset \mathcal{F}(L_0, r_0)$. Choose $\omega = \log^2 d / \sqrt{r}$. Let $\Psi^* = \Psi^*((\mathbf{z}^{(t)})_{t \in \mathcal{T}}, (f^{(m)})_{m \in \mathcal{M}}, d, r, \omega, L_0, r_0)$ be the parameter of transformer layers as in Proposition C.1. Then, for any $m \in \mathcal{M}$, $t \in \mathcal{T}$, $\eta \geq (1/\sqrt{r}) \log d$, and any $P_{X_1, Y_1 | M=m, T=t, U, \eta}$ described in Section 3.2.1, with the choice $\tau = \eta$,

$$D_{\text{KL}}(P_{X_1; T=t, U, \eta} \| Q_{\tilde{X}_s; \Psi^*, \tau, \mathcal{D}_n}) \lesssim \frac{1}{\sqrt{d}} + \frac{\log d}{\sqrt{n}}, \quad (39)$$

$$\mathbb{E} \left[D_{\text{KL}}(P_{Y_1 | X_1; M=m, U, \eta} \| Q_{\tilde{Y}_s | X_1; \Psi^*, \tau, \mathcal{D}_n}) \mid M = m, T = t, U, \eta \right] \lesssim \frac{1}{\sqrt{d}} + \frac{\log d}{\sqrt{n}} \quad (40)$$

hold for all $s \in \mathbb{N}^+$ with high probability. Hence,

$$D_{\text{KL}}(P_{X_1, Y_1; T=t, M=m, U, \eta} \| Q_{\tilde{X}_s, \tilde{Y}_s; \Psi^*, \tau, \mathcal{D}_n}) \lesssim \frac{1}{\sqrt{d}} + \frac{\log d}{\sqrt{n}}$$

holds for all $s \in \mathbb{N}^+$ with high probability.

The following corollary states that transformer can perfectly recover the input distribution with sufficiently large number of samples under stronger identifiability conditions.

Corollary C.1. Suppose that Assumptions C.1 and C.2 hold. For the transformer layers TF_{Ψ^*} in Proposition C.1, if

$$n \geq 2\omega \left(\frac{\xi_{\mathcal{T}}}{\eta r} \wedge \eta \xi_{\mathcal{M}} \right)^{-1},$$

then, given H_n and $\mathbf{h}_{2n+1}, \dots, \mathbf{h}_{2n+\ell}$ defined in equation 38, it outputs

$$\text{TF}_{\Psi^*}([H_n; \mathbf{h}_{2n+1}; \dots; \mathbf{h}_{2n+\ell}])_{2n+\ell} = \begin{cases} (f^{(\widehat{M})}(\mathbf{u}_{X_{n+s}})^\top, \mathbf{0}^\top)^\top & \text{if } \ell = 2s - 1, \\ (\mathbf{z}^{(\widehat{T})^\top}, \mathbf{0}^\top)^\top & \text{if } \ell = 2s \end{cases}$$

for all $s \in \mathbb{N}^+$ with high probability, where \widehat{T} and \widehat{M} are defined in equation 17 and equation 31.

Corollary C.1 states the with sufficiently large number of in-context samples pre-trained transformers can perfectly recover the distribution of (X_1, Y_1) under identifiability conditions. Corollary C.1 follows directly from Proposition C.1, Lemma C.1 and Lemma C.2, and its proof is omitted.

We next provide the proofs.

Proof of Theorem 3.2. We only focus on the first two steps to generate \tilde{X}_1 and \tilde{Y}_1 . We construct a transformer with the following properties: (1) For the $(2i - 1)$ -th tokens, it performs the argmax operation $\hat{f} = \arg \max_{f^{(m)}: m \in \mathcal{M}} \sum_{i' \in [n]} \langle \mathbf{u}_{Y_{i'}}, f^{(m)}(\mathbf{u}_{X_{i'}}) \rangle$ approximately, and outputs $\hat{f}(\mathbf{u}_{X_i})$. For the tokens with even index, it performs the argmax operation $\hat{z} = \arg \max_{z^{(t)}: t \in \mathcal{T}} \sum_{i' \in [n]} \langle \mathbf{u}_{Y_{i'}}, z^{(t)} \rangle$ approximately, and outputs \hat{z} .

We then sample from $\mathbf{u}_1, \dots, \mathbf{u}_d$ with a softmax probability applied on the last output token. When the current task is to generate \tilde{X}_1 , i.e., the length of the input is $2n$, the last output token is \hat{z} ; otherwise it is $\hat{f}(\mathbf{u}_{\tilde{X}_1})$. Thus we can sample \tilde{X}_1, \tilde{Y}_1 sequentially from a distribution close to that of X_1, Y_1 . By bounding the error that comes from approximating the argmax operation and sampling variation of seed data, we obtain the desired result. This completes the proof of Theorem 3.2. \square

Proof of Proposition C.1. We choose $B = \max_{x \in \mathcal{X}} \|\mathbf{u}_x\|$ so that $\sup_{z: \|z\|=1} |z^\top \mathbf{u}_x| \leq B$ holds for all $x \in \mathcal{X}$. For brevity, define $\bar{m} = |\mathcal{M}|$, $\bar{t} = |\mathcal{T}|$ and write $\mathcal{M} = [\bar{m}]$, $\mathcal{T} = [\bar{t}]$. Recall that $\bar{m} \geq \bar{t}$ by assumption. Fix $\ell \in \{0\} \cup \mathbb{N}^+$. To ease notation, let $N := 2n + \ell$, $D := r + r\bar{m} + \bar{m} + 4$ and $H_n^{(\ell)} := [\mathbf{h}_1; \dots; \mathbf{h}_{2n}; \mathbf{h}_{2n+1}; \dots; \mathbf{h}_{2n+\ell}] := [H_n; \mathbf{h}_{2n+1}; \dots; \mathbf{h}_{2n+\ell}]$.

We show the existence of transformer layers TF_{Ψ^*} such that for any $\ell \geq 0$, given the input $H_n^{(\ell)} \in \mathbb{R}^{D \times (2n+\ell)}$ at the ℓ -th step, the last token is transformed to :

$$(\text{TF}_{\Psi^*}(H_n^{(\ell)}))_{2n+\ell} = \begin{cases} \begin{pmatrix} \hat{f}(\mathbf{u}_{X_i}) \\ * \end{pmatrix} & \text{if } \ell \text{ is even,} \\ \begin{pmatrix} \hat{z} \\ * \end{pmatrix} & \text{if } \ell \text{ is odd.} \end{cases}$$

Define $\mathbf{z}^{(m)} = 0$ for $m \in [\bar{m}] \setminus [\bar{t}]$. We divide the proof into 4 steps.

Step 1. Here we aim to construct transformer layers with parameter Ψ_1^* such that it outputs

$$\text{TF}_{\Psi_1^*}(H_n^{(\ell)})_{2i-1} = \begin{pmatrix} \mathbf{u}_{X_i} \\ f^{(1)}(\mathbf{u}_{X_i}) \\ \vdots \\ f^{(\bar{m})}(\mathbf{u}_{X_i}) \\ \mathbf{0}_{\bar{m}} \\ \mathbf{p}_{2i-1} \end{pmatrix}, \quad \text{TF}_{\Psi_1^*}(H_n^{(\ell)})_{2i} = \begin{pmatrix} \mathbf{u}_{Y_i} \\ \mathbf{z}^{(1)} \\ \vdots \\ \mathbf{z}^{(\bar{m})} \\ \mathbf{0}_{\bar{m}} \\ \mathbf{p}_{2i} \end{pmatrix}.$$

Note that by assumption, there exist weights $\{(W_{\text{pre},k,1}^{(m)}, W_{\text{pre},k,2}^{(m)})\}_{k \in [L_0], m \in [\bar{m}]} \subset \mathbb{R}^{r_0 \times r} \times \mathbb{R}^{r \times r_0}$ such that

$$f^{(m)}(\mathbf{u}) = g_{L_0}^{(m)} \circ g_{L_0-1}^{(m)} \circ \dots \circ g_1^{(m)}(\mathbf{u}), \quad g_k^{(m)}(\mathbf{u}) = W_{\text{pre},k,2}^{(m)} \sigma(W_{\text{pre},k,1}^{(m)} \mathbf{u}).$$

For $k \in [L_0]$, choose parameters $\nu_{1,k}^* = (W_{1,k,1}^*, W_{1,k,2}^*) \in \mathbb{R}^{(\bar{m}r_0) \times D} \times \mathbb{R}^{D \times (\bar{m}r_0)}$ with

$$W_{1,k,1}^* = \begin{bmatrix} W_{\text{pre},k,1}^{(1)} & O_{r_0 \times (D-r)} \\ \vdots & \\ W_{\text{pre},k,1}^{(\bar{m})} & O_{r_0 \times (D-r)} \end{bmatrix}, \quad W_{1,k,2}^* = \begin{bmatrix} & O_{r \times (\bar{m}r_0)} & & & & \\ & W_{\text{pre},k,2}^{(1)} & O_{r \times ((\bar{m}-1)r_0)} & & & \\ O_{r \times r_0} & W_{\text{pre},k,2}^{(2)} & O_{r \times ((\bar{m}-2)r_0)} & & & \\ & \vdots & & & & \\ O_{r \times ((\bar{m}-1)r_0)} & W_{\text{pre},k,2}^{(\bar{m})} & & & & \\ & O_{(D-r(1+\bar{m})) \times (\bar{m}r_0)} & & & & \end{bmatrix}.$$

Let $\psi_{1,k}^* = (\mu_{\text{id}}, \nu_{1,k}^*)$ and $H_n^{(\ell)[0.5]} = [\mathbf{h}_1^{[0.5]}; \dots; \mathbf{h}_N^{[0.5]}] := \text{TF}_{(\psi_{1,1}^*, \dots, \psi_{1,L_0}^*)}(H_n^{(\ell)})$. Notice that

$$\mathbf{h}_{2i-1}^{[0.5]} = \begin{pmatrix} \mathbf{u}_{X_i} \\ f^{(1)}(\mathbf{u}_{X_i}) \\ \vdots \\ f^{(\bar{m})}(\mathbf{u}_{X_i}) \\ \mathbf{0}_{\bar{m}} \\ \mathbf{p}_{2i-1} \end{pmatrix}, \quad \mathbf{h}_{2i}^{[0.5]} = \begin{pmatrix} \mathbf{u}_{Y_i} \\ f^{(1)}(\mathbf{u}_{Y_i}) \\ \vdots \\ f^{(\bar{m})}(\mathbf{u}_{Y_i}) \\ \mathbf{0}_{\bar{m}} \\ \mathbf{p}_{2i} \end{pmatrix}.$$

Choose $\psi_{1,L_0+1}^* = (\mu_{L_0+1}^*, \nu_{\text{id}})$ with $\mu_{L_0+1}^* := \{(Q_{1,L_0+1,j}^*, K_{1,L_0+1,j}^*, V_{1,L_0+1,j}^*)\}_{j \in [4]}$ such that

$$\begin{aligned} Q_{1,L_0+1,1}^* \mathbf{h}_s^{[0.5]} &= \begin{pmatrix} (\mathbf{p}_s)_2/4 \\ -2(\mathbf{p}_s)_1 - (\mathbf{p}_s)_2 \\ 1 \\ 1 \\ \mathbf{0}_{D-4} \end{pmatrix}, & K_{1,L_0+1,1}^* \mathbf{h}_s^{[0.5]} &= \begin{pmatrix} 1 \\ 1 \\ 2(\mathbf{p}_s)_1 + (\mathbf{p}_s)_2 \\ 1/2 \\ \mathbf{0}_{D-4} \end{pmatrix}, \\ Q_{1,L_0+1,2}^* \mathbf{h}_s^{[0.5]} &= \begin{pmatrix} (\mathbf{p}_s)_2/4 \\ -2(\mathbf{p}_s)_1 - (\mathbf{p}_s)_2 \\ 1 \\ 1 \\ \mathbf{0}_{D-4} \end{pmatrix}, & K_{1,L_0+1,2}^* \mathbf{h}_s^{[0.5]} &= \begin{pmatrix} 1 \\ 1 \\ 2(\mathbf{p}_s)_1 + (\mathbf{p}_s)_2 \\ 1/4 \\ \mathbf{0}_{D-4} \end{pmatrix}, \\ Q_{1,L_0+1,3}^* \mathbf{h}_s^{[0.5]} &= \begin{pmatrix} (\mathbf{p}_s)_2/4 \\ -2(\mathbf{p}_s)_1 - (\mathbf{p}_s)_2 \\ 1 \\ 1 \\ \mathbf{0}_{D-4} \end{pmatrix}, & K_{1,L_0+1,3}^* \mathbf{h}_s^{[0.5]} &= \begin{pmatrix} 1 \\ 1 \\ 2(\mathbf{p}_s)_1 + (\mathbf{p}_s)_2 \\ -1/4 \\ \mathbf{0}_{D-4} \end{pmatrix}, \\ Q_{1,L_0+1,4}^* \mathbf{h}_s^{[0.5]} &= \begin{pmatrix} (\mathbf{p}_s)_2/4 \\ -2(\mathbf{p}_s)_1 - (\mathbf{p}_s)_2 \\ 1 \\ 1 \\ \mathbf{0}_{D-4} \end{pmatrix}, & K_{1,L_0+1,4}^* \mathbf{h}_s^{[0.5]} &= \begin{pmatrix} 1 \\ 1 \\ 2(\mathbf{p}_s)_1 + (\mathbf{p}_s)_2 \\ -1/2 \\ \mathbf{0}_{D-4} \end{pmatrix}, \end{aligned}$$

and

$$\begin{aligned} V_{1,L_0+1,1}^* \mathbf{h}_s^{[0.5]} &= -4\bar{\mathbf{h}}_s^{[0.5]}, & V_{1,L_0+1,2}^* \mathbf{h}_s^{[0.5]} &= 8\bar{\mathbf{h}}_s^{[0.5]}, \\ V_{1,L_0+1,3}^* \mathbf{h}_s^{[0.5]} &= -8\bar{\mathbf{h}}_s^{[0.5]}, & V_{1,L_0+1,4}^* \mathbf{h}_s^{[0.5]} &= 4\bar{\mathbf{h}}_s^{[0.5]}, \end{aligned}$$

where

$$\bar{\mathbf{h}}_s^{[0.5]} = \begin{pmatrix} \mathbf{0}_r \\ \mathbf{z}^{(1)} - (\mathbf{h}_{s'}^{[0.5]})_{(r+1):(2r)} \\ \vdots \\ \mathbf{z}^{(\bar{m})} - (\mathbf{h}_{s'}^{[0.5]})_{(r\bar{m}+1):(r\bar{m}+r)} \\ \mathbf{0}_{\bar{m}+4} \end{pmatrix}. \quad (41)$$

Then,

$$\begin{aligned} & \text{TF}_{\psi_{1,L_0+1}^*} (H_n^{(\ell)[0.5]})_s \\ &= \mathbf{h}_s^{[0.5]} + \sum_{s' \in [N]} \phi_1((\mathbf{p}_s)_2; 2(\mathbf{p}_s)_1 + (\mathbf{p}_s)_2, 2(\mathbf{p}_{s'})_1 + (\mathbf{p}_{s'})_2) \begin{pmatrix} \mathbf{0}_r \\ \mathbf{z}^{(1)} - (\mathbf{h}_{s'}^{[0.5]})_{(r+1):(2r)} \\ \vdots \\ \mathbf{z}^{(\bar{m})} - (\mathbf{h}_{s'}^{[0.5]})_{(r\bar{m}+1):(r\bar{m}+r)} \\ \mathbf{0}_{\bar{m}+4} \end{pmatrix} \\ &= \mathbf{h}_s^{[0.5]} + (\mathbf{p}_s)_2 \begin{pmatrix} \mathbf{0}_r \\ \mathbf{z}^{(1)} - (\mathbf{h}_s^{[0.5]})_{(r+1):(2r)} \\ \vdots \\ \mathbf{z}^{(\bar{m})} - (\mathbf{h}_s^{[0.5]})_{(r\bar{m}+1):(r\bar{m}+r)} \\ \mathbf{0}_{\bar{m}+4} \end{pmatrix}, \end{aligned}$$

where we used $2(\mathbf{p}_s)_1 + (\mathbf{p}_s)_2 = 2(\mathbf{p}_{s'})_1 + (\mathbf{p}_{s'})_2$ if and only if $s = s'$. Hence $\text{TF}_{\Psi_1^*}$ with $\Psi_1^* = (\psi_{1,1}^*, \dots, \psi_{1,L_0}^*, \psi_{1,L_0+1}^*)$ is the desired transformer.

Step 2. Let $H_n^{(\ell)[1]} = [\mathbf{h}_1^{[1]}; \dots; \mathbf{h}_N^{[1]}] := \text{TF}_{\Psi_1^*} (H_n^{(\ell)})$ be the output from $\text{TF}_{\Psi_1^*}$ constructed in Step 1. In Step 2, we aim to construct transformer layers with parameter Ψ_2^* satisfying

$$\text{TF}_{\Psi_2^*} (H_n^{(\ell)[1]})_{2i-1} = \begin{pmatrix} \mathbf{u}_{X_i} \\ f^{(1)}(\mathbf{u}_{X_i}) \\ \vdots \\ f^{(\bar{m})}(\mathbf{u}_{X_i}) \\ \mathbf{u}_{Y_i}^\top f^{(1)}(\mathbf{u}_{X_i}) \\ \vdots \\ \mathbf{u}_{Y_i}^\top f^{(\bar{m})}(\mathbf{u}_{X_i}) \\ \mathbf{p}_{2i-1} \end{pmatrix}, \quad \text{TF}_{\Psi_2^*} (H_n^{(\ell)[1]})_{2i} = \begin{pmatrix} \mathbf{u}_{Y_i} \\ \mathbf{z}^{(1)} \\ \vdots \\ \mathbf{z}^{(\bar{m})} \\ \mathbf{u}_{X_i}^\top \mathbf{z}^{(1)} \\ \vdots \\ \mathbf{u}_{X_i}^\top \mathbf{z}^{(\bar{m})} \\ \mathbf{p}_{2i} \end{pmatrix}.$$

Let ϕ_B be a function defined in equation 37. Let $\text{Attn}_{\mu_2^*}$ be an attention layer with parameters $\mu_2^* = \{(Q_{2,j,j'}^*, K_{2,j,j'}^*, V_{2,j,j'}^*)\}_{j \in [\bar{m}], j' \in [4]}$ defined as

$$Q_{2,j,1}^* \mathbf{h}_s^{[1]} = \begin{pmatrix} (\mathbf{h}_s^{[1]})_{1:r/(4B)} \\ -2(\mathbf{p}_s)_1 - (\mathbf{p}_s)_2 \\ 1 \\ 1/2 \\ \mathbf{0}_{D-3-r} \end{pmatrix}, \quad Q_{2,j,2}^* \mathbf{h}_s^{[1]} = \begin{pmatrix} (\mathbf{h}_s^{[1]})_{1:r/(4B)} \\ -2(\mathbf{p}_s)_1 - (\mathbf{p}_s)_2 \\ 1 \\ 1/4 \\ \mathbf{0}_{D-3-r} \end{pmatrix},$$

$$\begin{aligned}
Q_{2,j,3}^* \mathbf{h}_s^{[1]} &= \begin{pmatrix} (\mathbf{h}_s^{[1]})_{1:r}/(4B) \\ -2(\mathbf{p}_s)_1 - (\mathbf{p}_s)_2 \\ 1 \\ -1/4 \\ \mathbf{0}_{D-3-r} \end{pmatrix}, & Q_{2,j,4}^* \mathbf{h}_s^{[1]} &= \begin{pmatrix} (\mathbf{h}_s^{[1]})_{1:r}/(4B) \\ -2(\mathbf{p}_s)_1 - (\mathbf{p}_s)_2 \\ 1 \\ -1/2 \\ \mathbf{0}_{D-3-r} \end{pmatrix}, \\
K_{2,j,1}^* \mathbf{h}_s^{[1]} &= \begin{pmatrix} (\mathbf{h}_s^{[1]})_{(jr+1):((1+j)r)} \\ 1 \\ 2(\mathbf{p}_s)_1 + 1 - (\mathbf{p}_s)_2 \\ 1 \\ \mathbf{0}_{D-3-r} \end{pmatrix}, & K_{2,j,2}^* \mathbf{h}_s^{[1]} &= \begin{pmatrix} (\mathbf{h}_s^{[1]})_{(jr+1):((1+j)r)} \\ 1 \\ 2(\mathbf{p}_s)_1 + 1 - (\mathbf{p}_s)_2 \\ 1 \\ \mathbf{0}_{D-3-r} \end{pmatrix}, \\
K_{2,j,3}^* \mathbf{h}_s^{[1]} &= \begin{pmatrix} (\mathbf{h}_s^{[1]})_{(jr+1):((1+j)r)} \\ 1 \\ 2(\mathbf{p}_s)_1 + 1 - (\mathbf{p}_s)_2 \\ 1 \\ \mathbf{0}_{D-3-r} \end{pmatrix}, & K_{2,j,4}^* \mathbf{h}_s^{[1]} &= \begin{pmatrix} (\mathbf{h}_s^{[1]})_{(jr+1):((1+j)r)} \\ 1 \\ 2(\mathbf{p}_s)_1 + 1 - (\mathbf{p}_s)_2 \\ 1 \\ \mathbf{0}_{D-3-r} \end{pmatrix}, \\
V_{2,j,1}^* \mathbf{h}_s^{[1]} &= -4B\mathbf{e}_{r(1+\bar{m})+j}, & V_{2,j,2}^* \mathbf{h}_s^{[1]} &= 8B\mathbf{e}_{r(1+\bar{m})+j}, \\
V_{2,j,3}^* \mathbf{h}_s^{[1]} &= -8B\mathbf{e}_{r(1+\bar{m})+j}, & V_{2,j,4}^* \mathbf{h}_s^{[1]} &= 4B\mathbf{e}_{r(1+\bar{m})+j}.
\end{aligned}$$

Then, the s -th column of the output of $\text{Attn}_{\mu_2^*}$ is

$$\begin{aligned}
&\text{Attn}_{\mu_2^*}(H_n^{(\ell)[1]})_s \\
&= \mathbf{h}_s^{[1]} + \sum_{j \in [\bar{m}]} \sum_{j' \in [4]} \sum_{s' \in [N]} \sigma(\langle Q_{2,j,j'}^* \mathbf{h}_s^{[1]}, K_{2,j,j'}^* \mathbf{h}_{s'}^{[1]} \rangle) V_{2,j,j'}^* \mathbf{h}_{s'}^{[1]} \\
&= \mathbf{h}_s^{[1]} + \sum_{j \in [\bar{m}]} \sum_{s' \in [N]} \phi_B((\mathbf{h}_s^{[1]})_{1:r}^\top (\mathbf{h}_{s'}^{[1]})_{(jr+1):((1+j)r)}; 2(\mathbf{p}_s)_1 + (\mathbf{p}_s)_2, 2(\mathbf{p}_{s'})_1 + 1 - (\mathbf{p}_{s'})_2) \mathbf{e}_{r(1+\bar{m})+j}.
\end{aligned}$$

Since $2(\mathbf{p}_s)_1 + (\mathbf{p}_s)_2 = 2(\mathbf{p}_{s'})_1 + 1 - (\mathbf{p}_{s'})_2$ if and only if $(\mathbf{p}_s)_1 = (\mathbf{p}_{s'})_1$ and $(\mathbf{p}_s)_2 = 1 - (\mathbf{p}_{s'})_2$,

$$\text{Attn}_{\mu_2^*}(H_n^{(\ell)[1]})_s = \mathbf{h}_s^{[1]} + \sum_{s' \in [N]} \begin{pmatrix} \mathbf{0}_{r(1+\bar{m})} \\ (\mathbf{h}_s^{[1]})_{1:r}^\top (\mathbf{h}_{s'}^{[1]})_{(jr+1):((1+j)r)} \\ \vdots \\ (\mathbf{h}_s^{[1]})_{1:r}^\top (\mathbf{h}_{s'}^{[1]})_{(jr+1):((1+j)r)} \\ \mathbf{0}_4 \end{pmatrix} \mathbb{1}\{(\mathbf{p}_s)_1 = (\mathbf{p}_{s'})_1, (\mathbf{p}_s)_2 = 1 - (\mathbf{p}_{s'})_2\},$$

where we used $|(\mathbf{h}_s^{[1]})_{1:r}^\top (\mathbf{h}_{s'}^{[1]})_{(jr+1):((1+j)r)}| \leq B$. The desired transformer is obtained by choosing parameter $\Psi_2^* = (\psi_2^*)$, where $\psi_2^* = (\mu_2^*, \nu_{\text{id}})$. Define $H_n^{(\ell)[2]} = [\mathbf{h}_1^{[2]}; \dots; \mathbf{h}_n^{[2]}] = \text{TF}_{\Psi_2^*}(H_n^{(\ell)[1]})$.

Step 3. In this step, we aim to construct transformer layers $\text{TF}_{\Psi_3^*}$ satisfying

$$\text{TF}_{\Psi_3^*}(H_n^{(\ell)[2]})_{2i-1} = \begin{pmatrix} (\mathbf{h}_{2i-1}^{[2]})_{1:(r(\bar{m}+1))} \\ \sum_{i' \in [n]} \mathbf{u}_{Y_{i'}}^\top f^{(1)}(\mathbf{u}_{X_{i'}}) \\ \vdots \\ \sum_{i' \in [n]} \mathbf{u}_{Y_{i'}}^\top f^{(\bar{m})}(\mathbf{u}_{X_{i'}}) \\ (\mathbf{h}_{2i-1}^{[2]})_{(D-3):D} \end{pmatrix}, \quad \text{TF}_{\Psi_3^*}(H_n^{(\ell)[2]})_{2i} = \begin{pmatrix} (\mathbf{h}_{2i}^{[2]})_{1:(r(\bar{m}+1))} \\ \sum_{i' \in [n]} \mathbf{u}_{X_{i'}}^\top \mathbf{z}^{(1)} \\ \vdots \\ \sum_{i' \in [n]} \mathbf{u}_{X_{i'}}^\top \mathbf{z}^{(\bar{m})} \\ (\mathbf{h}_{2i}^{[2]})_{(D-3):D} \end{pmatrix}.$$

Note that the summations are over all $i' \in [n]$. We choose the parameter $\psi_3^* = (\mu_{\text{id}}, \nu_3^*)$ with $\nu_3^* = (W_{3,1}^*, W_{3,2}^*)$ defined as

$$\begin{aligned} W_{3,2}^* \sigma(W_{3,1}^* \mathbf{h}_s) &= W_{3,2}^* \begin{pmatrix} \sigma((\mathbf{p}_s)_2) \\ \sigma((\mathbf{p}_s)_3) \\ \sigma(2(\mathbf{p}_s)_1 - (\mathbf{p}_s)_3) \end{pmatrix} \\ &= \begin{pmatrix} \mathbf{0}_{D-2} \\ -\sigma((\mathbf{p}_s)_3) + \sigma((\mathbf{p}_s)_2) + \sigma(2(\mathbf{p}_s)_1 - (\mathbf{p}_s)_3) \\ 0 \end{pmatrix}. \end{aligned}$$

Then, it follows that

$$\begin{aligned} \text{TF}_{\psi_3^*}(H_n^{(\ell)[2]})_{2i-1} &= \begin{pmatrix} (\mathbf{h}_{2i-1}^{[2]})_{1:(D-4)} \\ i \\ 0 \\ \sigma(2(i-n)) \\ 1 \end{pmatrix} =: \begin{pmatrix} (\mathbf{h}_{2i-1}^{[2]})_{1:(D-4)} \\ \tilde{\mathbf{p}}_{2i-1} \end{pmatrix}, \\ \text{TF}_{\psi_3^*}(H_n^{(\ell)[2]})_{2i} &= \begin{pmatrix} (\mathbf{h}_{2i}^{[2]})_{1:(D-4)} \\ i \\ 1 \\ 1 + \sigma(2(i-n)) \\ 1 \end{pmatrix} =: \begin{pmatrix} (\mathbf{h}_{2i}^{[2]})_{1:(D-4)} \\ \tilde{\mathbf{p}}_{2i} \end{pmatrix}. \end{aligned}$$

Let $H_n^{(\ell)[2.5]} = [\mathbf{h}_1^{[2.5]}, \dots, \mathbf{h}_N^{[2.5]}] := \text{TF}_{\psi_3^*}(H_n^{(\ell)[2]})$. By a similar argument as in Part 1 and Part 2, we can choose $\psi_4^* = (\mu_4^*, \nu_{\text{id}})$ with $\mu_4^* = \{(Q_{4,j}^*, K_{4,j}^*, V_{4,j}^*)\}_{j \in [8]}$ such that

$$\begin{aligned} \text{TF}_{\psi_4^*}(H_n^{(\ell)[2.5]})_s &= \mathbf{h}_s^{[2.5]} + \sum_{s' \in [N]} \phi_1(1; (\tilde{\mathbf{p}}_s)_2, (\tilde{\mathbf{p}}_{s'})_3) \begin{pmatrix} \mathbf{0}_{r(\tilde{m}+1)} \\ (\mathbf{h}_{s'}^{[2.5]})_{(r(\tilde{m}+1)+1):(D-4)} \\ \mathbf{0}_4 \end{pmatrix} \\ &\quad - \sum_{s' \in [N]} \phi_1(1; 2(\tilde{\mathbf{p}}_s)_1 + (\tilde{\mathbf{p}}_s)_2, 2(\tilde{\mathbf{p}}_{s'})_1 + (\tilde{\mathbf{p}}_{s'})_2) \begin{pmatrix} \mathbf{0}_{r(\tilde{m}+1)} \\ (\mathbf{h}_{s'}^{[2.5]})_{(r(\tilde{m}+1)+1):(D-4)} \\ \mathbf{0}_4 \end{pmatrix} \\ &= \begin{pmatrix} (\mathbf{h}_s^{[2.5]})_{1:(r(\tilde{m}+1))} \\ \mathbf{0}_{r\tilde{m}} \\ (\mathbf{h}_s^{[2.5]})_{(D-3):D} \end{pmatrix} + \sum_{s' \in [N]} \phi_1(1; (\tilde{\mathbf{p}}_s)_2, (\tilde{\mathbf{p}}_{s'})_3) \begin{pmatrix} \mathbf{0}_{r(\tilde{m}+1)} \\ (\mathbf{h}_{s'}^{[2.5]})_{(r(\tilde{m}+1)+1):(D-4)} \\ \mathbf{0}_4 \end{pmatrix}. \end{aligned}$$

Note that $(\tilde{\mathbf{p}}_s)_2 = (\mathbf{p}_s)_2 \in \{0, 1\}$, $(\tilde{\mathbf{p}}_s)_3 = (\tilde{\mathbf{p}}_s)_2$ for $s \leq 2n$, and $(\tilde{\mathbf{p}}_s)_3 \geq 2$ for $s \geq 2n+1$. Thus,

$$\text{TF}_{\psi_4^*}(H_n^{(\ell)[2.5]})_s = \begin{pmatrix} (\mathbf{h}_s^{[2.5]})_{1:(r(\tilde{m}+1))} \\ \mathbf{0}_{r\tilde{m}} \\ (\mathbf{h}_s^{[2.5]})_{(D-3):D} \end{pmatrix} + \sum_{s' \in [2n]} \phi_1(1; (\mathbf{p}_s)_2, (\mathbf{p}_{s'})_3) \begin{pmatrix} \mathbf{0}_{r(\tilde{m}+1)} \\ (\mathbf{h}_{s'}^{[2.5]})_{(r(\tilde{m}+1)+1):(D-4)} \\ \mathbf{0}_4 \end{pmatrix}.$$

This gives

$$\text{TF}_{\psi_4^*}(H_n^{(\ell)[2.5]})_{2i-1} = \begin{pmatrix} (\mathbf{h}_{2i-1}^{[2.5]})_{1:(r(\tilde{m}+1))} \\ \sum_{i' \in [n]} \mathbf{u}_{Y_{i'}}^\top f^{(1)}(\mathbf{u}_{X_{i'}}) \\ \vdots \\ \sum_{i' \in [n]} \mathbf{u}_{Y_{i'}}^\top f^{(\tilde{m})}(\mathbf{u}_{X_{i'}}) \\ (\mathbf{h}_{2i-1}^{[2.5]})_{(D-3):D} \end{pmatrix}, \quad \text{TF}_{\psi_4^*}(H_n^{(\ell)[2.5]})_{2i} = \begin{pmatrix} (\mathbf{h}_{2i}^{[2.5]})_{1:(r(\tilde{m}+1))} \\ \sum_{i' \in [n]} \mathbf{u}_{X_{i'}}^\top \mathbf{z}^{(1)} \\ \vdots \\ \sum_{i' \in [n]} \mathbf{u}_{X_{i'}}^\top \mathbf{z}^{(\tilde{m})} \\ (\mathbf{h}_{2i}^{[2.5]})_{(D-3):D} \end{pmatrix}.$$

$\text{TF}_{\Psi_3^*}$ with $\Psi_3^* = (\psi_3^*, \psi_4^*)$ is the desired transformer. Let $H_n^{(\ell)[3]} = \text{TF}_{\Psi_3^*}(H_n^{(\ell)[2]})$.

Step 4. In this step, we aim to construct transformer layers satisfying

$$\text{TF}_{\Psi_4^*}(H_n^{(\ell)[3]})_{2i-1} = \begin{pmatrix} \widehat{f}(\mathbf{u}_{X_i}) \\ \mathbf{0}_{(r+1)\bar{m}} \\ \mathbf{p}_{2i-1} \end{pmatrix}, \quad \text{TF}_{\Psi_4^*}(H_n^{(\ell)[3]})_{2i} = \begin{pmatrix} \widehat{\mathbf{z}} \\ \mathbf{0}_{(r+1)\bar{m}} \\ \mathbf{p}_{2i} \end{pmatrix}.$$

where \widehat{f} and $\widehat{\mathbf{z}}$ satisfy

$$\widehat{f}(\mathbf{u}_{X_i}) \in \text{conv} \left\{ f^{(m')}(\mathbf{u}_{X_i}) : \frac{1}{n} \sum_{i \in [n]} \langle \mathbf{u}_{Y_i}, f^{(m')}(\mathbf{u}_{X_i}) \rangle \geq \max_{m'' \in [\bar{m}]} \frac{1}{n} \sum_{i \in [n]} \langle \mathbf{u}_{Y_i}, f^{(m'')}(\mathbf{u}_{X_i}) \rangle - \frac{\omega}{n} \right\},$$

$$\widehat{\mathbf{z}} \in \text{conv} \left\{ \mathbf{z}^{(t')} : \frac{1}{n} \sum_{i \in [n]} \langle \mathbf{u}_{X_i}, \mathbf{z}^{(t')} \rangle \geq \max_{t'' \in [\bar{t}]} \frac{1}{n} \sum_{i \in [n]} \langle \mathbf{u}_{X_i}, \mathbf{z}^{(t'')} \rangle - \frac{\omega}{n} \right\}.$$

To this aim, we directly apply Lemma D.2. Let $\Psi_4^* = \Psi^{\min}$. The desired transformer is $\text{TF}_{\Psi_4^*} \circ \text{TF}_{\Psi_3^*} \circ \text{TF}_{\Psi_2^*} \circ \text{TF}_{\Psi_1^*}$. This completes the proof of Proposition C.1. \square

Proof of Theorem C.1. Fix any distributions $P_{X_1; T=t, U, \eta}$ and $P_{Y_1 | X_1; M=m, U, \eta}$ introduced in Section 3.2.1. Let $\bar{m} = |\mathcal{M}|$, $\bar{t} = |\mathcal{T}|$ and write $\mathcal{M} = [\bar{m}]$, $\mathcal{T} = [\bar{t}]$. Recall that $\bar{m} \geq \bar{t}$ by assumption. We divide the proof into three parts.

Part 1. In this part we prove equation 39. For any $T = t$ and U , from Proposition C.1, there exists some $\mathcal{T}' \subset \mathcal{T} = [\bar{t}]$ such that

$$\widehat{\mathbf{z}} = \sum_{t' \in \mathcal{T}'} \alpha^{(t')} \mathbf{z}^{(t')}, \quad (42)$$

where $\alpha^{(t')} \geq 0$ for any $t' \in \mathcal{T}'$, $\sum_{t' \in \mathcal{T}'} \alpha^{(t')} = 1$, and

$$\frac{1}{n} \sum_{i \in [n]} \langle \mathbf{u}_{X_i}, \mathbf{z}^{(t')} \rangle \geq \max_{t'' \in [\bar{t}]} \frac{1}{n} \sum_{i \in [n]} \langle \mathbf{u}_{X_i}, \mathbf{z}^{(t'')} \rangle - \frac{\omega}{n} \quad (43)$$

holds for all $t' \in \mathcal{T}'$. From Lemma C.1, there exists some constant $C > 0$ such that

$$\max_{t \in [\bar{t}]} \mathbb{P} \left(\max_{t' \in \mathcal{T}'} \left| \mathbf{z}^{(t')\top} \left(\frac{1}{n} \sum_{i \in [n]} \mathbf{u}_{X_i} \right) - \frac{1}{\eta r} \mathbf{z}^{(t')\top} \mathbf{z}^{(t)} \right| \leq C\epsilon \left| T = t, U, \eta \right. \right) = 1 - \exp(-\Omega(\log^2 d)),$$

where $\epsilon := \log^2 d / \sqrt{nr} + \log d / \sqrt{dr}$. This gives

$$\begin{aligned} \frac{1}{\eta r} \langle \mathbf{z}^{(t)}, \mathbf{z}^{(t')} \rangle + C\epsilon &\geq \max_{t'' \in [\bar{t}]} \frac{1}{\eta r} \langle \mathbf{z}^{(t)}, \mathbf{z}^{(t'')} \rangle - C\epsilon - \frac{\omega}{n} \\ &= \frac{1}{\eta r} - C\epsilon - \frac{\omega}{n} \end{aligned}$$

with high probability for all $t' \in \mathcal{T}'$. Thus we have

$$\min_{t' \in \mathcal{T}'} \mathbf{z}^{(t')\top} \mathbf{z}^{(t)} \geq 1 - 2C\eta r\epsilon - \frac{\eta r\omega}{n} \quad (44)$$

with high probability. We next bound $D_{\text{KL}}(P_{X_1; T=t, U, \eta} \| Q_{\tilde{X}_s; \Psi^*, \tau, \mathcal{D}_n})$. We specifically choose $\tau \leftarrow \eta$. To this aim, we first bound the difference between log normalizing constants of two distributions:

$$\log \sum_{x' \in \mathcal{X}} \exp(\eta^{-1} \langle \mathbf{u}_{x'}, \widehat{\mathbf{z}} \rangle) - \log \sum_{x' \in \mathcal{X}} \exp(\eta^{-1} \langle \mathbf{u}_{x'}, \mathbf{z}^{(t)} \rangle).$$

From Lemma D.1, we have

$$\sup_{\mathbf{z}: \|\mathbf{z}\| \leq 1} \left| \frac{d \exp(\|\mathbf{z}\|^2/(2r\eta^2))}{\sum_{x' \in \mathcal{X}} \exp(\eta^{-1} \mathbf{z}^\top \mathbf{u}_{x'})} - 1 \right| \lesssim \frac{1}{\sqrt{d}} \log d \quad (45)$$

with high probability. Hereafter we focus on the event for U where equation 45 holds. Using $\|\mathbf{z}^{(t)}\| = 1$, we obtain

$$\log \sum_{x' \in \mathcal{X}} \exp(\eta^{-1} \langle \mathbf{u}_{x'}, \hat{\mathbf{z}} \rangle) - \log \sum_{x' \in \mathcal{X}} \exp(\eta^{-1} \langle \mathbf{u}_{x'}, \mathbf{z}^{(t)} \rangle) \quad (46)$$

$$= \log \frac{\exp(\|\hat{\mathbf{z}}\|^2/(2r\eta^2))}{\exp(\|\mathbf{z}^{(t)}\|^2/(2r\eta^2))} + O\left(\frac{\log d}{\sqrt{dr}} + \frac{\log d}{\eta r \sqrt{d}}\right) \quad (47)$$

$$= \frac{1}{2\eta^2 r} (\|\hat{\mathbf{z}} - \mathbf{z}^{(t)}\|^2 + 2(\hat{\mathbf{z}}^\top \mathbf{z}^{(t)} - 1)) + O\left(\frac{\log d}{\sqrt{dr}}\right) \quad (48)$$

$$\lesssim \frac{\|\hat{\mathbf{z}} - \mathbf{z}^{(t)}\|^2}{r\eta^2} + \frac{\log d}{\sqrt{dr}}, \quad (49)$$

where we used $\hat{\mathbf{z}}^\top \mathbf{z}^{(t)} \leq 1$ and $\eta\sqrt{r} \geq \log d$. Therefore,

$$\begin{aligned} & D_{\text{KL}}(P_{X_1; T=t, U, \eta} \| Q_{\tilde{X}_s; \Psi^*, \tau, \mathcal{D}_n}) \\ &= \sum_{x \in \mathcal{X}} P_{X_1=x|T=t, U, \eta} \left(\log \frac{\exp(\eta^{-1} \mathbf{z}^{(t)\top} \mathbf{u}_x)}{\sum_{x' \in \mathcal{X}} \exp(\eta^{-1} \mathbf{z}^{(t)\top} \mathbf{u}_{x'})} - \log \frac{\exp(\eta^{-1} \hat{\mathbf{z}}^\top \mathbf{u}_x)}{\sum_{x' \in \mathcal{X}} \exp(\eta^{-1} \hat{\mathbf{z}}^\top \mathbf{u}_{x'})} \right) \\ &= \eta^{-1} \mathbb{E}[(\mathbf{z}^{(t)} - \hat{\mathbf{z}})^\top \mathbf{u}_{X_1} | T=t, U, \eta] + \log \sum_{x' \in \mathcal{X}} \exp(\eta^{-1} \langle \mathbf{u}_{x'}, \hat{\mathbf{z}} \rangle) - \log \sum_{x' \in \mathcal{X}} \exp(\eta^{-1} \langle \mathbf{u}_{x'}, \mathbf{z}^{(t)} \rangle) \\ &= \frac{1}{\eta^2 r} (\mathbf{z}^{(t)} - \hat{\mathbf{z}})^\top \mathbf{z}^{(t)} + \frac{\|\hat{\mathbf{z}} - \mathbf{z}^{(t)}\|^2}{r\eta^2} + \frac{\log d}{\sqrt{dr}} + \frac{\log d}{\eta r \sqrt{d}} \\ &\lesssim \frac{1}{\eta} \left(\epsilon + \frac{\omega}{n} \right) + \frac{\log d}{\sqrt{dr}} \end{aligned}$$

holds with high probability, where we used Lemma D.1, equation 44 and equation 49. equation 39 follows from $\eta \geq (1/\sqrt{r}) \log d$ and $\omega = \log^2 d/\sqrt{r}$.

Part 2. In this part we prove equation 40. For any fixed $M = m$ and U , from Proposition C.1, there exists some $\mathcal{M}' \subset \mathcal{M} = [\bar{m}]$ such that

$$\hat{f}(\mathbf{u}_x) = \sum_{m' \in \mathcal{M}'} \beta^{(m')} f^{(m')}(\mathbf{u}_x), \quad (50)$$

where $\beta^{(m')} \geq 0$ for any $m' \in \mathcal{M}'$, $\sum_{m' \in \mathcal{M}'} \beta^{(m')} = 1$, and

$$\begin{aligned} \frac{1}{n} \sum_{i \in [n]} \langle \mathbf{u}_{Y_i}, f^{(m')}(\mathbf{u}_x) \rangle &\geq \max_{m'' \in [\bar{m}]} \frac{1}{n} \sum_{i \in [n]} \langle \mathbf{u}_{Y_i}, f^{(m'')}(\mathbf{u}_x) \rangle - \frac{\omega}{n} \\ &\geq \frac{1}{n} \sum_{i \in [n]} \langle \mathbf{u}_{Y_i}, f^{(m)}(\mathbf{u}_x) \rangle - \frac{\omega}{n} \end{aligned}$$

holds for all $m' \in \mathcal{M}'$. From Lemma D.1 and equation 64, Note that $\|\mathbf{u}_x\| \lesssim (1/\sqrt{r}) \log d$ holds with high probability from Lemma D.1. Thus $\max_{m \in [\bar{m}], x \in \mathcal{X}} \|f^{(m)}(\mathbf{u}_x)\| \leq 1$ holds with high probability by assumption.

$$\sup_{\mathbf{z}, \mathbf{z}' \in \mathbb{B}_r(1)} \left| \sum_{x \in \mathcal{X}} \mathbf{z}'^\top \mathbf{u}_x \exp(\eta^{-1} \mathbf{z}'^\top \mathbf{u}_x) - \frac{1}{\eta r} \mathbf{z}'^\top \mathbf{z} \exp\left(\frac{\|\mathbf{z}\|^2}{2\eta^2 r}\right) \right| \lesssim \sqrt{\frac{d}{r}} \log d, \quad (51)$$

$$\sup_{\mathbf{z} \in \mathbb{B}_r(1), x \in \mathcal{X}} \left| \mathbf{z}^\top \mathbf{u}_x \right| \lesssim \frac{\log d}{\sqrt{r}}, \quad \sup_{\mathbf{z} \in \mathbb{B}_r(1)} \left| \frac{d \exp(\|\mathbf{z}\|^2 / (2\eta^2 r))}{\sum_{x' \in \mathcal{X}} \exp(\eta^{-1} \mathbf{z}^\top \mathbf{u}_{x'})} - 1 \right| \lesssim \frac{1}{\sqrt{d}} \log d \quad (52)$$

hold with high probability with respect to U . Hereafter we focus on the event for U , where equation 51 and equation 52 hold, and $\max_{m \in [\bar{m}], x \in \mathcal{X}} \|f^{(m)}(\mathbf{u}_x)\| \leq 1$ holds. From Lemma C.2, we have

$$\begin{aligned} & \max_{m \in \mathcal{M}, t \in \mathcal{T}} \mathbb{P} \left(\max_{m' \in \mathcal{M}} \left| \frac{1}{n} \sum_{i \in [n]} \langle f^{(m')}(\mathbf{u}_{X_i}), \mathbf{u}_{Y_i} \rangle - \mathbb{E} \left[\langle f^{(m')}(\mathbf{u}_{X_1}), \mathbf{u}_{Y_1} \rangle \mid M = m, T = t, U, \eta \right] \right| \right. \\ & \quad \left. > \frac{\log^2 d}{\sqrt{nr}} \mid M = m, T = t, U, \eta \right) \\ & = \exp(-\Omega(\log^2 d)). \end{aligned}$$

Thus, we have

$$\begin{aligned} & \mathbb{E} \left[\langle f^{(m')}(\mathbf{u}_{X_1}), \mathbf{u}_{Y_1} \rangle \mid M = m, T = t, U, \eta \right] \\ & \geq \max_{m'' \in [\bar{m}]} \mathbb{E} \left[\langle f^{(m'')}(\mathbf{u}_{X_1}), \mathbf{u}_{Y_1} \rangle \mid M = m, T = t, U, \eta \right] - \frac{\omega}{n} - \frac{2 \log^2 d}{\sqrt{nr}} \\ & \geq \mathbb{E} \left[\langle f^{(m)}(\mathbf{u}_{X_1}), \mathbf{u}_{Y_1} \rangle \mid M = m, T = t, U, \eta \right] - \frac{\omega}{n} - \frac{2 \log^2 d}{\sqrt{nr}} \end{aligned}$$

and hence

$$\mathbb{E} \left[\langle f^{(m)}(\mathbf{u}_{X_1}), \mathbf{u}_{Y_1} \rangle \mid M = m, T = t, U, \eta \right] - \mathbb{E} \left[\langle \hat{f}(\mathbf{u}_{X_1}), \mathbf{u}_{Y_1} \rangle \mid M = m, T = t, U, \eta \right] \leq \frac{\omega}{n} + \frac{2 \log^2 d}{\sqrt{nr}}$$

with high probability for all $m' \in \mathcal{M}'$. By the same argument as in Part 1 combined with equation 51 and equation 52,

$$\left| \mathbb{E} \left[\langle f^{(m)}(\mathbf{u}_{X_1}), \mathbf{u}_{Y_1} \rangle - \langle f^{(m')}(\mathbf{u}_{X_1}), \mathbf{u}_{Y_1} \rangle \mid X_1 = x, T = t, M = m, U \right] \right| \quad (53)$$

$$- \frac{1}{\eta r} \left(\|f^{(m)}(\mathbf{u}_x)\|^2 - f^{(m')}(\mathbf{u}_x)^\top f^{(m)}(\mathbf{u}_x) \right) \lesssim \frac{\log d}{\sqrt{dr}} \quad (54)$$

holds for all $m' \in \mathcal{M}$ with high probability. Therefore,

$$\left| \mathbb{E} \left[\|f^{(m)}(\mathbf{u}_{X_1})\|^2 - f^{(m')}(\mathbf{u}_{X_1})^\top f^{(m)}(\mathbf{u}_{X_1}) \mid T = t, U, \eta \right] \right| \lesssim \eta r \left(\frac{\omega}{n} + \frac{\log^2 d}{\sqrt{nr}} + \frac{\log d}{\sqrt{dr}} \right) =: \epsilon \quad (55)$$

holds with high probability.

We next bound $\mathbb{E}[D_{\text{KL}}(P_{Y_1|X_1; M=m, U, \eta} \| Q_{\tilde{Y}_s|X_1; \Psi^*, \tau, \mathcal{D}_n}) \mid M = m, T = t, U, \eta]$ with the choice $\tau \leftarrow \eta$. Then,

$$\begin{aligned} & \mathbb{E}[D_{\text{KL}}(P_{Y_1|X_1; M=m, U, \eta} \| Q_{\tilde{X}_s; \Psi^*, \tau, \mathcal{D}_n}) \mid M = m, T = t, U, \eta] \\ & = \sum_{x \in \mathcal{X}} p_x^{(t)} \sum_{y \in \mathcal{X}} P_{Y_1|X_1=x, M=m, U, \eta}(y) \log \frac{P_{Y_1|X_1=x, M=m, U, \eta}(y)}{Q_{\tilde{X}_s; \Psi^*, \tau, \mathcal{D}_n}(y)}, \end{aligned}$$

where $p_x^{(t)} := \mathbb{P}(X_1 = x \mid T = t, U, \eta)$. Observe that

$$\mathbb{E}[D_{\text{KL}}(P_{Y_1|X_1; M=m, U, \eta} \| Q_{\tilde{Y}_s|X_1; \Psi^*, \mathcal{D}_n}) \mid M = m, T = t, U, \eta]$$

$$\begin{aligned}
&= \sum_{x \in \mathcal{X}} p_x^{(t)} \sum_{y \in \mathcal{X}} P_{Y_1|X_1=x, M=m, U, \eta}(y) \left(\eta^{-1} \langle f^{(m)}(\mathbf{u}_x), \mathbf{u}_y \rangle - \eta^{-1} \langle \hat{f}(\mathbf{u}_x), \mathbf{u}_y \rangle \right) \\
&\quad - \sum_{x \in \mathcal{X}} p_x^{(t)} \sum_{y \in \mathcal{X}} P_{Y_1|X_1=x, M=m, U, \eta}(y) \log \frac{\sum_{y' \in \mathcal{X}} \exp(\eta^{-1} \langle f^{(m)}(\mathbf{u}_x), \mathbf{u}_{y'} \rangle)}{\sum_{y' \in \mathcal{X}} \exp(\eta^{-1} \langle \hat{f}(\mathbf{u}_x), \mathbf{u}_{y'} \rangle)} \\
&= \eta^{-1} \mathbb{E}[\langle f^{(m)}(\mathbf{u}_{X_1}), \mathbf{u}_{Y_1} \rangle - \langle \hat{f}(\mathbf{u}_{X_1}), \mathbf{u}_{Y_1} \rangle | M = m, T = t, U, \eta] \\
&\quad - \sum_{x \in \mathcal{X}} p_x^{(t)} \log \frac{\sum_{y' \in \mathcal{X}} \exp(\eta^{-1} \langle f^{(m)}(\mathbf{u}_x), \mathbf{u}_{y'} \rangle)}{\sum_{y' \in \mathcal{X}} \exp(\eta^{-1} \langle \hat{f}(\mathbf{u}_x), \mathbf{u}_{y'} \rangle)} \\
&\lesssim \frac{\log^2 d}{\eta \sqrt{nr}} + \frac{\omega}{\eta n} + \frac{\mathbb{E}[\|\hat{f}(\mathbf{u}_x)\|^2 - \|f^{(m)}(\mathbf{u}_x)\|^2 | T = t, U, \eta]}{\eta^2 r}
\end{aligned}$$

holds with high probability, where the last inequality follows from the same argument as in the proof of Lemma C.2. Note that

$$\begin{aligned}
&\mathbb{E}[\|\hat{f}(\mathbf{u}_{X_1})\|^2 - \|f^{(m)}(\mathbf{u}_{X_1})\|^2 | T = t, U, \eta] \\
&= \mathbb{E}[\|\hat{f}(\mathbf{u}_{X_1}) - f^{(m)}(\mathbf{u}_{X_1})\|^2 | T = t, U, \eta] + 2\mathbb{E}[\hat{f}(\mathbf{u}_{X_1})^\top f^{(m)}(\mathbf{u}_{X_1}) - \|f^{(m)}(\mathbf{u}_{X_1})\|^2 | T = t, U, \eta] \\
&\leq \max_{m' \in \mathcal{M}'} \mathbb{E}[\|f^{(m')}(\mathbf{u}_{X_1}) - f^{(m)}(\mathbf{u}_{X_1})\|^2 | T = t, U, \eta] \\
&\quad + 2\mathbb{E}[\hat{f}(\mathbf{u}_{X_1})^\top f^{(m)}(\mathbf{u}_{X_1}) - \|f^{(m)}(\mathbf{u}_{X_1})\|^2 | T = t, U, \eta] \\
&\lesssim \frac{\log^2 d}{\eta \sqrt{nr}} + \frac{\omega}{\eta n} + \frac{\epsilon}{\eta^2 r} \lesssim \frac{1}{\eta} \left(\frac{\omega}{n} + \frac{\log^2 d}{\sqrt{nr}} + \frac{\log d}{\sqrt{dr}} \right)
\end{aligned}$$

holds with high probability, where the inequalities follow from Assumption C.3. The second claim follows from $\eta \geq (1/\sqrt{r}) \log d$ and $\omega = \log^2 d / \sqrt{r}$.

Part 3. The last claim follows since

$$\begin{aligned}
&D_{\text{KL}}(P_{X_1, Y_1; T=t, M=m, U, \eta} \| Q_{\tilde{X}_s; \Psi^*, \tau, \mathcal{D}_n}) \\
&= D_{\text{KL}}(P_{X_1; T=t, U, \eta} \| Q_{\tilde{X}_s; \Psi^*, \tau, \mathcal{D}_n}) + \mathbb{E}[D_{\text{KL}}(P_{Y_1|X_1; M=m, U, \eta} \| Q_{\tilde{Y}_s|X_1; \Psi^*, \tau, \mathcal{D}_n}) | M = m, T = t, U, \eta].
\end{aligned}$$

This completes the proof of Theorem C.1. \square

D Additional Auxiliary Results in Support of the Proofs

D.1 Existence of good word embeddings

Here we provide a lemma for the existence of a good event for the prior of $U = [\mathbf{u}_1, \dots, \mathbf{u}_x]^\top$.

Lemma D.1. *Let $\mathbf{u}_x \sim N(0, (1/r)I_r)$ i.i.d. Suppose that $\eta \geq (1/\sqrt{r}) \log d$. If $r = o(\log d)$, then*

$$\max_{x \in \mathcal{X}} \|\mathbf{u}_x\| \lesssim \frac{\log d}{\sqrt{r}},$$

and

$$\sup_{\mathbf{z} \in \mathbb{B}_r(1)} \left| \sum_{x \in \mathcal{X}} \left\{ \exp(\eta^{-1} \mathbf{z}^\top \mathbf{u}_x) - \exp\left(\frac{\|\mathbf{z}\|^2}{2\eta^2 r}\right) \right\} \right| \lesssim \sqrt{d} \log d, \quad (56)$$

$$\sup_{\mathbf{z} \in \mathbb{B}_r(1)} \left| \frac{d \exp(\|\mathbf{z}\|^2/(2\eta^2 r))}{\sum_{x' \in \mathcal{X}} \exp(\eta^{-1} \mathbf{z}^\top \mathbf{u}_{x'})} - 1 \right| \lesssim \frac{1}{\sqrt{d}} \log d, \quad (57)$$

$$\sup_{\mathbf{z}, \mathbf{z}' \in \mathbb{B}_r(1)} \left| \sum_{x \in \mathcal{X}} \left\{ \mathbf{z}'^\top \mathbf{u}_x \exp(\eta^{-1} \mathbf{z}^\top \mathbf{u}_x) - \mathbb{E} \left[\mathbf{z}'^\top \mathbf{u}_x \exp(\eta^{-1} \mathbf{z}^\top \mathbf{u}_x) \right] \right\} \right| \lesssim \sqrt{\frac{d}{r}} \log d, \quad (58)$$

$$\sup_{\mathbf{z}, \mathbf{z}' \in \mathbb{B}_r(1)} \left| \sum_{x \in \mathcal{X}} \frac{\mathbf{z}'^\top \mathbf{u}_x \exp(\eta^{-1} \mathbf{z}^\top \mathbf{u}_x)}{\sum_{x' \in \mathcal{X}} \exp(\eta^{-1} \mathbf{z}^\top \mathbf{u}_{x'})} - \frac{\mathbb{E}[\mathbf{z}'^\top \mathbf{u}_x \exp(\eta^{-1} \mathbf{z}^\top \mathbf{u}_x)]}{\exp(\|\mathbf{z}\|^2/(2\eta^2 r))} \right| \lesssim \frac{1}{\sqrt{dr}} \log d, \quad (59)$$

hold with probability $1 - \exp(-\Omega(\log^2 d))$.

Proof of Lemma D.1. We first derive the concentration for $(\|\mathbf{u}_x\|)_{x \in \mathcal{X}}$. Fix any $x \in \mathcal{X}$. Note that $r\|\mathbf{u}_x\|^2 \sim \chi_2^2(r)$. The concentration inequality for chi-squared distribution (see, for example, Lemma 1 in Laurent and Massart (2000)) gives

$$\mathbb{P}(r\|\mathbf{u}_x\|^2 \geq r + 2\sqrt{r\epsilon} + 2\epsilon) \leq \exp(-\epsilon).$$

Choosing $\epsilon \leftarrow \log^2 d$ gives $r\|\mathbf{u}_x\|^2 \leq (\sqrt{r} + 2 \log d)^2$ with high probability. By a union bound argument, we have

$$\max_{x \in \mathcal{X}} \|\mathbf{u}_x\| \leq \frac{\sqrt{r} + 2 \log d}{\sqrt{r}} \leq \frac{C \log d}{\sqrt{r}} \quad (60)$$

for some constant $C > 0$ with probability $1 - |\mathcal{X}| \exp(-\Omega(\log^2 d)) = 1 - \exp(-\Omega(\log^2 d))$, where we used $r = o(\log d)$. Let \mathcal{E} be the event where equation 60 holds. Let $\mathbf{z}_1, \mathbf{z}_2, \dots, \mathbf{z}_J \in \mathbb{B}_r(1)$ be the centers of a δ -covering ($\delta > 0$) of a ball in \mathbb{R}^r with radius 1, that is,

$$\mathbb{B}_r(1) \subset \bigcup_{j \in [J]} \{\mathbf{z} \in \mathbb{R}^r : \|\mathbf{z} - \mathbf{z}_j\| \leq \delta\}.$$

From a standard argument of covering number, we can take the δ -covering $(\mathbf{z}_j)_{j \in [J]}$ with $\log J = O(r \log(1 + 1/\delta))$. We specifically choose $\delta = 1/\sqrt{d}$.

Part 1: Proof of equation 56 and equation 57. In this part we first derive the uniform convergence of $\sup_{\mathbf{z} \in \mathbb{B}_r(1)} |\tilde{C}_x(\mathbf{z}) - \mathbb{E}[\tilde{C}_x(\mathbf{z})]|$, where $\tilde{C}_x(\mathbf{z}) := \exp(\eta^{-1} \mathbf{z}^\top \mathbf{u}_x) \mathbb{1}_{\mathcal{E}}$. Since $\eta^2 r \geq \log^2 d$, we have

$$\max_{x \in \mathcal{X}} \max_{j \in [J]} |\tilde{C}_x(\mathbf{z}_j)| \leq \exp\left(\frac{C \log d}{\eta \sqrt{r}}\right) \leq e^C.$$

Now fix any $j \in [J]$. From Hoeffding's inequality,

$$\mathbb{P}\left(\left| \sum_{x \in \mathcal{X}} (\tilde{C}_x(\mathbf{z}_j) - \mathbb{E}[\tilde{C}_x(\mathbf{z}_j)]) \right| > \epsilon\right) \leq 2 \exp\left(-\frac{\epsilon^2}{2de^{2C}}\right).$$

Choosing $\epsilon \leftarrow \sqrt{d} \log d$ gives $|\sum_{x \in \mathcal{X}} (\tilde{C}_x(\mathbf{z}_j) - \mathbb{E}[\tilde{C}_x(\mathbf{z}_j)])| \leq \sqrt{d} \log d$ with probability $1 - \exp(-\Omega(\log^2 d))$. By a union bound, we have $\max_{j \in [J]} |\sum_{x \in \mathcal{X}} (\tilde{C}_x(\mathbf{z}_j) - \mathbb{E}[\tilde{C}_x(\mathbf{z}_j)])| \leq \sqrt{d} \log d$ with probability

$$1 - J \exp(-\Omega(\log^2 d)) = 1 - \exp(-\Omega(\log^2 d) + O(r \log d)) = 1 - \exp(-\Omega(\log^2 d)).$$

Let $C_x(\mathbf{z}) := \exp(\eta^{-1}\mathbf{z}^\top \mathbf{u}_x)$. For any fixed $\mathbf{z} \in \mathbb{B}_r(1)$, there exists some $j' \in [J]$ such that $\|\mathbf{z} - \mathbf{z}_{j'}\| \leq \delta$. Note that on the event \mathcal{E} , $C_x(\mathbf{z}) = \tilde{C}_x(\mathbf{z})$ and thus

$$\begin{aligned} |C_x(\mathbf{z}) - \tilde{C}_x(\mathbf{z}_{j'})| &\leq \left| \exp(\eta^{-1}\mathbf{z}^\top \mathbf{u}_x) - \exp(\eta^{-1}\mathbf{z}_{j'}^\top \mathbf{u}_x) \right| \\ &= \exp(\eta^{-1}\mathbf{z}_{j'}^\top \mathbf{u}_x) \left| \exp(\eta^{-1}(\mathbf{z} - \mathbf{z}_{j'})^\top \mathbf{u}_x) - 1 \right| \\ &\leq 2e\eta^{-1} |(\mathbf{z}_{j'} - \mathbf{z})^\top \mathbf{u}_x| \\ &\lesssim \delta \frac{\log d}{\eta\sqrt{r}} \leq \frac{1}{\sqrt{d}}, \end{aligned}$$

where we used $\exp(\eta^{-1}\mathbf{z}_{j'}^\top \mathbf{u}_x) \leq \exp(\eta^{-1} \max_{x \in \mathcal{X}} \|\mathbf{u}_x\|) \lesssim 1$ by equation 60, $|1 - e^x| \leq 2|x|$ for $x \in [-1, 1]$ and $|\eta^{-1}(\mathbf{z} - \mathbf{z}_{j'})^\top \mathbf{u}_x| \leq \eta^{-1}\delta \max_{x \in \mathcal{X}} \|\mathbf{u}_x\| \leq 1$ for sufficiently large d in the second inequality. Furthermore, a similar argument combined with Cauchy-Schwarz inequality gives

$$\begin{aligned} |\mathbb{E}[C_x(\mathbf{z})] - \mathbb{E}[\tilde{C}_x(\mathbf{z}_{j'})]| &\leq |\mathbb{E}[C_x(\mathbf{z})] - \mathbb{E}[C_x(\mathbf{z}_{j'})]| + |\mathbb{E}[C_x(\mathbf{z}_{j'})] - \mathbb{E}[\tilde{C}_x(\mathbf{z}_{j'})]| \\ &= \left| \exp\left(\frac{\|\mathbf{z}\|^2}{2\eta^2 r}\right) - \exp\left(\frac{\|\mathbf{z}_{j'}\|^2}{2\eta^2 r}\right) \right| + \mathbb{E} \left[\exp(\eta^{-1}\mathbf{z}_{j'}^\top \mathbf{u}_x) \mathbb{1}_{\mathcal{E}^c} \right] \\ &\leq \exp\left(\frac{\|\mathbf{z}\|^2}{2\eta^2 r}\right) \left| 1 - \exp\left(\frac{\|\mathbf{z}_{j'}\|^2 - \|\mathbf{z}\|^2}{2\eta^2 r}\right) \right| + \sqrt{\mathbb{E} \left[\exp(2\eta^{-1}\mathbf{z}_{j'}^\top \mathbf{u}_x) \right] \mathbb{P}(\mathcal{E}^c)} \\ &\leq \exp\left(\frac{\|\mathbf{z}\|^2}{2\eta^2 r}\right) \left| 1 - \exp\left(\frac{(\|\mathbf{z}_{j'}\| - \|\mathbf{z}\|)(\|\mathbf{z}_{j'}\| + \|\mathbf{z}\|)}{2\eta^2 r}\right) \right| + \exp\left(\frac{\|\mathbf{z}_{j'}\|^2}{\eta^2 r}\right) \exp(-\Omega(\log^2 d)) \\ &\leq \frac{2\sqrt{e}\delta}{\eta^2 r} + \exp(-\Omega(\log^2 d)) \\ &\lesssim \frac{1}{\sqrt{d} \log^2 d} + \exp(-\Omega(\log^2 d)). \end{aligned}$$

Hence by a union bound argument,

$$\sup_{\mathbf{z} \in \mathbb{B}_r(1)} \left| \sum_{x \in \mathcal{X}} (C_x(\mathbf{z}) - \mathbb{E}[C_x(\mathbf{z})]) \right| \lesssim d \left(\frac{1}{\sqrt{d}} + \frac{1}{\sqrt{d} \log^2 d} + \exp(-\Omega(\log^2 d)) \right) + \sqrt{d} \log d \quad (61)$$

$$\lesssim \sqrt{d} \log d \quad (62)$$

holds with high probability.

Using $\mathbb{E}[C_x(\mathbf{z})] = \exp(\|\mathbf{z}\|^2/(2\eta^2 r)) \geq 1$ and equation 62, we obtain

$$\sup_{\mathbf{z} \in \mathbb{B}_r(1)} \left| \frac{1}{d\mathbb{E}[C_x(\mathbf{z})]} \sum_{x \in \mathcal{X}} C_x(\mathbf{z}) - 1 \right| \lesssim \frac{1}{\sqrt{d}} \log d. \quad (63)$$

Thus

$$\sup_{\mathbf{z} \in \mathbb{B}_r(1)} \left| \frac{d\mathbb{E}[C_x(\mathbf{z})]}{\sum_{x \in \mathcal{X}} C_x(\mathbf{z})} - 1 \right| \lesssim \frac{1}{\sqrt{d}} \log d$$

holds with high probability for sufficiently large d .

Part 2: Proof of equation 58 We first derive a concentration inequality for $\sum_{x \in \mathcal{X}} \mathbf{z}_{j'}^\top \mathbf{u}_x \exp(\eta^{-1} \mathbf{z}_j^\top \mathbf{u}_x)$ uniformly over all $j, j' \in [J]$. Fix any $j, j' \in [J]$. Define $D_x(\mathbf{z}, \mathbf{z}') := \mathbf{z}'^\top \mathbf{u}_x \exp(\eta^{-1} \mathbf{z}^\top \mathbf{u}_x)$ and $\tilde{D}_x(\mathbf{z}, \mathbf{z}') := \mathbf{z}'^\top \mathbf{u}_x \exp(\eta^{-1} \mathbf{z}^\top \mathbf{u}_x) \mathbb{1}_{\mathcal{E}}$. Note that since $\eta \geq \log d / \sqrt{r}$,

$$|\tilde{D}_x(\mathbf{z}_j, \mathbf{z}_{j'})| \leq \frac{1}{2\sqrt{r}} \exp\left(\frac{1}{2\eta\sqrt{r}} \log d\right) \log d \leq \frac{\sqrt{e}}{2\sqrt{r}} \log d$$

holds for $d \geq 4$. Furthermore,

$$\begin{aligned} \mathbb{E}[\tilde{D}_x(\mathbf{z}_j, \mathbf{z}_{j'})] &\leq \mathbb{E}[D_x(\mathbf{z}_j, \mathbf{z}_{j'})] = \mathbf{z}_{j'}^\top \mathbb{E}\left[\mathbf{u}_x \exp(\eta^{-1} \mathbf{z}_j^\top \mathbf{u}_x)\right] \\ &= \eta \mathbf{z}_{j'}^\top \mathbb{E}\left[\frac{d}{d\mathbf{z}} \exp(\eta^{-1} \mathbf{z}^\top \mathbf{u}_x) \Big|_{\mathbf{z}=\mathbf{z}_j}\right] \\ &= \eta \mathbf{z}_{j'}^\top \frac{d}{d\mathbf{z}} \mathbb{E}\left[\exp(\eta^{-1} \mathbf{z}^\top \mathbf{u}_x)\right] \Big|_{\mathbf{z}=\mathbf{z}_j} \\ &= \eta \mathbf{z}_{j'}^\top \frac{d}{d\mathbf{z}} \exp\left(\frac{\|\mathbf{z}\|^2}{2\eta^2 r}\right) \Big|_{\mathbf{z}=\mathbf{z}_j} \\ &= \frac{1}{\eta r} \mathbf{z}_{j'}^\top \mathbf{z}_j \exp\left(\frac{\|\mathbf{z}_j\|^2}{2\eta^2 r}\right), \end{aligned} \tag{64}$$

and

$$\begin{aligned} \mathbb{E}[\tilde{D}_x(\mathbf{z}_j, \mathbf{z}_{j'})^2] &\leq \mathbb{E}[D_x(\mathbf{z}_j, \mathbf{z}_{j'})^2] = \mathbb{E}\left[(\mathbf{z}_{j'}^\top \mathbf{u}_x)^2 \exp(2\eta^{-1} \mathbf{z}_j^\top \mathbf{u}_x)\right] \\ &= \mathbb{E}\left[\text{tr}\left(\mathbf{z}_{j'} \mathbf{z}_{j'}^\top \mathbf{u}_x \mathbf{u}_x^\top \exp(2\eta^{-1} \mathbf{z}_j^\top \mathbf{u}_x)\right)\right] \\ &= \frac{\eta^2}{4} \mathbb{E}\left[\text{tr}\left(\mathbf{z}_{j'} \mathbf{z}_{j'}^\top \frac{d}{d\mathbf{z}} \frac{d}{d\mathbf{z}^\top} \exp(2\eta^{-1} \mathbf{z}^\top \mathbf{u}_x) \Big|_{\mathbf{z}=\mathbf{z}_j}\right)\right] \\ &= \frac{\eta^2}{4} \text{tr}\left(\mathbf{z}_{j'} \mathbf{z}_{j'}^\top \frac{d}{d\mathbf{z}} \frac{d}{d\mathbf{z}^\top} \mathbb{E}\left[\exp(2\eta^{-1} \mathbf{z}^\top \mathbf{u}_x)\right] \Big|_{\mathbf{z}=\mathbf{z}_j}\right) \\ &= \frac{\eta^2}{4} \text{tr}\left(\mathbf{z}_{j'} \mathbf{z}_{j'}^\top \frac{d}{d\mathbf{z}} \frac{d}{d\mathbf{z}^\top} \exp\left(\frac{2\|\mathbf{z}\|^2}{\eta^2 r}\right) \Big|_{\mathbf{z}=\mathbf{z}_j}\right) \\ &= \frac{\eta^2}{4} \text{tr}\left(\mathbf{z}_{j'} \mathbf{z}_{j'}^\top \left(\frac{4}{\eta^2 r} I + \frac{16}{\eta^4 r^2} \mathbf{z}_j \mathbf{z}_j^\top\right) \exp\left(\frac{2\|\mathbf{z}_j\|^2}{\eta^2 r}\right)\right) \\ &= \frac{\eta^2}{4} \left(\frac{4}{\eta^2 r} + \frac{16}{\eta^4 r^2} (\mathbf{z}_j \mathbf{z}_j^\top)^2\right) \exp\left(\frac{2\|\mathbf{z}_j\|^2}{\eta^2 r}\right) \\ &\leq \frac{5e^2}{r}, \end{aligned} \tag{65}$$

where we used $\eta^2 r \geq \log^2 d \geq 1$ for $d \geq 4$, and $\|\mathbf{z}_j\| \leq 1$ in the last inequality. From Bernstein inequality, we obtain

$$\mathbb{P}\left(\left|\sum_{x \in \mathcal{X}} (\tilde{D}_x(\mathbf{z}_j, \mathbf{z}_{j'}) - \mathbb{E}[\tilde{D}_x(\mathbf{z}_j, \mathbf{z}_{j'})])\right| \geq \epsilon\right) \leq 2 \exp\left(-\frac{(1/2)\epsilon^2}{5de^2/r + (1/6)\sqrt{e/r} \log de}\right).$$

Choosing $\epsilon \leftarrow \sqrt{d/r} \log d$ gives

$$\mathbb{P}\left(\left|\sum_{x \in \mathcal{X}} (\tilde{D}_x(\mathbf{z}_j, \mathbf{z}_{j'}) - \mathbb{E}[\tilde{D}_x(\mathbf{z}_j, \mathbf{z}_{j'})])\right| \leq \sqrt{\frac{d}{r}} \log d\right) \leq \exp\left(-\Omega\left(\frac{(d/r) \log^2 d}{d/r + (\sqrt{d}/r) \log^2 d}\right)\right)$$

$$= \exp(-\Omega(\log^2 d)).$$

By a union bound argument, we have $\max_{j,j' \in [J]} |\sum_{x \in \mathcal{X}} (\tilde{D}_x(\mathbf{z}_j, \mathbf{z}_{j'}) - \mathbb{E}[\tilde{D}_x(\mathbf{z}_j, \mathbf{z}_{j'})])| \leq \sqrt{d/r} \log d$ with high probability. From Cauchy-Schwarz inequality, we have

$$\begin{aligned} 0 &\leq \mathbb{E}[D_x(\mathbf{z}_j, \mathbf{z}_{j'})] - \mathbb{E}[\tilde{D}_x(\mathbf{z}_j, \mathbf{z}_{j'})] = \mathbb{E}\left[\mathbf{z}_{j'}^\top \mathbf{u}_x \exp\left(\eta^{-1} \mathbf{z}_j^\top \mathbf{u}_x\right) \mathbb{1}_{\mathcal{E}^c}\right] \\ &\leq \sqrt{\mathbb{E}[D_x(\mathbf{z}_j, \mathbf{z}_{j'})^2] \mathbb{P}(\mathcal{E}^c)} \leq \sqrt{\frac{5e^2}{r}} \exp(-\Omega(\log^2 d)), \end{aligned}$$

where the last inequality follows from equation 65. Since $\tilde{D}_x(\mathbf{z}_j, \mathbf{z}_{j'}) = D_x(\mathbf{z}_j, \mathbf{z}_{j'})$ on the event \mathcal{E} , we have

$$\max_{j,j' \in [J]} \left| \sum_{x \in \mathcal{X}} (D_x(\mathbf{z}_j, \mathbf{z}_{j'}) - \mathbb{E}[D_x(\mathbf{z}_j, \mathbf{z}_{j'})]) \right| \lesssim \sqrt{\frac{d}{r}} \log d + \frac{1}{\sqrt{r}} \exp(-\Omega(\log^2 d)) \lesssim \sqrt{\frac{d}{r}} \log d \quad (66)$$

with probability $1 - \exp(-\Omega(\log^2 d)) - \mathbb{P}(\mathcal{E}^c) = 1 - \exp(-\Omega(\log^2 d))$. A similar argument as in Part 1 gives equation 58.

Part 3: Proof of equation 59. Fix any $\mathbf{z}, \mathbf{z}' \in \mathbb{B}_r(1)$. equation 57 and equation 58 yield

$$\begin{aligned} &\left| \sum_{x \in \mathcal{X}} \frac{D_x(\mathbf{z}, \mathbf{z}')}{\sum_{x' \in \mathcal{X}} C_{x'}(\mathbf{z})} - \frac{\mathbb{E}[D_x(\mathbf{z}, \mathbf{z}')]}{\mathbb{E}[C_x(\mathbf{z})]} \right| \\ &\leq \frac{1}{d\mathbb{E}[C_{x'}(\mathbf{z})]} \left| \sum_{x \in \mathcal{X}} D_x(\mathbf{z}, \mathbf{z}') \left(1 - \frac{d\mathbb{E}[C_{x'}(\mathbf{z})]}{\sum_{x' \in \mathcal{X}} C_{x'}(\mathbf{z})}\right) \right| + \frac{1}{d\mathbb{E}[C_{x'}(\mathbf{z})]} \left| \sum_{x \in \mathcal{X}} (D_x(\mathbf{z}, \mathbf{z}') - \mathbb{E}[D_x(\mathbf{z}, \mathbf{z}')]) \right| \\ &\leq \left| \frac{1}{d} \sum_{x \in \mathcal{X}} D_x(\mathbf{z}, \mathbf{z}') \right| \left| 1 - \frac{d\mathbb{E}[C_{x'}(\mathbf{z})]}{\sum_{x' \in \mathcal{X}} C_{x'}(\mathbf{z})} \right| + \frac{1}{d} \left| \sum_{x \in \mathcal{X}} (D_x(\mathbf{z}, \mathbf{z}') - \mathbb{E}[D_x(\mathbf{z}, \mathbf{z}')]) \right| \\ &\lesssim \left(\frac{\mathbf{z}'^\top \mathbf{z}}{\eta r} \exp\left(\frac{\|\mathbf{z}\|^2}{2\eta^2 r}\right) + \frac{1}{\sqrt{dr}} \log d \right) \left(\frac{1}{\sqrt{d}} \log d \right) + \frac{1}{\sqrt{dr}} \log d \\ &\lesssim \frac{1}{\sqrt{dr}} \log d, \end{aligned}$$

where we used $\mathbb{E}[C_{x'}(\mathbf{z})] \geq 1$ in the second inequality, and equation 64 in the third inequality. The last inequality follows since $\|\mathbf{z}\|^2 \leq 1$, $|\mathbf{z}'^\top \mathbf{z}| \leq 1$ and $\eta^2 r \geq \log^2 d$. Since $\mathbf{z}, \mathbf{z}' \in \mathbb{B}_r(1)$ are arbitrary, this gives equation 59.

This completes the proof of Lemma D.1. \square

D.2 Construction of selection layers

We implement the deletion layer that performs argmin operation. The lemma is a direct application of Proposition M.2 of Bai et al. (2023).

Lemma D.2 (Minimum by Transformer). *Fix $\omega > 0$, $r \in \mathbb{N}^+$ and $\bar{m} \geq 2$. Then, there exist transformer layers $\text{TF}_{\Psi^{\min}}$ with $\Psi^{\min} = \Psi^{\min}(\omega, \bar{m}, r)$ satisfying that*

- it consists of 5 transformer layers with the width of FNN $O(\bar{m}^2)$, and the number of heads of attention layers $O(\bar{m})$,

- for any $N \in \mathbb{N}^+$ and $H = [\mathbf{h}_1, \dots, \mathbf{h}_N] \in \mathbb{R}^{r(\bar{m}+1)+\bar{m}+4}$ of the form

$$\mathbf{h}_s = \begin{pmatrix} \mathbf{x}_0 \\ \mathbf{x}_1 \\ \vdots \\ \mathbf{x}_{\bar{m}} \\ v_1 \\ \vdots \\ v_{\bar{m}} \\ \mathbf{p}_s \end{pmatrix},$$

where $\mathbf{x}_m \in \mathbb{R}^r$ for $m \in \{0\} \cup [\bar{m}]$, $v_m \in [-1, 1]$ for $m \in [\bar{m}]$, and \mathbf{p}_s is defined in Section 3.2.1, $\text{TF}_{\Psi^{\min}}$ outputs

$$\text{TF}_{\Psi^{\min}}(H)_s = (\mathbf{x}^\top, \mathbf{0}^\top)^\top,$$

where $\mathbf{x} \in \text{conv}\{\mathbf{x}_m : m \in [\bar{m}], v_m \leq \min_{m' \in [\bar{m}]} v_{m'} + \omega\}$.

Proof of Lemma D.2. To ease notation we write $D = r + r\bar{m} + \bar{m} + 4$. We divide the proof into 4 parts.

Part 1. Let $\text{FFN}_{\nu_1^{\min}}$ be a feed-forward neural network with $\nu_1^{\min} = (W_{1,1}^{\min}, W_{1,2}^{\min})$ such that

$$\begin{aligned} W_{1,2}^{\min} \sigma(W_{1,1}^{\min} \mathbf{h}) &= W_{1,2}^{\min} \begin{pmatrix} \sigma((\mathbf{h})_{r(1+\bar{m})+1} - (\mathbf{h})_{r(1+\bar{m})+2}) \\ \sigma((\mathbf{h})_{r(1+\bar{m})+1} - (\mathbf{h})_{r(1+\bar{m})+3}) \\ \vdots \\ \sigma((\mathbf{h})_{r(1+\bar{m})+1} - (\mathbf{h})_{r(1+\bar{m})+\bar{m}}) \\ \vdots \\ \sigma((\mathbf{h})_{r(1+\bar{m})+\bar{m}} - (\mathbf{h})_{r(1+\bar{m})+1}) \\ \vdots \\ \sigma((\mathbf{h})_{r(1+\bar{m})+\bar{m}} - (\mathbf{h})_{r(1+\bar{m})+\bar{m}-1}) \\ \sigma((\mathbf{h})_{(r(1+\bar{m})+1):(r(1+\bar{m})+\bar{m})}) \\ \sigma(-(\mathbf{h})_{(r(1+\bar{m})+1):(r(1+\bar{m})+\bar{m})}) \end{pmatrix} \\ &= \begin{pmatrix} \mathbf{0}_{r(1+\bar{m})} \\ -(\mathbf{h})_{r(1+\bar{m})+1} + \sum_{m':m' \neq 1} \sigma((\mathbf{h})_{r(1+\bar{m})+1} - (\mathbf{h})_{r(1+\bar{m})+m'}) \\ \vdots \\ -(\mathbf{h})_{r(1+\bar{m})+\bar{m}} + \sum_{m':m' \neq \bar{m}} \sigma((\mathbf{h})_{r(1+\bar{m})+\bar{m}} - (\mathbf{h})_{r(1+\bar{m})+m'}) \\ \mathbf{0}_4 \end{pmatrix}. \end{aligned}$$

Then,

$$\text{FFN}_{\nu_1^{\min}}(\mathbf{h}_s) = \begin{pmatrix} \mathbf{x}_0 \\ \mathbf{x}_1 \\ \vdots \\ \mathbf{x}_{\bar{m}} \\ v_1^{(1)} \\ \vdots \\ v_{\bar{m}}^{(1)} \\ \mathbf{p}_s \end{pmatrix},$$

where $v_m^{(1)} = \sum_{m':m' \neq m} \sigma(v_m - v_{m'})$. Note that $v_m^{(1)} \leq \omega$ implies $v_m \leq \min_{m':m' \neq m} v_{m'} + \omega$. Choose $\psi_1^{\min} := (\mu_{\text{id}}, \nu_1^{\min})$.

Part 2. Define $\text{FFN}_{\nu_2^{\min}}$ as a feed-forward neural network with $\nu_2^{\min} = (W_{2,1}^{\min}, W_{2,2}^{\min})$ such that

$$\begin{aligned} W_{2,2}^{\min} \sigma(W_{2,1}^{\min} \mathbf{h}) &= W_{2,2}^{\min} \begin{pmatrix} \sigma((\mathbf{h})_{r(1+\bar{m})+1}) \\ \vdots \\ \sigma((\mathbf{h})_{r(1+\bar{m})+\bar{m}}) \\ \sigma(-(\mathbf{h})_{r(1+\bar{m})+1}) \\ \vdots \\ \sigma(-(\mathbf{h})_{r(1+\bar{m})+\bar{m}}) \\ \sigma((\mathbf{h})_D - (\mathbf{h})_{r(1+\bar{m})+1}/\omega) \\ \vdots \\ \sigma((\mathbf{h})_D - (\mathbf{h})_{r(1+\bar{m})+\bar{m}}/\omega) \end{pmatrix} \\ &= \begin{pmatrix} \mathbf{0}_{r(1+\bar{m})} \\ -(\mathbf{h})_{r(1+\bar{m})+1} + \sigma((\mathbf{h})_D - (\mathbf{h})_{r(1+\bar{m})+1}/\omega) \\ \vdots \\ -(\mathbf{h})_{r(1+\bar{m})+\bar{m}} + \sigma((\mathbf{h})_D - (\mathbf{h})_{r(1+\bar{m})+\bar{m}}/\omega) \\ \mathbf{0}_4 \end{pmatrix}, \end{aligned}$$

Then,

$$\text{FFN}_{\nu_2^{\min}}(\mathbf{h}_s) = \begin{pmatrix} \mathbf{x}_0 \\ \mathbf{x}_1 \\ \vdots \\ \mathbf{x}_{\bar{m}} \\ v_1^{(2)} \\ \vdots \\ v_{\bar{m}}^{(2)} \\ \mathbf{p}_s \end{pmatrix},$$

where $v_m^{(2)} = \sigma(1 - v_m^{(1)}/\omega)$. Let $\psi_2^{\min} := (\mu_{\text{id}}, \nu_2^{\min})$.

Part 3. Define $\text{FFN}_{\nu_3^{\min}}$ as a feed-forward neural network with $\nu_3^{\min} = (W_{3,1}^{\min}, W_{3,2}^{\min})$ such that

$$W_{3,2}^{\min} \sigma(W_{3,1}^{\min} \mathbf{h}) = W_{3,2}^{\min} \begin{pmatrix} \sigma((\mathbf{h})_{r(1+\bar{m})+1}) \\ \vdots \\ \sigma((\mathbf{h})_{r(1+\bar{m})+\bar{m}}) \\ \sigma(-(\mathbf{h})_{r(1+\bar{m})+1}) \\ \vdots \\ \sigma(-(\mathbf{h})_{r(1+\bar{m})+\bar{m}}) \\ \sigma((\mathbf{h})_D) \\ \sigma((\mathbf{h})_D - (\mathbf{h})_{r(1+\bar{m})+1}) \\ \sigma((\mathbf{h})_D - (\mathbf{h})_{r(1+\bar{m})+1} - (\mathbf{h})_{r(1+\bar{m})+2}) \\ \vdots \\ \sigma((\mathbf{h})_D - (\mathbf{h})_{r(1+\bar{m})+1} - (\mathbf{h})_{r(1+\bar{m})+2} - \cdots - (\mathbf{h})_{r(1+\bar{m})+\bar{m}}) \end{pmatrix}$$

$$= \begin{pmatrix} \mathbf{0}_{r(1+\bar{m})} \\ -(\mathbf{h})_{r(1+\bar{m})+1} + V_1^{(3)}(\mathbf{h}) \\ -(\mathbf{h})_{r(1+\bar{m})+2} + V_2^{(3)}(\mathbf{h}) \\ \vdots \\ -(\mathbf{h})_{r(1+\bar{m})+\bar{m}} + V_{\bar{m}}^{(3)}(\mathbf{h}) \\ \mathbf{0}_4 \end{pmatrix},$$

where

$$V_m^{(3)}(\mathbf{h}) := \sigma((\mathbf{h})_D - (\mathbf{h})_{r(1+\bar{m})+1} - \cdots - (\mathbf{h})_{r(1+\bar{m})+m-1}) \\ - \sigma((\mathbf{h})_D - (\mathbf{h})_{r(1+\bar{m})+1} - \cdots - (\mathbf{h})_{r(1+\bar{m})+m}).$$

Then,

$$\text{FFN}_{\nu_3^{\min}}(\mathbf{h}_s) = \mathbf{h}_s + W_{3,2}^{\min} \sigma(W_{3,1}^{\min} \mathbf{h}_s) = \begin{pmatrix} \mathbf{x}_0 \\ \mathbf{x}_1 \\ \vdots \\ \mathbf{x}_{\bar{m}} \\ v_1^{(3)} \\ \vdots \\ v_{\bar{m}}^{(3)} \\ \mathbf{0} \\ * \end{pmatrix},$$

where $v_m^{(3)} = \sigma(1 - \sum_{m' \in [m-1]} v_{m'}^{(2)}) - \sigma(1 - \sum_{m' \in [m]} v_{m'}^{(2)})$. Note that since there always exists some $m^* \in [\bar{m}]$ with $v_{m^*} = \min_{m \in [\bar{m}]} v_m$, $v_{m^*}^{(1)} = 0$ and $v_{m^*}^{(2)} = 1$. This implies $v_{\bar{m}}^{(2)} = 0$. Thus

$$\sum_{m \in [\bar{m}]} v_m^{(3)} = \sigma(1) - \sigma\left(1 - \sum_{m' \in [\bar{m}]} v_{m'}^{(2)}\right) = 1 - 0 = 1.$$

We also have $v_m^{(3)} \geq 0$ for all $m \in [\bar{m}]$. Furthermore, $v_m^{(3)} > 0$ implies $v_m^{(1)} < \omega$ and thus $v_m \leq \min_{m' \in [\bar{m}]} v_{m'} + \omega$. Then, $\sum_m v_m^{(3)} \mathbf{x}_m$ is a convex combination of $\{\mathbf{x}_m : v_m \leq \min_{m' \in [\bar{m}]} v_{m'} + \omega\}$. Let $\psi_{\min,3} := (\mu_{\text{id}}, \nu_3^{\min})$.

Part 4. Define $\text{TF}_{\mu_4^{\min}}$ with a parameter $\mu_4^{\min} = \{(Q_{4,j,j'}^{\min}, K_{4,j,j'}^{\min}, V_{4,j,j'}^{\min})\}_{j \in [\bar{m}], j' \in [8]}$ such that

$$Q_{4,j,1}^{\min} \mathbf{h} = \begin{pmatrix} (\mathbf{h})_{r(1+\bar{m})+j/4} \\ -2(\mathbf{h})_{D-3} - (\mathbf{h})_{D-2} \\ (\mathbf{h})_D \\ (\mathbf{h})_{D/2} \\ \mathbf{0}_{D-4} \end{pmatrix}, Q_{4,j,2}^{\min} \mathbf{h} = \begin{pmatrix} (\mathbf{h})_{r(1+\bar{m})+j/4} \\ -2(\mathbf{h})_{D-3} - (\mathbf{h})_{D-2} \\ (\mathbf{h})_D \\ (\mathbf{h})_{D/4} \\ \mathbf{0}_{D-4} \end{pmatrix}, \\ Q_{4,j,3}^{\min} \mathbf{h} = \begin{pmatrix} (\mathbf{h})_{r(1+\bar{m})+j/4} \\ -2(\mathbf{h})_{D-3} - (\mathbf{h})_{D-2} \\ (\mathbf{h})_D \\ -(\mathbf{h})_{D/4} \\ \mathbf{0}_{D-4} \end{pmatrix}, Q_{4,j,4}^{\min} \mathbf{h} = \begin{pmatrix} (\mathbf{h})_{r(1+\bar{m})+j/4} \\ -2(\mathbf{h})_{D-3} - (\mathbf{h})_{D-2} \\ (\mathbf{h})_D \\ -(\mathbf{h})_{D/2} \\ \mathbf{0}_{D-4} \end{pmatrix},$$

$$\begin{aligned}
Q_{4,j,5}^{\min} \mathbf{h} &= \begin{pmatrix} (\mathbf{h})_{D/4} \\ -2(\mathbf{h})_{D-3} - (\mathbf{h})_{D-2} \\ (\mathbf{h})_D \\ (\mathbf{h})_{D/2} \\ \mathbf{0}_{D-4} \end{pmatrix}, Q_{4,j,6}^{\min} \mathbf{h} = \begin{pmatrix} (\mathbf{h})_{D/4} \\ -2(\mathbf{h})_{D-3} - (\mathbf{h})_{D-2} \\ (\mathbf{h})_D \\ (\mathbf{h})_{D/4} \\ \mathbf{0}_{D-4} \end{pmatrix}, \\
Q_{4,j,7}^{\min} \mathbf{h} &= \begin{pmatrix} (\mathbf{h})_{D/4} \\ -2(\mathbf{h})_{D-3} - (\mathbf{h})_{D-2} \\ (\mathbf{h})_D \\ -(\mathbf{h})_{D/4} \\ \mathbf{0}_{D-4} \end{pmatrix}, Q_{4,j,8}^{\min} \mathbf{h} = \begin{pmatrix} (\mathbf{h})_{D/4} \\ -2(\mathbf{h})_{D-3} - (\mathbf{h})_{D-2} \\ (\mathbf{h})_D \\ -(\mathbf{h})_{D/2} \\ \mathbf{0}_{D-4} \end{pmatrix}, \\
K_{4,j,1}^{\min} \mathbf{h} &= \begin{pmatrix} (\mathbf{h})_D \\ (\mathbf{h})_D \\ 2(\mathbf{h})_{D-3} + (\mathbf{h})_{D-2} \\ (\mathbf{h})_D \\ \mathbf{0}_{D-4} \end{pmatrix}, K_{4,j,2}^{\min} \mathbf{h} = \begin{pmatrix} (\mathbf{h})_D \\ (\mathbf{h})_D \\ 2(\mathbf{h})_{D-3} + (\mathbf{h})_{D-2} \\ (\mathbf{h})_D \\ \mathbf{0}_{D-4} \end{pmatrix}, \\
K_{4,j,3}^{\min} \mathbf{h} &= \begin{pmatrix} (\mathbf{h})_D \\ (\mathbf{h})_D \\ 2(\mathbf{h})_{D-3} + (\mathbf{h})_{D-2} \\ (\mathbf{h})_D \\ \mathbf{0}_{D-4} \end{pmatrix}, K_{4,j,4}^{\min} \mathbf{h} = \begin{pmatrix} (\mathbf{h})_D \\ (\mathbf{h})_D \\ 2(\mathbf{h})_{D-3} + (\mathbf{h})_{D-2} \\ (\mathbf{h})_D \\ \mathbf{0}_{D-4} \end{pmatrix}, \\
K_{4,j,5}^{\min} &= K_{4,j,1}^{\min}, K_{4,j,6}^{\min} = K_{4,j,2}^{\min}, K_{4,j,7}^{\min} = K_{4,j,3}^{\min}, K_{4,j,8}^{\min} = K_{4,j,4}^{\min}, \\
V_{4,j,1}^{\min} \mathbf{h} &= -4 \begin{pmatrix} (\mathbf{h})_{(jr+1):(j+1)r} \\ \mathbf{0}_{D-r} \end{pmatrix}, V_{4,j,2}^{\min} \mathbf{h} = 8 \begin{pmatrix} (\mathbf{h})_{(jr+1):(j+1)r} \\ \mathbf{0}_{D-r} \end{pmatrix}, \\
V_{4,j,3}^{\min} \mathbf{h} &= -8 \begin{pmatrix} (\mathbf{h})_{(jr+1):(j+1)r} \\ \mathbf{0}_{D-r} \end{pmatrix}, V_{4,j,4}^{\min} \mathbf{h} = 4 \begin{pmatrix} (\mathbf{h})_{(jr+1):(j+1)r} \\ \mathbf{0}_{D-r} \end{pmatrix}, \\
V_{4,j,5}^{\min} \mathbf{h} &= 4 \begin{pmatrix} (\mathbf{h})_{1:(r(1+\bar{m}))} \\ \mathbf{0}_{D-r(1+\bar{m})} \end{pmatrix}, V_{4,j,6}^{\min} \mathbf{h} = -8 \begin{pmatrix} (\mathbf{h})_{1:(r(1+\bar{m}))} \\ \mathbf{0}_{D-r(1+\bar{m})} \end{pmatrix}, \\
V_{4,j,7}^{\min} \mathbf{h} &= 8 \begin{pmatrix} (\mathbf{h})_{1:(r(1+\bar{m}))} \\ \mathbf{0}_{D-r(1+\bar{m})} \end{pmatrix}, V_{4,j,8}^{\min} \mathbf{h} = -4 \begin{pmatrix} (\mathbf{h})_{1:(r(1+\bar{m}))} \\ \mathbf{0}_{D-r(1+\bar{m})} \end{pmatrix}.
\end{aligned}$$

Let $\tilde{H} = [\tilde{\mathbf{h}}_1; \dots; \tilde{\mathbf{h}}_N] := \text{TF}_{(\psi_1^{\min}, \psi_2^{\min}, \psi_3^{\min})}(H)$. Then,

$$\begin{aligned}
&\text{Attn}_{\mu_4^{\min}}(\tilde{H})_s \\
&= \tilde{\mathbf{h}}_s + \sum_{s' \in [N]} \phi_1((\tilde{\mathbf{h}}_s)_{r(1+\bar{m})+j}; 2(\tilde{\mathbf{h}}_s)_{D-3} + (\tilde{\mathbf{h}}_s)_{D-2}, 2(\tilde{\mathbf{h}}_{s'})_{D-3} + (\tilde{\mathbf{h}}_{s'})_{D-2}) \begin{pmatrix} (\tilde{\mathbf{h}}_{s'})_{(jr+1):(j+1)r} \\ \mathbf{0}_{D-r} \end{pmatrix} \\
&\quad - \sum_{s' \in [N]} \phi_1(1; 2(\tilde{\mathbf{h}}_s)_{D-3} + (\tilde{\mathbf{h}}_s)_{D-2}, 2(\tilde{\mathbf{h}}_{s'})_{D-3} + (\tilde{\mathbf{h}}_{s'})_{D-2}) \begin{pmatrix} (\tilde{\mathbf{h}}_{s'})_{1:(r(1+\bar{m}))} \\ \mathbf{0}_{D-r} \end{pmatrix} \\
&= \begin{pmatrix} \sum_{m \in [\bar{m}]} v_m^{(3)} \mathbf{x}_m \\ \mathbf{0}_{(r+1)\bar{m}} \\ \mathbf{p}_s \end{pmatrix}.
\end{aligned}$$

Define $\psi_4^{\min} = (\mu_4^{\min}, \nu_{\text{id}})$. We can easily implement a transformer layer $\text{TF}_{\psi_5^{\min}}$ such that $\text{TF}_{\psi_5^{\min}}(H)_s = ((\mathbf{h}_s)_{1:D-4}, \mathbf{0}_4^\top)^\top$. The desired transformer is obtained by $\text{TF}_{\Psi^{\min}}$ with $\Psi^{\min} = (\psi_1^{\min}, \psi_2^{\min}, \psi_3^{\min}, \psi_4^{\min}, \psi_5^{\min})$.

This completes the proof of Lemma D.2. \square

E More Details for Numerical Experiments

In this section, we provide more details regarding the numerical experiments in Section 4.

E.1 Prompts

We show an example of the serialized tables and the prompts we have used.

The serialized seed data.

```
preg is 3.0, plas is 128.0, pres is 68.0, skin is 25.0, insu is 155.0,  
  ↪ mass is 34.3, pedi is 0.372, age is 29.0, class is 0.0.  
preg is 1.0, plas is 85.0, pres is 66.0, skin is 29.0, insu is 0.0,  
  ↪ mass is 26.6, pedi is 0.351, age is 31.0, class is 0.0.  
preg is 4.0, plas is 112.0, pres is 78.0, skin is 39.0, insu is 0.0,  
  ↪ mass is 37.6, pedi is 0.412, age is 22.0, class is 0.0.  
preg is 0.0, plas is 137.0, pres is 40.0, skin is 35.0, insu is 168.0,  
  ↪ mass is 43.1, pedi is 2.288, age is 33.0, class is 1.0.  
preg is 3.0, plas is 173.0, pres is 82.0, skin is 48.0, insu is 465.0,  
  ↪ mass is 38.4, pedi is 2.137, age is 25.0, class is 1.0.  
preg is 10.0, plas is 115.0, pres is 70.0, skin is 30.0, insu is 0.0,  
  ↪ mass is 35.3, pedi is 0.134, age is 29.0, class is 0.0.
```

The prompts.

```
Sys: You are an expert statistician in analyzing diabetes condition. Your  
  ↪ objective is to predict/guess new chunk of records that closely  
  ↪ mirrors the statistical properties of a provided real-world records.  
  ↪ This predicted/guessed records collection will be instrumental for  
  ↪ downstream tasks such as developing personalized treatment plans,  
  ↪ conducting epidemiological studies, and optimizing healthcare  
  ↪ resource allocation. You are good at in-context learning. You always  
  ↪ think step-by-step, use chain-of-thoughts, and your common sense.  
User: The following is the text of the observed records of diabetes  
  ↪ condition. Investigate it carefully. Each row represents the number  
  ↪ of times pregnant, plasma glucose concentration, diastolic blood  
  ↪ pressure, triceps skin fold thickness, 2-Hour serum insulin, body  
  ↪ mass index, diabetes pedigree function, age, class (class value 1 is  
  ↪ interpreted as tested positive for diabetes) . Guess and craft new  
  ↪ 20 records of textural representation as if they were from the same  
  ↪ source of the given records. Do not replicate the real records and  
  ↪ the good example predicted records I will give you. Discover the  
  ↪ pattern and trends of the real records. Your guess should preserve  
  ↪ statistical properties. All pairs of correlation of variables should  
  ↪ be very close to real-world records. All variables marginal  
  ↪ distribution should be closely align with the real dataset. Learn  
  ↪ complicated associations and interplays. Introduce interpretable  
  ↪ variation. The guess should closely resemble real records in terms  
  ↪ of trends and patterns. Use your domain knowledge and understanding  
  ↪ of diabetes and other factors when you are predicting. Output  
  ↪ predicted records in the same format as real-world records format.  
  ↪ Do not order the guessed records.
```

```
User: [serialized seed data]
```

```
User: Your response must only exclusively contain your guessed records with  
  ↪ the same format as the provided example (e.g. object is value). No  
  ↪ other words. Please always think step-by-step, use chain-of-thoughts,  
  ↪ and your common sense. The guessed 20 records are:
```

E.2 More details about the spurious correlation experiment

We evaluate spurious correlations across three datasets: Diabetes, Heart Failure, and Gender, and investigate four groups: the minority group, the majority group, the overall group, and the worst group. Among them, the worst group identifies the subgroup of subjects with the highest errors in predictions, and the overall group includes all subjects.

For the Diabetes data, $(y, a) = (\text{class}, \text{skin})$. The minority group includes patients diagnosed with diabetes who have no triceps skinfold thickness measurements, i.e., $\{\text{class} = 1, \text{skin} = 0\}$, and those without diabetes but with positive measurements, i.e., $\{\text{class} = 0, \text{skin} > 0\}$, reflecting negative correlations. The majority group includes patients with diabetes and measured skin thickness, i.e., $\{\text{class} = 1, \text{skin} > 0\}$, and those without diabetes and no skin thickness measurements, i.e., $\{\text{class} = 0, \text{skin} = 0\}$, reflecting positive correlations.

For the HeartFailure data, $(y, a) = (\text{death event}, \text{sex})$. The minority group includes female patients who have death events, i.e., $\{\text{death event} = 1, \text{sex} = 0\}$, and those male patients who have not experienced death events, i.e., $\{\text{death event} = 0, \text{sex} = 1\}$. The majority group includes male patients with death events, i.e., $\{\text{death event} = 1, \text{sex} = 1\}$, as well as those female patients without death events, i.e., $\{\text{death event} = 0, \text{sex} = 0\}$.

For the Gender data, $(y, a) = (\text{gender}, \text{long hair})$. The minority group include female subjects without long hair, i.e., $\{\text{gender} = 1, \text{long hair} = 0\}$, and male subjects with long hair, i.e., $\{\text{gender} = 0, \text{long hair} = 1\}$. The majority group includes female subjects with long hair, i.e., $\{\text{gender} = 1, \text{long hair} = 1\}$, and male subjects without long hair, i.e., $\{\text{gender} = 0, \text{long hair} = 0\}$.

We determine the spurious correlation by two main criteria: the meaning in practice, and the correlation in the whole data. For the Diabetes data, a `skin` value of 0 indicates missing the skinfold measurement. If the data trend reveals a strong positive correlation between `skin` and `class`, then there exists a risk of under-representation for those without skinfold measurement who have diabetes. For the Heart Failure data, an apparent correlation between `sex` and the `death event` indicator may suggest a potential gender bias in predictions. For the Gender data, while the gender does not inherently correlate with hair length, the observed data suggests that females typically have long hair and males typically have short hair, which could potentially lead to a biased classifier. Finally, we select the (y, a) pairs such that they exhibit minimal correlations in the complete dataset, and we ensure that neither positive nor negative correlations dominate.

E.3 Ablation studies

We show through simulations that the generated synthetic data remains effective even without contextual information, and GPT-4 learns the distribution of the tabular data, and does not memorize the individual samples, when asked to generate the synthetic data.

We consider the following simulation model with 9 features X_1, \dots, X_9 .

$$X_1 \sim \mathcal{N}(0, 1), \quad X_2 \sim \mathcal{N}(0, 1), \quad X_3 = 0.5X_1 + 0.3X_2 + \epsilon_3, \quad \epsilon_3 \sim \mathcal{N}(0, 0.5),$$

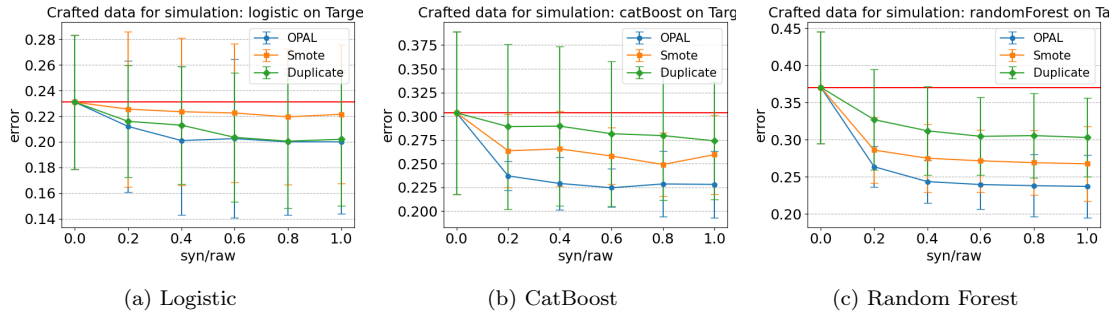


Figure 4: Imbalanced classification: comparison of OPAL, SMOTE, and duplication, with the simulated data, and the three classifiers, logistic regression, CatBoost, and random forest. The red line represents the mean error of the classifier trained with the raw data.

$$\begin{aligned}
 X_4 &= X_1 \cdot \epsilon_4, \quad \epsilon_4 \sim \mathcal{N}(0, 1), \quad X_5 = 0.5X_3 + \epsilon_5, \quad \epsilon_5 \sim \mathcal{N}(0, 1), \quad X_6 \sim \mathcal{N}(0, 1), \\
 X_7 &\sim \mathcal{N}(0, 1), \quad X_8 = X_2 \cdot X_3, \quad X_9 = X_1 \cdot X_2,
 \end{aligned}$$

Let $f(X_1, X_2, X_3, X_9) = 1.5 + 0.7X_1 - 0.6X_2 + 0.8X_3 + 0.4X_9$, and $Z_i = f(X_1^i, X_2^i, X_3^i, X_9^i) + \epsilon_i$, with $\epsilon_i \sim \mathcal{N}(0, 0.5)$, we generate the response

$$Y_i = \mathbb{1}\{Z_i > \text{median}(\{Z_j\}_{j \geq 1})\}.$$

To show that OPAL remains effective without contextual information, we generate a total of 1000 samples, with 400 as the testing samples. Among the remaining 600 samples, we randomly select 100 samples as the raw data, in which labels '0' and '1' are treated as the minority and majority groups, respectively, with a ratio of 1 : 9 between the two groups. We then use Algorithm 1 to perform LLM-based oversampling. Figure 4 reports the misclassification error rate based on 5 data replications with the tree classifiers. We see that OPAL consistently outperforms the benchmark solutions, and the improvement is more evident for nonlinear classifiers.

To show that GPT-4 learns the distribution of the tabular data, rather than memorizing the individual samples, we compute the median distance to the closest records (DCR) for our data. DCR quantifies the proximity between each synthetic sample and the nearest sample in the original data. A larger DCR suggests an enhanced diversity of the synthetic data compared to the original data Xu et al. (2019). Table 3 reports the DCR results for the three datasets, Diabetes, HeartFailure, and Gender. We see that OPAL achieves a comparable DCR to the DCR when using the rest of real samples not fed into GPT-4. Meanwhile, the DCR of OPAL is better or comparable to that of SMOTE.

Dataset	Real	OPAL	SMOTE
Diabetes	0.160	0.153	0.088
HeartFailure	0.361	0.304	0.242
Gender	0.049	0.056	0.070

Table 3: Median DCR across Real, OPAL, and SMOTE data.

We acknowledge the possibility that publicly available data might have been included in OpenAI’s pre-training, which is a common issue for all LLM-based synthetic data generators. Our simulation here seems to suggest that GPT-4 learns the underlying data pattern rather than memorizing the data, because it has not seen this simulated data before.

E.4 More numerical results

This section contains additional results for the numerical experiments in Section 4.

In particular, Figure 5 and Figure 6 report the results for imbalanced classification with logistic regression and CatBoost, which show similar qualitative patterns as Figure 2 in Section 4.2. Figure 7 and Figure 8 report the results for spurious correlations with logistic regression and CatBoost, which again show similar qualitative patterns as Figure 3 in Section 4.3.

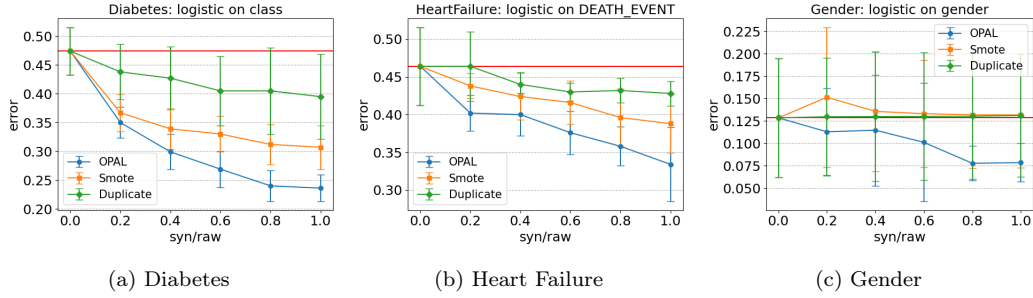


Figure 5: Imbalanced classification: comparison of OPAL, SMOTE, and duplication, with three datasets, Diabetes, Heart Failure, and Gender, and the logistic regression classifier. The red line represents the mean error of the classifier trained with the raw data.

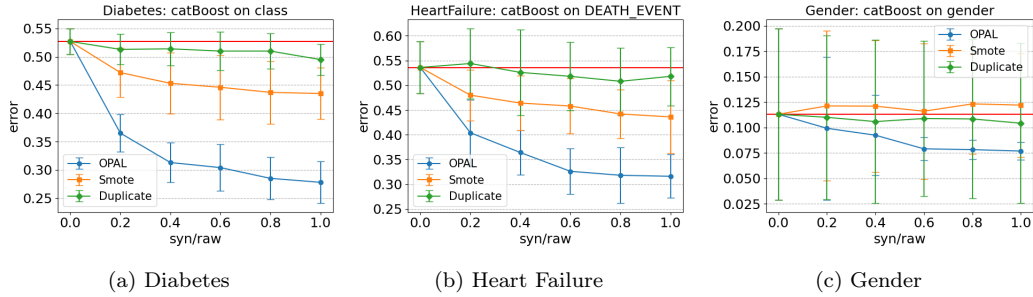


Figure 6: Imbalanced classification: comparison of OPAL, SMOTE, and duplication, with three datasets, Diabetes, Heart Failure, and Gender, and the CatBoost classifier. The red line represents the mean error of the classifier trained with the raw data.

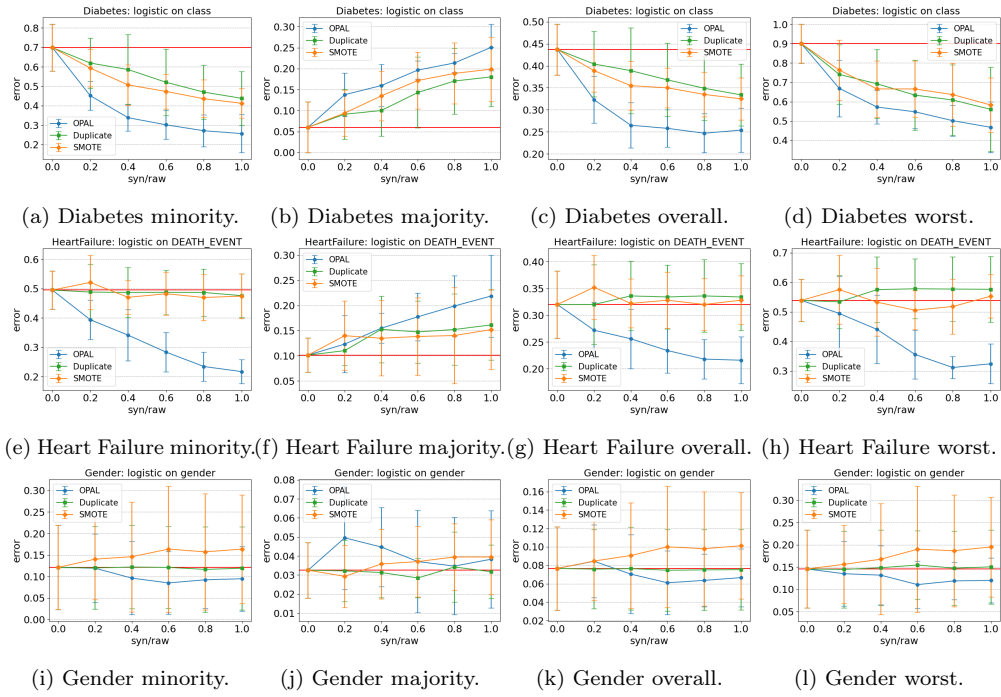


Figure 7: Spurious correlations: comparison of OPAL, SMOTE, and duplication, with three datasets, Diabetes, Heart Failure, Gender, and the logistic regression classifier. The red line represents the mean error of the classifier trained with the raw data



Figure 8: Spurious correlations: comparison of OPAL, SMOTE, and duplication, with three datasets, Diabetes, Heart Failure, Gender, and the CatBoost classifier. The red line represents the mean error of the classifier trained with the raw data.

Table 4: Errors for imbalanced classification tasks corresponding to Figure 2.

Dataset	Classifier	Method	$\frac{SN}{raw}$					
			0%	20%	40%	60%	80%	100%
Diabetes	Logistic	OPAL	0.474 ± 0.041	0.350 ± 0.027	0.299 ± 0.031	0.269 ± 0.032	0.240 ± 0.027	0.236 ± 0.023
		SMOTE	0.474 ± 0.041	0.367 ± 0.032	0.339 ± 0.035	0.330 ± 0.031	0.312 ± 0.035	0.307 ± 0.038
		Duplication	0.474 ± 0.041	0.438 ± 0.048	0.427 ± 0.054	0.405 ± 0.061	0.405 ± 0.075	0.395 ± 0.074
	CatBoost	OPAL	0.527 ± 0.023	0.365 ± 0.033	0.313 ± 0.035	0.304 ± 0.041	0.285 ± 0.037	0.278 ± 0.037
		SMOTE	0.527 ± 0.023	0.472 ± 0.043	0.453 ± 0.054	0.446 ± 0.057	0.437 ± 0.055	0.435 ± 0.045
		Duplication	0.527 ± 0.023	0.513 ± 0.027	0.514 ± 0.029	0.510 ± 0.034	0.510 ± 0.031	0.495 ± 0.027
	RandomForest	OPAL	0.541 ± 0.041	0.388 ± 0.028	0.339 ± 0.037	0.298 ± 0.045	0.291 ± 0.054	0.269 ± 0.029
		SMOTE	0.541 ± 0.041	0.489 ± 0.057	0.468 ± 0.075	0.459 ± 0.080	0.452 ± 0.081	0.452 ± 0.072
		Duplication	0.541 ± 0.041	0.515 ± 0.040	0.517 ± 0.052	0.519 ± 0.039	0.525 ± 0.027	0.519 ± 0.025
Heart Failure	Logistic	OPAL	0.464 ± 0.052	0.402 ± 0.024	0.400 ± 0.028	0.376 ± 0.029	0.358 ± 0.026	0.334 ± 0.049
		SMOTE	0.463 ± 0.052	0.438 ± 0.016	0.424 ± 0.030	0.416 ± 0.029	0.396 ± 0.038	0.388 ± 0.039
		Duplication	0.464 ± 0.052	0.464 ± 0.046	0.440 ± 0.016	0.430 ± 0.012	0.432 ± 0.016	0.428 ± 0.016
	CatBoost	OPAL	0.536 ± 0.052	0.404 ± 0.066	0.364 ± 0.045	0.326 ± 0.046	0.318 ± 0.057	0.316 ± 0.044
		SMOTE	0.536 ± 0.052	0.480 ± 0.051	0.464 ± 0.055	0.458 ± 0.055	0.442 ± 0.050	0.436 ± 0.073
		Duplication	0.536 ± 0.052	0.544 ± 0.071	0.526 ± 0.087	0.518 ± 0.069	0.508 ± 0.068	0.518 ± 0.059
	RandomForest	OPAL	0.604 ± 0.077	0.458 ± 0.085	0.372 ± 0.063	0.344 ± 0.073	0.306 ± 0.056	0.290 ± 0.045
		SMOTE	0.604 ± 0.077	0.516 ± 0.077	0.478 ± 0.083	0.470 ± 0.080	0.460 ± 0.062	0.466 ± 0.072
		Duplication	0.604 ± 0.077	0.582 ± 0.066	0.574 ± 0.055	0.566 ± 0.063	0.560 ± 0.070	0.544 ± 0.060
Gender	Logistic	OPAL	0.128 ± 0.066	0.113 ± 0.049	0.115 ± 0.062	0.101 ± 0.066	0.078 ± 0.019	0.078 ± 0.021
		SMOTE	0.128 ± 0.066	0.151 ± 0.078	0.136 ± 0.067	0.133 ± 0.060	0.132 ± 0.060	0.132 ± 0.059
		Duplication	0.128 ± 0.066	0.130 ± 0.066	0.130 ± 0.072	0.130 ± 0.071	0.130 ± 0.070	0.131 ± 0.069
	CatBoost	OPAL	0.113 ± 0.084	0.099 ± 0.070	0.092 ± 0.040	0.079 ± 0.011	0.078 ± 0.009	0.077 ± 0.009
		SMOTE	0.113 ± 0.084	0.121 ± 0.074	0.121 ± 0.065	0.116 ± 0.067	0.123 ± 0.049	0.122 ± 0.051
		Duplication	0.113 ± 0.084	0.110 ± 0.081	0.106 ± 0.080	0.109 ± 0.077	0.108 ± 0.078	0.104 ± 0.079
	RandomForest	OPAL	0.120 ± 0.070	0.105 ± 0.054	0.087 ± 0.025	0.074 ± 0.008	0.071 ± 0.007	0.070 ± 0.008
		SMOTE	0.120 ± 0.070	0.116 ± 0.068	0.116 ± 0.060	0.109 ± 0.059	0.115 ± 0.052	0.121 ± 0.050
		Duplication	0.120 ± 0.070	0.117 ± 0.075	0.115 ± 0.069	0.115 ± 0.067	0.115 ± 0.068	0.114 ± 0.070

Table 5: Errors under spurious correlation corresponding to subplots (a), (b), (c), (d) in Figure 7, Figure 8, and Figure 3, Diabetes.

Dataset	Class	Classifier	Method	$\frac{syn}{raw}$					
				0%	20%	40%	60%	80%	100%
Diabetes	Minority	Logistic	OPAL	0.699 ± 0.121	0.451 ± 0.074	0.338 ± 0.069	0.301 ± 0.074	0.271 ± 0.083	0.256 ± 0.099
			Duplication	0.699 ± 0.121	0.619 ± 0.130	0.586 ± 0.181	0.520 ± 0.171	0.470 ± 0.139	0.438 ± 0.139
			SMOTE	0.699 ± 0.121	0.593 ± 0.097	0.507 ± 0.104	0.473 ± 0.089	0.436 ± 0.097	0.412 ± 0.076
		CatBoost	OPAL	0.731 ± 0.102	0.593 ± 0.060	0.506 ± 0.035	0.449 ± 0.032	0.410 ± 0.046	0.403 ± 0.056
			Duplication	0.731 ± 0.102	0.721 ± 0.098	0.698 ± 0.091	0.680 ± 0.105	0.673 ± 0.117	0.654 ± 0.107
			SMOTE	0.731 ± 0.102	0.698 ± 0.105	0.664 ± 0.085	0.641 ± 0.092	0.613 ± 0.097	0.565 ± 0.086
		RandomForest	OPAL	0.853 ± 0.081	0.629 ± 0.056	0.528 ± 0.027	0.460 ± 0.049	0.430 ± 0.054	0.416 ± 0.052
			Duplication	0.853 ± 0.081	0.738 ± 0.104	0.676 ± 0.077	0.619 ± 0.067	0.569 ± 0.099	0.542 ± 0.036
			SMOTE	0.853 ± 0.081	0.742 ± 0.081	0.658 ± 0.125	0.594 ± 0.124	0.556 ± 0.134	0.536 ± 0.108
	Majority	Logistic	OPAL	0.060 ± 0.061	0.138 ± 0.052	0.160 ± 0.050	0.197 ± 0.022	0.214 ± 0.023	0.251 ± 0.056
			Duplication	0.060 ± 0.061	0.091 ± 0.060	0.100 ± 0.061	0.143 ± 0.085	0.171 ± 0.078	0.180 ± 0.071
			SMOTE	0.060 ± 0.061	0.094 ± 0.055	0.135 ± 0.059	0.172 ± 0.068	0.189 ± 0.073	0.199 ± 0.077
		CatBoost	OPAL	0.049 ± 0.033	0.083 ± 0.060	0.095 ± 0.046	0.100 ± 0.048	0.119 ± 0.055	0.114 ± 0.053
			Duplication	0.049 ± 0.033	0.056 ± 0.040	0.061 ± 0.046	0.075 ± 0.038	0.080 ± 0.039	0.102 ± 0.043
			SMOTE	0.049 ± 0.033	0.070 ± 0.038	0.092 ± 0.037	0.094 ± 0.055	0.114 ± 0.055	0.109 ± 0.046
		RandomForest	OPAL	0.022 ± 0.038	0.044 ± 0.024	0.074 ± 0.033	0.098 ± 0.047	0.114 ± 0.047	0.119 ± 0.047
			Duplication	0.022 ± 0.038	0.041 ± 0.029	0.065 ± 0.031	0.089 ± 0.038	0.103 ± 0.048	0.122 ± 0.051
			SMOTE	0.022 ± 0.038	0.036 ± 0.037	0.073 ± 0.031	0.101 ± 0.050	0.108 ± 0.053	0.128 ± 0.054
	Overall	Logistic	OPAL	0.437 ± 0.058	0.323 ± 0.053	0.265 ± 0.052	0.258 ± 0.042	0.247 ± 0.044	0.254 ± 0.050
			Duplication	0.437 ± 0.058	0.404 ± 0.074	0.389 ± 0.097	0.368 ± 0.083	0.349 ± 0.072	0.334 ± 0.070
			SMOTE	0.437 ± 0.058	0.389 ± 0.049	0.355 ± 0.051	0.350 ± 0.046	0.335 ± 0.051	0.325 ± 0.048
		CatBoost	OPAL	0.449 ± 0.042	0.382 ± 0.020	0.336 ± 0.017	0.305 ± 0.024	0.290 ± 0.047	0.284 ± 0.052
			Duplication	0.449 ± 0.042	0.446 ± 0.038	0.435 ± 0.036	0.430 ± 0.045	0.428 ± 0.057	0.426 ± 0.045
			SMOTE	0.449 ± 0.042	0.439 ± 0.047	0.428 ± 0.037	0.416 ± 0.037	0.408 ± 0.043	0.378 ± 0.040
RandomForest		OPAL	0.510 ± 0.035	0.388 ± 0.032	0.340 ± 0.018	0.311 ± 0.043	0.300 ± 0.045	0.294 ± 0.048	
		Duplication	0.510 ± 0.035	0.451 ± 0.055	0.424 ± 0.037	0.401 ± 0.031	0.378 ± 0.047	0.370 ± 0.011	
		SMOTE	0.510 ± 0.035	0.452 ± 0.045	0.418 ± 0.053	0.393 ± 0.069	0.374 ± 0.073	0.370 ± 0.060	
Worst	Logistic	OPAL	0.900 ± 0.101	0.669 ± 0.146	0.572 ± 0.087	0.548 ± 0.086	0.502 ± 0.080	0.467 ± 0.131	
		Duplication	0.900 ± 0.101	0.741 ± 0.153	0.692 ± 0.178	0.634 ± 0.181	0.609 ± 0.182	0.560 ± 0.218	
		SMOTE	0.900 ± 0.101	0.764 ± 0.157	0.666 ± 0.146	0.666 ± 0.146	0.637 ± 0.163	0.583 ± 0.141	
	CatBoost	OPAL	0.872 ± 0.071	0.831 ± 0.115	0.672 ± 0.080	0.672 ± 0.068	0.576 ± 0.102	0.572 ± 0.077	
		Duplication	0.872 ± 0.071	0.880 ± 0.069	0.845 ± 0.134	0.808 ± 0.126	0.825 ± 0.129	0.780 ± 0.102	
		SMOTE	0.872 ± 0.071	0.898 ± 0.125	0.850 ± 0.138	0.810 ± 0.161	0.810 ± 0.117	0.766 ± 0.115	
	RandomForest	OPAL	0.974 ± 0.040	0.851 ± 0.109	0.706 ± 0.049	0.637 ± 0.090	0.630 ± 0.056	0.611 ± 0.096	
		Duplication	0.974 ± 0.040	0.839 ± 0.038	0.762 ± 0.083	0.725 ± 0.123	0.670 ± 0.134	0.673 ± 0.124	
		SMOTE	0.974 ± 0.040	0.860 ± 0.127	0.811 ± 0.151	0.794 ± 0.171	0.759 ± 0.149	0.719 ± 0.127	

Table 6: Errors under spurious correlation corresponding to subplots (e), (f), (g), (h) in Figure 7, Figure 8, and Figure 3, Heart Failure.

Dataset	Class	Classifier	Method	$\frac{svm}{raw}$					
				0%	20%	40%	60%	80%	100%
Heart Failure	Minority	Logistic	OPAL	0.495 ± 0.065	0.394 ± 0.067	0.341 ± 0.088	0.284 ± 0.067	0.234 ± 0.050	0.217 ± 0.041
			Duplication	0.495 ± 0.065	0.488 ± 0.095	0.487 ± 0.085	0.487 ± 0.076	0.487 ± 0.081	0.476 ± 0.075
			SMOTE	0.495 ± 0.065	0.521 ± 0.093	0.470 ± 0.058	0.482 ± 0.073	0.470 ± 0.078	0.474 ± 0.077
		CatBoost	OPAL	0.419 ± 0.094	0.271 ± 0.051	0.253 ± 0.048	0.230 ± 0.046	0.218 ± 0.060	0.197 ± 0.047
			Duplication	0.419 ± 0.094	0.417 ± 0.088	0.391 ± 0.083	0.395 ± 0.072	0.382 ± 0.093	0.392 ± 0.067
			SMOTE	0.419 ± 0.094	0.415 ± 0.068	0.373 ± 0.068	0.361 ± 0.088	0.354 ± 0.083	0.386 ± 0.094
		RandomForest	OPAL	0.449 ± 0.046	0.321 ± 0.048	0.257 ± 0.041	0.245 ± 0.049	0.233 ± 0.066	0.215 ± 0.058
			Duplication	0.449 ± 0.046	0.411 ± 0.048	0.378 ± 0.062	0.382 ± 0.080	0.388 ± 0.100	0.359 ± 0.061
			SMOTE	0.449 ± 0.046	0.440 ± 0.075	0.352 ± 0.066	0.377 ± 0.027	0.371 ± 0.074	0.358 ± 0.033
	Majority	Logistic	OPAL	0.101 ± 0.034	0.123 ± 0.056	0.155 ± 0.030	0.177 ± 0.047	0.199 ± 0.060	0.219 ± 0.081
			Duplication	0.101 ± 0.034	0.110 ± 0.029	0.153 ± 0.066	0.147 ± 0.062	0.152 ± 0.071	0.161 ± 0.070
			SMOTE	0.101 ± 0.034	0.140 ± 0.093	0.135 ± 0.134	0.138 ± 0.077	0.140 ± 0.096	0.152 ± 0.079
		CatBoost	OPAL	0.091 ± 0.027	0.121 ± 0.037	0.136 ± 0.029	0.145 ± 0.027	0.148 ± 0.022	0.154 ± 0.021
			Duplication	0.091 ± 0.027	0.091 ± 0.027	0.108 ± 0.037	0.121 ± 0.064	0.111 ± 0.056	0.125 ± 0.067
			SMOTE	0.091 ± 0.027	0.090 ± 0.044	0.092 ± 0.053	0.136 ± 0.065	0.124 ± 0.045	0.126 ± 0.052
		RandomForest	OPAL	0.105 ± 0.047	0.138 ± 0.051	0.165 ± 0.059	0.183 ± 0.052	0.162 ± 0.034	0.167 ± 0.054
			Duplication	0.105 ± 0.047	0.122 ± 0.066	0.143 ± 0.056	0.135 ± 0.059	0.144 ± 0.067	0.139 ± 0.068
			SMOTE	0.105 ± 0.047	0.104 ± 0.067	0.129 ± 0.059	0.129 ± 0.059	0.135 ± 0.079	0.134 ± 0.051
	Overall	Logistic	OPAL	0.320 ± 0.063	0.272 ± 0.053	0.256 ± 0.055	0.234 ± 0.042	0.218 ± 0.037	0.216 ± 0.044
			Duplication	0.320 ± 0.063	0.320 ± 0.075	0.336 ± 0.065	0.334 ± 0.059	0.336 ± 0.068	0.334 ± 0.063
			SMOTE	0.320 ± 0.063	0.352 ± 0.060	0.322 ± 0.046	0.328 ± 0.053	0.320 ± 0.049	0.328 ± 0.046
		CatBoost	OPAL	0.274 ± 0.072	0.206 ± 0.038	0.200 ± 0.028	0.190 ± 0.021	0.186 ± 0.030	0.176 ± 0.025
			Duplication	0.274 ± 0.072	0.272 ± 0.064	0.266 ± 0.063	0.272 ± 0.068	0.262 ± 0.078	0.272 ± 0.067
			SMOTE	0.274 ± 0.072	0.272 ± 0.061	0.248 ± 0.059	0.258 ± 0.061	0.252 ± 0.070	0.268 ± 0.063
RandomForest		OPAL	0.294 ± 0.044	0.238 ± 0.053	0.214 ± 0.022	0.214 ± 0.022	0.200 ± 0.036	0.192 ± 0.044	
		Duplication	0.294 ± 0.044	0.280 ± 0.055	0.274 ± 0.062	0.270 ± 0.072	0.278 ± 0.071	0.260 ± 0.066	
		SMOTE	0.294 ± 0.044	0.292 ± 0.064	0.254 ± 0.065	0.266 ± 0.047	0.264 ± 0.066	0.256 ± 0.034	
Worst	Logistic	OPAL	0.539 ± 0.071	0.495 ± 0.125	0.440 ± 0.116	0.356 ± 0.083	0.312 ± 0.038	0.324 ± 0.068	
		Duplication	0.539 ± 0.071	0.534 ± 0.090	0.575 ± 0.111	0.578 ± 0.101	0.577 ± 0.109	0.576 ± 0.111	
		SMOTE	0.539 ± 0.071	0.574 ± 0.117	0.533 ± 0.115	0.506 ± 0.067	0.518 ± 0.093	0.553 ± 0.074	
	CatBoost	OPAL	0.495 ± 0.131	0.300 ± 0.033	0.287 ± 0.051	0.279 ± 0.049	0.286 ± 0.042	0.265 ± 0.031	
		Duplication	0.495 ± 0.131	0.523 ± 0.129	0.493 ± 0.136	0.477 ± 0.119	0.466 ± 0.146	0.481 ± 0.119	
		SMOTE	0.495 ± 0.131	0.492 ± 0.104	0.412 ± 0.089	0.383 ± 0.095	0.399 ± 0.092	0.420 ± 0.111	
	RandomForest	OPAL	0.526 ± 0.100	0.369 ± 0.067	0.322 ± 0.055	0.320 ± 0.071	0.277 ± 0.061	0.268 ± 0.057	
		Duplication	0.526 ± 0.100	0.495 ± 0.121	0.471 ± 0.112	0.456 ± 0.153	0.463 ± 0.149	0.426 ± 0.145	
		SMOTE	0.526 ± 0.100	0.504 ± 0.047	0.406 ± 0.058	0.422 ± 0.011	0.425 ± 0.067	0.423 ± 0.056	

Table 7: Errors under spurious correlation corresponding to subplots (i), (j), (k), (l) in Figure 7, Figure 3, and Figure 3, Gender.

Dataset	Class	Classifier	Method	$\frac{svm}{faw}$					
				0%	20%	40%	60%	80%	100%
Gender	Minority	Logistic	OPAL	0.121 ± 0.098	0.119 ± 0.080	0.096 ± 0.085	0.085 ± 0.073	0.092 ± 0.066	0.095 ± 0.075
			Duplication	0.121 ± 0.098	0.120 ± 0.096	0.122 ± 0.097	0.121 ± 0.095	0.116 ± 0.099	0.119 ± 0.097
			SMOTE	0.121 ± 0.098	0.140 ± 0.094	0.146 ± 0.128	0.164 ± 0.147	0.157 ± 0.135	0.164 ± 0.127
		CatBoost	OPAL	0.144 ± 0.109	0.106 ± 0.056	0.104 ± 0.073	0.122 ± 0.093	0.106 ± 0.054	0.097 ± 0.064
			Duplication	0.144 ± 0.109	0.162 ± 0.161	0.170 ± 0.170	0.169 ± 0.169	0.169 ± 0.175	0.168 ± 0.170
			SMOTE	0.144 ± 0.109	0.152 ± 0.160	0.146 ± 0.126	0.157 ± 0.156	0.155 ± 0.143	0.137 ± 0.097
		RandomForest	OPAL	0.147 ± 0.051	0.096 ± 0.036	0.085 ± 0.045	0.089 ± 0.045	0.090 ± 0.054	0.101 ± 0.060
			Duplication	0.147 ± 0.051	0.125 ± 0.051	0.107 ± 0.031	0.111 ± 0.051	0.117 ± 0.068	0.125 ± 0.081
			SMOTE	0.147 ± 0.051	0.132 ± 0.048	0.111 ± 0.050	0.109 ± 0.047	0.100 ± 0.038	0.098 ± 0.043
	Majority	Logistic	OPAL	0.033 ± 0.015	0.050 ± 0.027	0.045 ± 0.021	0.037 ± 0.027	0.035 ± 0.026	0.038 ± 0.026
			Duplication	0.033 ± 0.015	0.032 ± 0.016	0.031 ± 0.013	0.028 ± 0.010	0.034 ± 0.018	0.032 ± 0.014
			SMOTE	0.033 ± 0.015	0.037 ± 0.018	0.036 ± 0.057	0.037 ± 0.037	0.039 ± 0.039	0.039 ± 0.039
		CatBoost	OPAL	0.041 ± 0.043	0.055 ± 0.037	0.055 ± 0.042	0.044 ± 0.044	0.046 ± 0.041	0.049 ± 0.041
			Duplication	0.041 ± 0.043	0.041 ± 0.043	0.041 ± 0.043	0.043 ± 0.041	0.043 ± 0.042	0.043 ± 0.043
			SMOTE	0.041 ± 0.043	0.041 ± 0.040	0.044 ± 0.044	0.043 ± 0.043	0.047 ± 0.047	0.049 ± 0.049
		RandomForest	OPAL	0.026 ± 0.044	0.045 ± 0.043	0.048 ± 0.044	0.045 ± 0.045	0.045 ± 0.042	0.046 ± 0.044
			Duplication	0.026 ± 0.044	0.034 ± 0.047	0.038 ± 0.040	0.038 ± 0.038	0.039 ± 0.039	0.042 ± 0.041
			SMOTE	0.026 ± 0.044	0.030 ± 0.044	0.037 ± 0.037	0.037 ± 0.037	0.043 ± 0.043	0.044 ± 0.044
	Overall	Logistic	OPAL	0.077 ± 0.045	0.084 ± 0.039	0.070 ± 0.043	0.061 ± 0.035	0.064 ± 0.029	0.067 ± 0.031
			Duplication	0.077 ± 0.045	0.076 ± 0.043	0.076 ± 0.045	0.075 ± 0.044	0.075 ± 0.044	0.075 ± 0.044
			SMOTE	0.077 ± 0.045	0.084 ± 0.048	0.090 ± 0.057	0.100 ± 0.065	0.098 ± 0.062	0.101 ± 0.058
		CatBoost	OPAL	0.093 ± 0.053	0.081 ± 0.033	0.080 ± 0.038	0.084 ± 0.046	0.076 ± 0.025	0.073 ± 0.030
			Duplication	0.093 ± 0.053	0.102 ± 0.075	0.106 ± 0.081	0.106 ± 0.080	0.106 ± 0.083	0.106 ± 0.083
			SMOTE	0.093 ± 0.053	0.096 ± 0.075	0.095 ± 0.059	0.101 ± 0.072	0.101 ± 0.068	0.093 ± 0.049
RandomForest		OPAL	0.087 ± 0.028	0.071 ± 0.028	0.067 ± 0.030	0.068 ± 0.029	0.068 ± 0.027	0.074 ± 0.031	
		Duplication	0.087 ± 0.028	0.080 ± 0.033	0.072 ± 0.024	0.075 ± 0.032	0.078 ± 0.039	0.084 ± 0.045	
		SMOTE	0.087 ± 0.028	0.081 ± 0.028	0.074 ± 0.031	0.073 ± 0.031	0.071 ± 0.029	0.071 ± 0.032	
Worst	Logistic	OPAL	0.146 ± 0.088	0.135 ± 0.072	0.132 ± 0.066	0.111 ± 0.053	0.119 ± 0.042	0.120 ± 0.051	
		Duplication	0.146 ± 0.088	0.145 ± 0.086	0.148 ± 0.085	0.155 ± 0.077	0.148 ± 0.083	0.150 ± 0.083	
		SMOTE	0.146 ± 0.088	0.155 ± 0.088	0.167 ± 0.125	0.190 ± 0.141	0.187 ± 0.126	0.195 ± 0.112	
	CatBoost	OPAL	0.164 ± 0.118	0.138 ± 0.047	0.135 ± 0.065	0.144 ± 0.090	0.123 ± 0.047	0.109 ± 0.058	
		Duplication	0.164 ± 0.118	0.187 ± 0.177	0.194 ± 0.190	0.199 ± 0.185	0.197 ± 0.193	0.191 ± 0.193	
		SMOTE	0.164 ± 0.118	0.173 ± 0.178	0.165 ± 0.140	0.181 ± 0.172	0.179 ± 0.159	0.155 ± 0.106	
	RandomForest	OPAL	0.162 ± 0.057	0.123 ± 0.030	0.115 ± 0.044	0.114 ± 0.045	0.114 ± 0.041	0.123 ± 0.051	
		Duplication	0.162 ± 0.057	0.140 ± 0.059	0.127 ± 0.039	0.130 ± 0.060	0.137 ± 0.079	0.146 ± 0.093	
		SMOTE	0.162 ± 0.057	0.146 ± 0.058	0.126 ± 0.058	0.125 ± 0.054	0.113 ± 0.041	0.110 ± 0.043	

Table 8: Spurious Correlations: maximum absolute difference of accuracy, the smaller difference the better fairness.

Dataset	Classifier	Method	$\frac{SVH}{raw}$					
			Raw	20%	40%	60%	80%	100%
Diabetes	Logistic	Duplication	0.8845 ± 0.1248	0.7190 ± 0.1761	0.6389 ± 0.2006	0.5431 ± 0.2178	0.5113 ± 0.2167	0.4576 ± 0.2541
		OPAL	0.8845 ± 0.1248	0.6114 ± 0.1583	0.5042 ± 0.1026	0.4614 ± 0.1085	0.3921 ± 0.1151	0.3184 ± 0.1397
		SMOTE	0.8845 ± 0.1248	0.7422 ± 0.1744	0.6114 ± 0.1642	0.5883 ± 0.1677	0.5282 ± 0.1628	0.4629 ± 0.1167
	CatBoost	Duplication	0.8636 ± 0.0703	0.8600 ± 0.0770	0.8157 ± 0.1531	0.7782 ± 0.1453	0.7869 ± 0.1506	0.7326 ± 0.1292
		OPAL	0.8636 ± 0.0703	0.7916 ± 0.1388	0.6234 ± 0.0990	0.6058 ± 0.0958	0.5086 ± 0.1025	0.5145 ± 0.0515
		SMOTE	0.8636 ± 0.0703	0.7422 ± 0.1744	0.6114 ± 0.1642	0.5883 ± 0.1677	0.5282 ± 0.1628	0.4629 ± 0.1167
	Random Forest	Duplication	0.9728 ± 0.0382	0.8565 ± 0.0970	0.8036 ± 0.0813	0.6867 ± 0.1241	0.6707 ± 0.1472	0.6299 ± 0.1686
		OPAL	0.9728 ± 0.0382	0.8747 ± 0.1027	0.7380 ± 0.1342	0.5966 ± 0.1040	0.5483 ± 0.1041	0.5555 ± 0.0769
		SMOTE	0.9728 ± 0.0382	0.8461 ± 0.1273	0.8331 ± 0.1629	0.7796 ± 0.2216	0.7031 ± 0.1984	0.6880 ± 0.1988
Heart Failure	Logistic	Duplication	0.4895 ± 0.0769	0.4589 ± 0.0623	0.4511 ± 0.1331	0.4635 ± 0.1283	0.4626 ± 0.1263	0.4617 ± 0.1271
		OPAL	0.4895 ± 0.0769	0.4142 ± 0.1768	0.3490 ± 0.1203	0.2395 ± 0.1179	0.1772 ± 0.0872	0.1847 ± 0.0686
		SMOTE	0.4896 ± 0.0769	0.4932 ± 0.1786	0.4423 ± 0.1795	0.4238 ± 0.1361	0.4369 ± 0.1731	0.4818 ± 0.1582
	CatBoost	Duplication	0.4347 ± 0.1212	0.4631 ± 0.1178	0.4344 ± 0.1346	0.3948 ± 0.1424	0.3904 ± 0.1458	0.3882 ± 0.1468
		OPAL	0.4347 ± 0.1212	0.2279 ± 0.0187	0.1932 ± 0.0426	0.1926 ± 0.0471	0.1989 ± 0.0468	0.1613 ± 0.0449
		SMOTE	0.4347 ± 0.1212	0.4383 ± 0.1206	0.3580 ± 0.1001	0.2894 ± 0.1250	0.3214 ± 0.0812	0.3513 ± 0.1094
	Random Forest	Duplication	0.4523 ± 0.1188	0.3887 ± 0.1342	0.4243 ± 0.1137	0.3814 ± 0.1458	0.3758 ± 0.1508	0.3805 ± 0.1491
		OPAL	0.4523 ± 0.1188	0.3131 ± 0.1078	0.2609 ± 0.0648	0.2286 ± 0.1140	0.1926 ± 0.0910	0.2034 ± 0.1050
		SMOTE	0.4523 ± 0.1188	0.4408 ± 0.0540	0.3967 ± 0.0477	0.3164 ± 0.0720	0.3143 ± 0.0639	0.3356 ± 0.0665
Gender	Logistic	Duplication	0.127 ± 0.086	0.128 ± 0.087	0.131 ± 0.083	0.134 ± 0.080	0.130 ± 0.084	0.132 ± 0.085
		OPAL	0.127 ± 0.086	0.107 ± 0.066	0.107 ± 0.059	0.093 ± 0.051	0.102 ± 0.047	0.103 ± 0.054
		SMOTE	0.127 ± 0.086	0.138 ± 0.087	0.146 ± 0.127	0.167 ± 0.148	0.160 ± 0.127	0.169 ± 0.111
	CatBoost	Duplication	0.135 ± 0.131	0.160 ± 0.190	0.166 ± 0.202	0.170 ± 0.196	0.169 ± 0.206	0.161 ± 0.203
		OPAL	0.135 ± 0.131	0.103 ± 0.058	0.100 ± 0.075	0.108 ± 0.103	0.082 ± 0.074	0.069 ± 0.077
		SMOTE	0.135 ± 0.131	0.143 ± 0.191	0.131 ± 0.154	0.146 ± 0.189	0.140 ± 0.170	0.114 ± 0.117
	Random Forest	Duplication	0.128 ± 0.052	0.113 ± 0.066	0.100 ± 0.048	0.101 ± 0.061	0.113 ± 0.081	0.105 ± 0.073
		OPAL	0.128 ± 0.052	0.069 ± 0.034	0.070 ± 0.040	0.078 ± 0.044	0.080 ± 0.063	0.072 ± 0.059
		SMOTE	0.128 ± 0.052	0.115 ± 0.060	0.093 ± 0.065	0.089 ± 0.050	0.084 ± 0.058	0.073 ± 0.045